รายงานวิจัยฉบับสมบูรณ์

โครงการเครื่องปฏิกรณ์แบบหลายหน้าที่สำหรับอุตสาหกรรมเคมีและปิโตรเคมี

โดย ศาสตราจารย์ ดร. สุทธิชัย อัสสะบำรุงรัตน์

พฤษภาคม 2551

สัญญาเลขที่ RMU4880017

รายงานวิจัยฉบับสมบูรณ์

โครงการเครื่องปฏิกรณ์แบบหลายหน้าที่สำหรับอุตสาหกรรมเคมีและปิโตรเคมี

ผู้วิจัย

ศาสตราจารย์ ดร. สุทธิชัย อัสสะบำรุงรัตน์

สังกัด

ภาควิชาวิศวกรรมเคมี

คณะวิศวกรรมศาสตร์

จุฬาลงกรณ์มหาวิทยาลัย

สนับสนุนโดยสำนักงานกองทุนสนับสนุนการวิจัย

(ความเห็นในรายงานนี้เป็นของผู้วิจัย สกว.ไม่จำเป็นต้องเห็นด้วยเสมอไป)

Abstract

Project Code: RMU4880017

Project Title: Multifunctional Reactors for Chemical and Petrochemical Industries

Investigator: Professor Suttichai Assabumrungrat,
Department of Chemical Engineering, Faculty of Engineering,
Chulalongkorn University

Email: Suttichai.A@chula.ac.th

Project Period: 1 August 2005 – 31 July 2008

This project was aimed to develop new basic knowledge related to multifunctional reactors for chemical and petrochemical industries. The works were focused on 3 sub-research topics including 1) Study on fuel cells, 2) Study on reaction and extraction system and 3) Study on periodic operation. From the works, 15 international papers have been accepted for publication and 3 international papers are under consideration. In addition, 5 papers were presented in international conferences. The followings summarize the lists of all outputs.

International Papers

1) W. Jamsak, S. Assabumrungrat, P.L. Douglas, N. Laosiripojana and S. Charojrochkul, "Theoretical Performance Analysis of Ethanol-Fueled Solid Oxide Fuel Cells with Different Electrolytes", Chemical Engineering Journal 119 (2006) 11–18. (IF-2006 = 1.594).
2) S. Assabumrungrat, N. Laosiripojana and P. Philunrekekun, "Determination of Boundary of Carbon Formation for Dry Reforming of Methane in Solid Oxide Fuel Cell", Journal of Power Sources, vol. 159 (2006) 1274-1282 (IF-2006 = 3.521).
3) Eakkapon Promaros, Suttichai Assabumrungrat, Navadol Laosiripojana, Piyasan Praserthdam, Tomohiko Tagawa and Shigeo Goto, "Carbon dioxide reforming of methane under periodic operation", Korean Journal of Chemical Engineering 24 (2007) 44-50 (IF-2006 = 0.808).
4) Garun tanarungsun, Worapon Kiatkittipong, Suttichai Assabumrungrat, Hiroshi Yamada, Tomohiko Tagawa and Piyasan Prasertdam, "Fe (III), Cu (II), V (V)/TiO2 for hydroxylation

of benzene to phenol with hydrogen peroxide at room temperature", Journal of Chemical Engineering of Japan, vol. 40 (2007) 415-421 (IF-2006 = 0.594).

5) Garun Tanarungsun, Worapon Kiatkittipong, Suttichai Assabumrungrat, Hiroshi Yamada, Tomohiko Tagawa and Piyasan Prasertdam, "Liquid phase hydroxylation of benzene to phenol with hydrogen peroxide catalyzed by Fe (III)/TiO_2 catalysts at room temperature", Journal of Industrial & Engineering Chemistry, vol. 13 (2007) 444-451 (IF-2006 = 0.957).
6) S. Vivanpatarakij, S. Assabumrungrat and N. Laosiripojana, "Improvement of SOFC performance by using non-uniform cell potential operation", Journal of Power Sources, vol. 167 (2007) 139-144 (IF-2006 = 3.521).
7) W. Jamsak, S. Assabumrungrat, P.L. Douglas, N. Laosiripojana, R. Suwanwarangkul, S. Charojrochkul and E. Croiset "Performance Assessment of Bioethanol-Fed Solid Oxide Fuel Cell System Integrated with a Distillation Column", ECS Transactions - Solid Oxide Fuel Cells vol. 7 (2007) 1475-1482 (IF-2006 = -).
8) W. Jamsak, S. Assabumrungrat, P.L. Douglas, N. Laosiripojana, R. Suwanwarangkul, S. Charojrochkul and E. Croiset "Performance of Ethanol-Fueled Solid Oxide Fuel Cells: Proton and Oxygen Ion Conductors", Chemical Engineering Journal, vol. 133/1-3 (2007) 187-194 (IF-2006 = 1.594).
9) Garun Tanarungsun, Worapon Kiatkittipong, Suttichai Assabumrungrat, Hiroshi Yamada, Tomohiko Tagawa and Piyasan Prasertdam, "Multi transition metal catalysts supported on TiO_2 for hydroxylation of benzene to phenol with hydrogen peroxide", Journal of Industrial & Engineering Chemistry, vol. 13 (2007) 870-877 (IF-2006 = 0.957).
10) W. Jamsak, S. Assabumrungrat, P.L. Douglas, E. Croiset, N. Laosiripojana, R. Suwanwarangkul and S. Charojrochkul, "Thermodynamic Assessment of Solid Oxide Fuel Cell System Integrated with Bioethanol Purification Unit", Journal of Power Sources, vol. 174 (2007) 191-198 (IF-2006 = 3.521).
11) W. Sangtongkitcharoen, S.Vivanpatarakij, N. Laosiripojana, A. Arpornwichanop and S. Assabumrungrat, "Performance analysis of methanol-fueled solid oxide fuel cell system incoporated with palladium membrane reactor", Chemical Engineering Journal, vol. 138 (2008) 436-441 (IF-2006 = 1.594).
12) Garun tanarungsun, Worapon Kiatkittipong, Suttichai Assabumrungrat, Hiroshi Yamada, Tomohiko Tagawa and Piyasan Prasertdam, "Hydroxylation of benzene to phenol on Fe/TiO_2

catalysts loaded with different types of second metal", Catalysis Communications, Vol. 9 (2008) 1886-1890 (IF-2006 = 1.878).

13) Hiroshi YAMADA, Tomoaki MIZUNO, Tomohiko TAGAWA, Garun TANARUNGSUN, Piyasan PRASERTHDAM and Suttichai ASSABUMRUNGRAT "Catalyst Regenerator for Partial Oxidation of Benzene in Reaction-Extraction System" Journal of the Japan Petroleum Institute, vol. 51 (2008), 114-117. (IF-2006 = 0.633)

14) P. Philunrekekun, S. Assabumrungrat, N. Laosiripojana and A.A. Adesina, "Selection of appropriate fuel processor for biogas-fuelled SOFC system", Chemical Engineering Journal, in press (IF-2006 = 1.594).

15) Garun Tanarungsun, Worapon Kiatkittipong, Suttichai Assabumrungrat, Hiroshi Yamada, Tomohiko Tagawa and Piyasan Prasertdam, "Ternary metal oxide catalysts for selective oxidation of benzene to phenol", accepted by Journal of Industrial & Engineering Chemistry, April 9, 2008 (IF-2005 = 0.957).

Submitted International Papers (under consideration)

1) S. Vivanpatarakij, S. Assabumrungrat, and N. Laosiripojana, "Performance improvement of solid oxide fuel cell system using palladium membrane reactor with different operation modes", submitted to Chemical Engineering Journal, December 2007 (IF-2006 = 1.594).

2) Boonrat Pholjaroen, Navadol Laosiripojana, Piyasan Praserthdam and Suttichai Assabumrungrat, "Reactivity of Ni/SiO_2.MgO toward carbon dioxide reforming of methane under steady state and periodic operations" submitted to Fuel Processing Technology, April 11, 2008 (IF-2006 = 1.323).

3) P. Philunrekekun, S. Assabumrungrat, N. Laosiripojana and A.A. Adesina, "Performance of biogas-fed solid oxide fuel cell systems integrated with membrane module for CO_2 removal", submitted to Chemical Engineering and Processing: Process Intensification, April 2, 2008 (IF-2006 = 1.129).

International Conferences

1) Eakkapon Promaros, Suttichai Assabumrungrat, Navadol Laosiripojana, Piyasan Praserthdam, Tomohiko Tagawa and Shigeo Goto, "Carbon dioxide reforming of methane under periodic operation", Fifth international conference on unsteady-state processes in catalysis, Suita City, Japan Nov. 22-25, 2006 (poster presentation).

2) Boonrat Pholjaroen, Eakkapon Promaros, Navadol Laosiripojana, Suttichai Assabumrungrat, Piyasan Praserthdam, Tomohiko Tagawa and Shigeo Goto "Characterization of deposited coke on Ni/SiO2.MgO catalyst from carbon dioxide reforming of methane under periodic operation", Singapore, December 3-5, 2006 (oral presentation).

3) W. Sangtongkitcharoen, S. Assabumrungrat, N. Laosiripojana, A. Arpornwichanop, S.Vivanpatarakij and P. Praserthdam "Performance analysis of methanol-fueled solid oxide fuel cell system Incorporated with palladium membrane reactor", The sixth International Symposium on Catalysis in Multiphase Reactors (CAMURE-6) and the fifth International Symposium on Multifunctional Reactors (ISMR-5), January 14-16, 2007 (poster presentation).

4) S. Vivanpatarakij, S. Assabumrungrat, N. Laosiripojana and P. Praserthdam, "Improvement of SOFC performance by using non-uniform cell potential operation", The sixth International Symposium on Catalysis in Multiphase Reactors (CAMURE-6) and the fifth International Symposium on Multifunctional Reactors (ISMR-5), January 14-16, 2007 (oral presentation).

5) W. Jamsak, S. Assabumrungrat, P.L. Douglas, N. Laosiripojana, R. Suwanwarangkul, S. Charojrochkul and E. Croiset "Performance Assessment of Bioethanol-Fed Solid Oxide Fuel Cell System Integrated with a Distillation Column", 10th International Symposium on Solid Oxide Fuel Cells (SOFC-X), Nara, Japan, June 3-8, 2007 (oral presentation).

บทคัดย่อ

รหัสโครงการ: RMU4880017

ชื่อโครงการ: เครื่องปฏิกรณ์แบบหลายหน้าที่สำหรับอุตสาหกรรมเคมีและปิโตรเคมี

ชื่อนักวิจัย: ศาสตราจารย์ ดร.สุทธิชัย อัสสะบำรุงรัตน์

Email: Suttichai.A@chula.ac.th

ระยะเวลาโครงการ: 1 สิงหาคม 2548 – 31 กรกฎาคม 2551

โครงการวิจัยนี้มีวัตถุประสงค์เพื่อสร้างองค์ความรู้พื้นฐานที่เกี่ยวข้องกับเครื่องปฏิกรณ์แบบหลายหน้าที่สำหรับอุตสาหกรรมเคมีและปิโตรเคมี งานที่ศึกษาสามารถแบ่งออกเป็น 3 หัวข้อย่อย คือ 1) การศึกษาทางด้านเซลล์เชื้อเพลิง 2) การศึกษาระบบการเกิดปฏิกิริยาที่มีการสกัด และ 3) การศึกษาการดำเนินงานแบบสลับ ผลงานที่ได้จากการศึกษานี้คือ บทความที่นำเสนอในวารสารระดับนานาชาติที่ได้รับการยอมรับให้ตีพิมพ์แล้ว 15 บทความ และบทความที่นำเสนอในวารสารระดับนานาชาติที่อยู่ระหว่างการพิจารณา 3 บทความ นอกจากนี้ยังมีการนำเสนอผลงานในที่ประชุมระดับนานาชาติอีก 5 บทความ โดยรายละเอียดสรุปได้ดังต่อไปนี้

บทความวิจัยระดับนานาชาติที่ได้รับการยอมรับให้ตีพิมพ์แล้ว

1) W. Jamsak, S. Assabumrungrat, P.L. Douglas, N. Laosiripojana and S. Charojrochkul, “Theoretical Performance Analysis of Ethanol-Fueled Solid Oxide Fuel Cells with Different Electrolytes”, Chemical Engineering Journal 119 (2006) 11–18. (IF-2006 = 1.594).
2) S. Assabumrungrat, N. Laosiripojana and P. Philunrekekun, “Determination of Boundary of Carbon Formation for Dry Reforming of Methane in Solid Oxide Fuel Cell”, Journal of Power Sources, vol. 159 (2006) 1274-1282 (IF-2006 = 3.521).
3) Eakkapon Promaros, Suttichai Assabumrungrat, Navadol Laosiripojana, Piyasan Praserthdam, Tomohiko Tagawa and Shigeo Goto, “Carbon dioxide reforming of methane under periodic operation”, Korean Journal of Chemical Engineering 24 (2007) 44-50 (IF-2006 = 0.808).
4) Garun Tanarungsun, Worapon Kiatkittipong, Suttichai Assabumrungrat, Hiroshi Yamada, Tomohiko Tagawa and Piyasan Prasertdam, “Fe (III), Cu (II), V (V)/TiO2 for hydroxylation of benzene to phenol with hydrogen peroxide at room temperature”, Journal of Chemical Engineering of Japan, vol. 40 (2007) 415-421 (IF-2006 = 0.594).
5) Garun Tanarungsun, Worapon Kiatkittipong, Suttichai Assabumrungrat, Hiroshi Yamada, Tomohiko Tagawa and Piyasan Prasertdam, “Liquid phase hydroxylation of benzene to

phenol with hydrogen peroxide catalyzed by Fe (III)/TiO_2 catalysts at room temperature", Journal of Industrial & Engineering Chemistry, vol. 13 (2007) 444-451 (IF-2006 = 0.957).

6) S. Vivanpatarakij, S. Assabumrungrat and N. Laosiripojana, "Improvement of SOFC performance by using non-uniform cell potential operation", Journal of Power Sources, vol. 167 (2007) 139-144 (IF-2006 = 3.521).
7) W. Jamsak, S. Assabumrungrat, P.L. Douglas, N. Laosiripojana, R. Suwanwarangkul, S. Charojrochkul and E. Croiset "Performance Assessment of Bioethanol-Fed Solid Oxide Fuel Cell System Integrated with a Distillation Column", ECS Transactions – Solid Oxide Fuel Cells vol. 7 (2007) 1475-1482 (IF-2006 = -).
8) W. Jamsak, S. Assabumrungrat, P.L. Douglas, N. Laosiripojana, R. Suwanwarangkul, S. Charojrochkul and E. Croiset "Performance of Ethanol-Fueled Solid Oxide Fuel Cells: Proton and Oxygen Ion Conductors", Chemical Engineering Journal, vol. 133/1-3 (2007) 187-194 (IF-2006 = 1.594).
9) Garun tanarungsun, Worapon Kiatkittipong, Suttichai Assabumrungrat, Hiroshi Yamada, Tomohiko Tagawa and Piyasan Prasertdam, "Multi transition metal catalysts supported on TiO_2 for hydroxylation of benzene to phenol with hydrogen peroxide", Journal of Industrial & Engineering Chemistry, vol. 13 (2007) 870-877 (IF-2006 = 0.957).
10) W. Jamsak, S. Assabumrungrat, P.L. Douglas, E. Croiset, N. Laosiripojana, R. Suwanwarangkul and S. Charojrochkul, "Thermodynamic Assessment of Solid Oxide Fuel Cell System Integrated with Bioethanol Purification Unit", Journal of Power Sources, vol. 174 (2007) 191-198 (IF-2006 = 3.521).
11) W. Sangtongkitcharoen, S.Vivanpatarakij, N. Laosiripojana, A. Arpornwichanop and S. Assabumrungrat, "Performance analysis of methanol-fueled solid oxide fuel cell system Incorporated with palladium membrane reactor", Chemical Engineering Journal, vol. 138 (2008) 436-441 (IF-2006 = 1.594).
12) Garun Tanarungsun, Worapon Kiatkittipong, Suttichai Assabumrungrat, Hiroshi Yamada, Tomohiko Tagawa and Piyasan Prasertdam, "Hydroxylation of benzene to phenol on Fe/TiO_2 catalysts loaded with different types of second metal", Catalysis Communications, Vol. 9 (2008) 1886-1890 (IF-2006 = 1.878).
13) Hiroshi YAMADA, Tomoaki MIZUNO, Tomohiko TAGAWA, Garun TANARUNGSUN, Piyasan PRASERTHDAM and Suttichai ASSABUMRUNGRAT "Catalyst Regenerator for

Partial Oxidation of Benzene in Reaction-Extraction System" Journal of the Japan Petroleum Institute, vol. 51 (2008), 114-117. (IF-2006 = 0.633)

14) P. Philunrekekun, S. Assabumrungrat, N. Laosiripojana and A.A. Adesina, "Selection of appropriate fuel processor for biogas-fuelled SOFC system", Chemical Engineering Journal, in press (IF-2006 = 1.594).

15) Garun Tanarungsun, Worapon Kiatkittipong, Suttichai Assabumrungrat, Hiroshi Yamada, Tomohiko Tagawa and Piyasan Prasertdam, "Ternary metal oxide catalysts for selective oxidation of benzene to phenol", accepted by Journal of Industrial & Engineering Chemistry, April 9, 2008 (IF-2005 = 0.957).

บทความวิจัยระดับนานาชาติที่อยู่ระหว่างการพิจารณา

1) S. Vivanpatarakij, S. Assabumrungrat, and N. Laosiripojana, "Performance improvement of solid oxide fuel cell system using palladium membrane reactor with different operation modes", submitted to Chemical Engineering Journal, December 2007 (IF-2006 = 1.594).

2) Boonrat Pholjaroen, Navadol Laosiripojana, Piyasan Praserthdam and Suttichai Assabumrungrat, "Reactivity of Ni/SiO_2.MgO toward carbon dioxide reforming of methane under steady state and periodic operations" submitted to Fuel Process Technol, April 11, 2008 (IF-2006 = 1.323).

3) P. Philunrekekun, S. Assabumrungrat, N. Laosiripojana and A.A. Adesina, "Performance of biogas-fed solid oxide fuel cell systems integrated with membrane module for CO_2 removal", submitted to Chemical Engineering and Processing: Process Intensification, April 2, 2008 (IF-2006 = 1.129).

การนำเสนอผลงานในที่ประชุมระดับนานาชาติ

1) Eakkapon Promaros, Suttichai Assabumrungrat, Navadol Laosiripojana, Piyasan Praserthdam, Tomohiko Tagawa and Shigeo Goto, "Carbon dioxide reforming of methane under periodic operation", Fifth international conference on unsteady-state processes in catalysis, Suita City, Japan Nov. 22-25, 2006 (poster presentation).

2) Boonrat Pholjaroen, Eakkapon Promaros, Navadol Laosiripojana, Suttichai Assabumrungrat, Piyasan Praserthdam, Tomohiko Tagawa and Shigeo Goto "Characterization of deposited coke on Ni/SiO2.MgO catalyst from carbon dioxide reforming of methane under periodic operation", Singapore, December 3-5, 2006 (oral presentation).

3) W. Sangtongkitcharoen, S. Assabumrungrat, N. Laosiripojana, A. Arpornwichanop, S.Vivanpatarakij and P. Praserthdam, "Performance analysis of methanol-fueled solid oxide fuel cell system Incorporated with palladium membrane reactor", The sixth International Symposium on Catalysis in Multiphase Reactors (CAMURE-6) and the fifth International Symposium on Multifunctional Reactors (ISMR-5), January 14-16, 2007 (poster presentation).
4) S. Vivanpatarakij, S. Assabumrungrat, N. Laosiripojana and P. Praserthdam, "Improvement of SOFC performance by using non-uniform cell potential operation", The sixth International Symposium on Catalysis in Multiphase Reactors (CAMURE-6) and the fifth International Symposium on Multifunctional Reactors (ISMR-5), January 14-16, 2007 (oral presentation).
5) W. Jamsak, S. Assabumrungrat, P.L. Douglas, N. Laosiripojana, R. Suwanwarangkul, S. Charojrochkul and E. Croiset "Performance Assessment of Bioethanol-Fed Solid Oxide Fuel Cell System Integrated with a Distillation Column", 10th International Symposium on Solid Oxide Fuel Cells (SOFC-X), Nara, Japan, June 3-8, 2007 (oral presentation).

Acknowledgement

This research project is financially supported by The Thailand Research Fund (TRF) and Commission of Higher Education. The project is completed successfully by the supports of my hard working students (Dr. Wasana Jamsak, Dr. Supawat Vivanpatarakij, Dr. Garun Tanarungsan, Mr. Wiboon Sangtongkitcharoen, Mr. Eakkapon Promaros, Mr. Boonrat Pholjaroen, Mr. Pakorn Philunrekekun and others), my good colleagues (Dr. Navadol Laosiripojana, Dr. Amornchai Arpornwichanop, Dr. Sumittra Charojrochkul, Dr. Rapeepong Suwanwarangkul) and my good collaborators (Professor Tomohiko Tagawa, Assistant Professor Hiroshi Yamada, Professor Peter Douglas, Associate Professor Eric Croiset and Professor Adesoji Adesina).

Table of Content

Research Outputs from the Study

The works on multifunctional reactors for chemical and petrochemical industries in this study were divided into 3 main parts as summarized below.

1) Study on fuel cell systems

The numbers of international papers that are published and being under consideration under this topic are 8 and 2, respectively (total = 10 papers).

Preliminary analysis of solid oxide fuel cell (SOFC) system fuelled by bioethanol was investigated. The performance of the SOFCs with an oxygen-conducting electrolyte (SOFC-O^{2-}) and a proton-conducting electrolyte (SOFC-H^{+}) was compared. It was found that although the theoretical performance of the SOFC-H^{+} is superior to that of the SOFC-O^{2-}, the presently available poor proton conductor makes the use of the proton-conducting electrolyte impractical. The development of novel proton conductor for SOFC is necessary. The possibility of the system integration between an SOFC and a distillation column for bioethanol purification was examined. Excessive heat from the SOFC system was utilized as a heat source for the reboiler of the distillation column. The study also focused on the performance of the integrated system under the energy-self sufficiency condition of the system.

Another SOFC system was focused on using biogas as a fuel. A suitable feed composition which was safe from anode deactivation by carbon formation was determined for different types of fuel processor (steam reforming, partial oxidation and dry reforming). Then the performance of the biogas-fuelled SOFC with different types of fuel processor was compared, considering the obtained electrical efficiency and power density of the SOFC stack.

The other project was focused on performance improvement of SOFC by using different approaches such as application of non-uniform potential operation and replacing a conventional reformer with a membrane reactor to increase hydrogen concentration in the product stream.

Publications

W. Jamsak, S. Assabumrungrat, P.L. Douglas, N. Laosiripojana and S. Charojrochkul, "Theoretical Performance Analysis of Ethanol-Fueled Solid Oxide Fuel Cells with Different

Electrolytes", Chemical Engineering Journal 119 (2006) 11–18. (IF-2006 = 1.594). **(Appendix 1)**

W. Jamsak, S. Assabumrungrat, P.L. Douglas, N. Laosiripojana, R. Suwanwarangkul, S. Charojrochkul and E. Croiset "Performance Assessment of Bioethanol-Fed Solid Oxide Fuel Cell System Integrated with a Distillation Column", ECS Transactions - Solid Oxide Fuel Cells vol. 7 (2007) 1475-1482 (IF-2006 = -). **(Appendix 2)**

W. Jamsak, S. Assabumrungrat, P.L. Douglas, N. Laosiripojana, R. Suwanwarangkul, S. Charojrochkul and E. Croiset "Performance of Ethanol-Fueled Solid Oxide Fuel Cells: Proton and Oxygen Ion Conductors", Chemical Engineering Journal, vol. 133/1-3 (2007) 187-194 (IF-2006 = 1.594). **(Appendix 3)**

W. Jamsak, S. Assabumrungrat, P.L. Douglas, E. Croiset, N. Laosiripojana, R. Suwanwarangkul and S. Charojrochkul, "Thermodynamic Assessment of Solid Oxide Fuel Cell System Integrated with Bioethanol Purification Unit", Journal of Power Sources, vol. 174 (2007) 191-198 (IF-2006 = 3.521). **(Appendix 4)**

S. Assabumrungrat, N. Laosiripojana and P. Philunrekekun, "Determination of Boundary of Carbon Formation for Dry Reforming of Methane in Solid Oxide Fuel Cell", Journal of Power Sources, vol. 159 (2006) 1274-1282 (IF-2006 = 3.521). **(Appendix 5)**

S. Vivanpatarakij, S. Assabumrungrat and N. Laosiripojana, "Improvement of SOFC performance by using non-uniform cell potential operation", Journal of Power Sources, vol. 167 (2007) 139-144 (IF-2006 = 3.521). **(Appendix 6)**

W. Sangtongkitcharoen, S.Vivanpatarakij, N. Laosiripojana, A. Arpornwichanop and S. Assabumrungrat, "Performance analysis of methanol-fueled solid oxide fuel cell system incoporated with palladium membrane reactor", Chemical Engineering Journal, vol. 138 (2008) 436-441 (IF-2006 = 1.594). **(Appendix 7)**

P. Philunrekekun, S. Assabumrungrat, N. Laosiripojana and A.A. Adesina, "Selection of appropriate fuel processor for biogas-fuelled SOFC system", Chem. Eng. J., accepted October 5, 2007 (IF-2006 = 1.594). **(Appendix 8)**

S. Vivanpatarakij, S. Assabumrungrat, and N. Laosiripojana, "Performance improvement of solid oxide fuel cell system using palladium membrane reactor with different operation modes", submitted to Chemical Engineering Journal, December 2007 (IF-2006 = 1.594). **(Appendix 9)**

P. Philunrekekun, S. Assabumrungrat, N. Laosiripojana and A.A. Adesina, "Performance of biogas-fed solid oxide fuel cell systems integrated with membrane module for CO_2 removal",

submitted to Chemical Engineering and Processing: Process Intensification, April 2, 2008 (IF-2006 = 1.129). **(Appendix 10)**

2) Study on reaction with separation

The number of international papers that are published under this topic is 6.

This work is aimed to study the reaction and extraction system by focusing on production of phenol from the liquid phase hydroxylation of benzene by hydrogen peroxide. The preliminary works were mainly focused on catalyst screening. Firstly a suitable TiO_2 support was selected and then various metal oxides (V, Cu and Fe) were tested. The Fe/TiO_2 was selected for further studies. Various second or third metals were added in the catalyst for the catalytic performance improvement. Some work was carried out to investigate the reaction system that combines both reaction and extraction functions.

Publications

Garun tanarungsun, Worapon Kiatkittipong, Suttichai Assabumrungrat, Hiroshi Yamada, Tomohiko Tagawa and Piyasan Prasertdam, "Fe (III), Cu (II), V (V)/TiO2 for hydroxylation of benzene to phenol with hydrogen peroxide at room temperature", Journal of Chemical Engineering of Japan, vol. 40 (2007) 415-421 (IF-2005 = 0.594). **(Appendix 11)**

Garun tanarungsun, Worapon Kiatkittipong, Suttichai Assabumrungrat, Hiroshi Yamada, Tomohiko Tagawa and Piyasan Prasertdam, "Liquid phase hydroxylation of benzene to phenol with hydrogen peroxide catalyzed by Fe (III)/TiO_2 catalysts at room temperature", Journal of Industrial & Engineering Chemistry, vol. 13 (2007) 444-451 (IF-2006 = 0.957). **(Appendix 12)**

Garun tanarungsun, Worapon Kiatkittipong, Suttichai Assabumrungrat, Hiroshi Yamada, Tomohiko Tagawa and Piyasan Prasertdam, "Multi transition metal catalysts supported on TiO_2 for hydroxylation of benzene to phenol with hydrogen peroxide", Journal of Industrial & Engineering Chemistry, vol. 13 (2007) 870-877 (IF-2006 = 0.957). **(Appendix 13)**

Garun tanarungsun, Worapon Kiatkittipong, Hiroshi Yamada, Tomohiko Tagawa, Piyasan Prasertdam and Suttichai Assabumrungrat, "Hydroxylation of benzene to phenol on Fe/TiO_2 catalysts loaded with different types of second metal", Catalysis Communications, vol. 9 (2008) 1886-1890 (IF-2006 = 1.878). **(Appendix 14)**

Hiroshi Yamada, Tomoaki Mizuno, Tomohiko Tagawa, Garun Tanarungsun, Piyasan Praserthdam and Suttichai Assabumrungrat "Catalyst Regenerator for Partial Oxidation of Benzene in Reaction-Extraction System" Journal of the Japan Petroleum Institute, vol. 51 (2008), 114-117. (IF-2006 = 0.633) **(Appendix 15)**

Garun tanarungsun, Worapon Kiatkittipong, Hiroshi Yamada, Tomohiko Tagawa, Piyasan Prasertdam and Suttichai Assabumrungrat, "Ternary metal oxide catalysts for selective oxidation of benzene to phenol", accepted by Journal of Industrial & Engineering Chemistry, April 9, 2008 (IF-2005 = 0.957). **(Appendix 16)**

3) Study on periodic operation

The numbers of international paper that are published and being under consideration under this topic are 1 and 1, respectively (total = 2 papers).

This work focuses on the use of periodic operation for hydrogen production from methane and carbon dioxide. The reactants were alternately fed to the catalyst bed. During the methane feed period, pure hydrogen was the product. Carbon dioxide was fed in the other period for catalyst regeneration, yielding carbon monoxide as the product. It was reported that only under some operating conditions, the periodic operation offered a comparable or superior performance over the conventional continuous operation. The operation was retarded by the incomplete regeneration of the catalyst covered by carbon from the methane cracking. Different types of carbon were observed from the operations at T = 650 and 750^{o}C.

Publication

Eakkapon Promaros, Suttichai Assabumrungrat, Navadol Laosiripojana, Piyasan Praserthdam, Tomohiko Tagawa and Shigeo Goto, "Carbon dioxide reforming of methane under periodic operation", Korean Journal of Chemical Engineering 24 (2007) 44-50 (IF-2006 = 0.808) **(Appendix 17)**

Boonrat Pholjaroen, Navadol Laosiripojana, Piyasan Praserthdam and Suttichai Assabumrungrat, "Reactivity of Ni/SiO_2.MgO toward carbon dioxide reforming of methane under steady state and periodic operations" submitted to Fuel Processing Technology, April 11, 2008 (IF-2006 = 1.323). **(Appendix 18)**

Appendix

Appendix 1

ELSEVIER

Chemical Engineering Journal 119 (2006) 11–18

Chemical Engineering Journal

www.elsevier.com/locate/cej

Theoretical performance analysis of ethanol-fuelled solid oxide fuel cells with different electrolytes

W. Jamsak [a], S. Assabumrungrat [a,*], P.L. Douglas [b], N. Laosiripojana [c], S. Charojrochkul [d]

[a] *Center of Excellence in Catalysis and Catalytic Reaction Engineering, Department of Chemical Engineering, Faculty of Engineering, Chulalongkorn University, Bangkok 10330, Thailand*

[b] *Department of Chemical Engineering, University of Waterloo, Ontario, Canada*

[c] *The Joint Graduate School of Energy and Environment, King Mongkut's University of Technology Thonburi, Bangkok 10140, Thailand*

[d] *National Metal and Materials Technology Center (MTEC), Thailand*

Received 31 July 2005; received in revised form 21 February 2006; accepted 4 March 2006

Abstract

The theoretical performance of ethanol-fuelled solid oxide fuel cells (SOFCs) with oxygen ion conducting and proton conducting electrolytes are presented in this paper. It was reported in a previous work that an SOFC with a proton conducting electrolyte (SOFC-H^+) offers higher efficiency than an SOFC with an oxygen ion conducting electrolyte (SOFC-O^{2-}). However, the study was based on the same steam-to-hydrocarbon feed ratio. Our previous work demonstrated the potential benefit of the SOFC-O^{2-} over the SOFC-H^+ in terms of a lower requirement for steam in the feed. Therefore, in this article, this benefit is taken into account in the performance comparison. Influences of mode of operation (i.e. plug flow (PF) and well-mixed (WM)) on the performance of SOFCs were also investigated. In the PF mode, two feeding patterns (i.e. co-current (Co) and counter-current (CC)) were considered.

The results show that theoretical SOFC efficiencies depend on the type of electrolyte, mode of operation, inlet H_2O:EtOH ratio and fuel utilization. Although it was found that the feeding pattern has an influence on EMF distribution along the cell, the average EMF is not affected. At the best conditions for each type of SOFC, it was observed that SOFC-O^{2-} yields a maximum efficiency at the minimum inlet H_2O:EtOH ratio which is the limit for carbon formation for each value of fuel utilization. On the other hand, in SOFC-H^+, optimum inlet H_2O:EtOH ratios are higher than the limit of carbon formation. At the optimum conditions, the rank of the various SOFCs is as follows: SOFC-H^+(PF) > SOFC-O^{2-}(PF) > SOFC-H^+(WM) > SOFC-O^{2-}(WM) over the temperature range (1000–1200 K). No difference in SOFC efficiency between both feeding patterns was observed. It is clear from our theoretical studies that the SOFC-H^+(PF) is the most promising SOFC system.

Keywords: Solid oxide fuel cells; Direct internal reforming; Oxygen ion conductor; Proton conductor; Efficiency

1. Introduction

Fuel cells are currently regarded as the most promising technology for conversion of chemical to electrical energy. Solid oxide fuel cells (SOFC) have attracted considerable interest as they offer the widest range of potential applications, possibility in operation with an internal reformer, and possessing a high system efficiency. Many fuels have been suggested for use in SOFCs; however, among these, ethanol is considered to be an attractive green fuel because of its renewability from various biomass sources including energy plants, waste materials from agro-industries, forestry residue materials, and even organic fractions from municipal solid wastes. They also offer advantages related to natural availability and safety in storage and handling.

There are a number of studies published dealing with the use of ethanol for fuel cells. Ethanol was found to provide higher electrical and overall efficiency than methane in a direct internal reforming molten carbonate fuel cell (DIR-MCFC) [1]. Thermodynamic analysis of an indirect internal reforming molten carbonate fuel cell (IIR-MCFC) revealed that among different fuels (i.e. methane, methanol, and ethanol), ethanol presented the highest power density and the highest cell voltage. At a constant power density, ethanol allows the system to operate close to its thermal equilibrium better than does methanol but not as well as methane [2]. Tsiakaras and Demin [3] investigated performances

* Corresponding author. Tel.: +662 218 6868; fax: +662 218 6877.
E-mail address: Suttichai.A@chula.ac.th (S. Assabumrungrat).

1385-8947/$ – see front matter © 2006 Elsevier B.V. All rights reserved.
doi:10.1016/j.cej.2006.03.001

Nomenclature

a	inlet moles of ethanol (mol)
b	inlet moles of steam (mol)
c	extent of the electrochemical reaction of hydrogen (mol)
E	electromotive force of a cell (V)
F	Faraday constant (C mol^{-1})
ΔH^0	lower heating value of ethanol (J mol^{-1})
K	equilibrium constant of the hydrogen oxidation reaction (kPa$^{-0.5}$)
n_i	number of moles of component i (mol)
p_i	partial pressure of component i (kPa)
$p_{r,i}$	relative partial pressure of component i
q	electrical charge (A)
R	gas constant (J mol^{-1} K^{-1})
T	temperature (K)
U_f	operating fuel utilization (%)
$U_{f,i,}$	partial fuel utilization (%)
W	electrical work (W)
x	converted moles associated with reaction (1) (mol)
y	converted moles associated with reaction (2) (mol)
z	converted moles associated with reaction (3) (mol)

Greek letters

η	electrical efficiency (%)
φ	potential (V)

Subscripts

a	anode
c	cathode

of SOFCs *fuelled* by products from different ethanol processing; i.e. steam reforming, dry reforming, and partial oxidation with air. The product from ethanol steam reforming showed the highest maximum efficiency. Performances of external reforming SOFCs (ER-SOFC) fed by different fuels, e.g. methane, methanol, ethanol, and gasoline, were compared within a temperature range of 800–1200 K [4]. It was observed that at low temperatures, methane required a lower inlet steam:fuel ratio to prevent unfavorable coke formation than did methanol and ethanol. Nevertheless, at high temperatures the steam:fuel ratio at the limit of coke formation for ethanol was the same as for methane.

Although two types of electrolytes are possible for the SOFC operation, an oxygen ion conducting electrolyte is more commonly used than a proton conducting electrolyte. Until now, there are very few studies related to the use of the proton conducting electrolytes in SOFCs in the open literature [5–8]. In addition, all the studies of the ethanol-fed SOFCs employed only the oxygen ion conducting electrolyte. Demin et al. [7] reported an interesting result that an SOFC with a proton conducting electrolyte (SOFC-H^+) provides higher efficiency than an SOFC with an oxygen ion conducting electrolyte (SOFC-O^{2-}) for the system fed with methane. The comparison study was based on the same steam:methane feed ratio for both SOFC-O^{2-} and SOFC-H^+. It was demonstrated in our previous work that the steam requirement of SOFC-O^{2-} *is* lower than that of the SOFC-H^+ because water produced from the electrochemical reaction of hydrogen appears in the anode chamber [9]. Therefore, when the benefit from the lower steam requirement in SOFC-O^{2-} is taken into account, it is unclear whether the SOFC-H^+ still shows better performance than the SOFC-O^{2-}.

In this study, the theoretical performance of ethanol-fuelled SOFCs with two electrolytes in different modes of operation (i.e. plug flow (PF) and well-mixed (WM)) were investigated. Two feeding patterns of the PF mode (i.e. co-current (Co) and counter-current (CC)) were also considered. The efficiencies of SOFC-O^{2-} and SOFC-H^+ were compared, taking into account the benefit from the lower steam requirement for SOFC-O^{2-}. This is important in determining whether future SOFCs should be based on the use of the proton conducting electrolyte.

2. Theory

The reaction system involving the production of hydrogen via ethanol steam reforming can be represented by the following reactions [1]:

$$C_2H_5OH + H_2O = 4H_2 + 2CO \quad (1)$$

$$CO + H_2O = H_2 + CO_2 \quad (2)$$

$$CO + 3H_2 = CH_4 + H_2O \quad (3)$$

Previous results confirmed that a gas mixture at thermodynamic equilibrium contains only five components with noticeable concentration, e.g. carbon monoxide, carbon dioxide, hydrogen, steam, and methane [10,11].

Two types of solid electrolytes can be employed in the SOFC, i.e. oxygen ion and proton conducting electrolytes. The reactions taking place in the anode and the cathode can be summarized as follows.

Oxygen ion conducting electrolyte:

$$\text{anode}: H_2 + O^{2-} = H_2O + 2e^- \quad (4)$$

$$\text{cathode}: \tfrac{1}{2}O_2 + 2e^- = O^{2-} \quad (5)$$

Proton conducting electrolyte:

$$\text{anode}: H_2 = 2H^+ + 2e^- \quad (6)$$

$$\text{cathode}: 2H^+ + \tfrac{1}{2}O_2 + 2e^- = H_2O \quad (7)$$

The difference between both electrolyte types is the location of the water produced. With the oxygen ion conducting electrolyte, water is produced in the reaction mixture in the anode chamber. In the case of the proton conducting electrolyte, water appears on the cathode side. The theoretical number of moles of each component at equilibrium is given by the following expressions:

$$n_{EtOH} = a - x \quad (8)$$

$$n_{CH_4} = z \tag{9}$$

$$n_{CO} = 2x - y - z \tag{10}$$

$$n_{CO_2} = y \tag{11}$$

$$n_{H_2} = 4x + y - 3z - c \tag{12}$$

$$\begin{aligned} n_{H_2O} &= b + c - y + z \text{ (for oxygen ion conducting electrolyte)} \\ n_{H_2O} &= b - y + z \text{ (for proton conducting electrolyte)} \end{aligned} \tag{13}$$

$$n_{tot} = \sum_{i=1}^{6} n_i \tag{14}$$

The following three reactions are the most probable reactions which lead to carbon formation in the reaction system.

$$2CO = CO_2 + C \tag{15}$$

$$CH_4 = 2H_2 + C \tag{16}$$

$$CO + H_2 = H_2O + C \tag{17}$$

The reactions take place under a carbon-free condition when the carbon activities are less than one [10].

2.1. Electromotive force (EMF) calculations

The EMF of a cell is the maximum possible voltage, which drives charges around an electrical circuit in an SOFC. In practice, the actual voltage is less than this theoretical value due to activation, ohmic, and concentration losses. In this article, only the maximum possible voltage or EMF of the cell was considered, neglecting all losses. The EMF can be calculated from a difference in potentials between both electrodes in the cell as shown in Eq. (18).

$$E = |\varphi_c - \varphi_a| \tag{18}$$

where φ_c and φ_a are the potentials at the cathode and the anode, respectively. The electrode potential can be calculated using the Nernst equation. Since the electrochemical reactions at the electrodes are different, depending on the type of electrolyte, the potential can be expressed as:

$$\begin{aligned} \text{SOFC} - O^{2-} : E &= \frac{RT}{4F} \ln p_{r,O_2} \\ &= -\frac{\Delta G}{2F} - \frac{RT}{2F} \ln \frac{P_{H_2O,a}}{P_{H_2,a} P_{O_2,c}^{0.5}} \end{aligned} \tag{19}$$

$$\begin{aligned} \text{SOFC} - H^{+} : E &= \frac{RT}{2F} \ln p_{r,H_2} \\ &= -\frac{\Delta G}{2F} - \frac{RT}{2F} \ln \frac{P_{H_2O,c}}{P_{H_2,a} P_{O_2,c}^{0.5}} \end{aligned} \tag{20}$$

where p_{r,O_2} and p_{r,H_2} are relative oxygen partial pressure and relative hydrogen partial pressure, respectively, R the universal gas constant, T the absolute temperature, F the Faraday's constant, ΔG the Gibb's free energy and P_i the partial pressure of component i. The second terms of the right-hand side expression of Eqs. (19) and (20) are the Nerstian term comprising the partial pressure of hydrogen, oxygen, and steam. It should be noted that the partial pressures of steam for the SOFC-H^+ and the SOFC-O^{2-} represent the values at the anode and the cathode, respectively.

Typically, conventional SOFC operations are close to plug flow mode in which the gas compositions vary along the length of the cell. However, SOFCs can be operated under a well-mixed mode by using a high recycle rate. In the PF mode, the feeding pattern of fuel and air to the SOFC stack affects the composition distribution and, consequently the, EMF distribution along the SOFC cell. Two feeding patterns (i.e. co-current and counter-current) were considered in this study. An average EMF ($\overline{E}$) in the PF mode can be determined by the numerical integration of EMF along the stack. It should be noted that the EMF also depends significantly on the inlet H_2O:EtOH ratio, operating temperature, and the fuel and air utilizations. To simplify the calculations, it was assumed that the gas compositions in the anode are at their equilibrium compositions along the stack. Deviation from this equilibrium condition would result in lower SOFC EMF values as less hydrogen was generated in the anode chamber to compensate for the hydrogen consumed by the electrochemical reaction. Therefore, the results shown in this work represent the best performances for all SOFC cases. Details of the calculations of the equilibrium composition were presented in our previous work [9]. It should be noted that our calculations were compared with the results of Hernandez-Pacheco et al. [12] and found to be in good agreement. Using the same operating conditions ($U_f = 80\%$, $T = 1200$ K and 100% hydrogen feed) our calculations gave an EMF of approximately 0.92 V whereas Hernandez obtained 0.9 V.

2.2. SOFC efficiency

When a current is drawn from the SOFC, the maximum work produced by the SOFC can be calculated using the following equation:

$$W = q\overline{E} \tag{21}$$

where W is the electrical work from the SOFC and q is an electrical charge passing through the electrolyte. The electrical efficiency is defined as the ratio of electrical work produced by the SOFC to the chemical energy of fuel fed to the SOFC. Therefore, the maximum SOFC efficiency is obtained from in the following equation:

$$\eta = \frac{q\overline{E}}{-\Delta H^0} \times 100\% \tag{22}$$

where $-\Delta H^0$ is lower heating value of ethanol at standard conditions.

3. Results and discussion

The influences of the mode of operation (plug flow and well-mixed), feeding pattern (co-current and counter-current) and

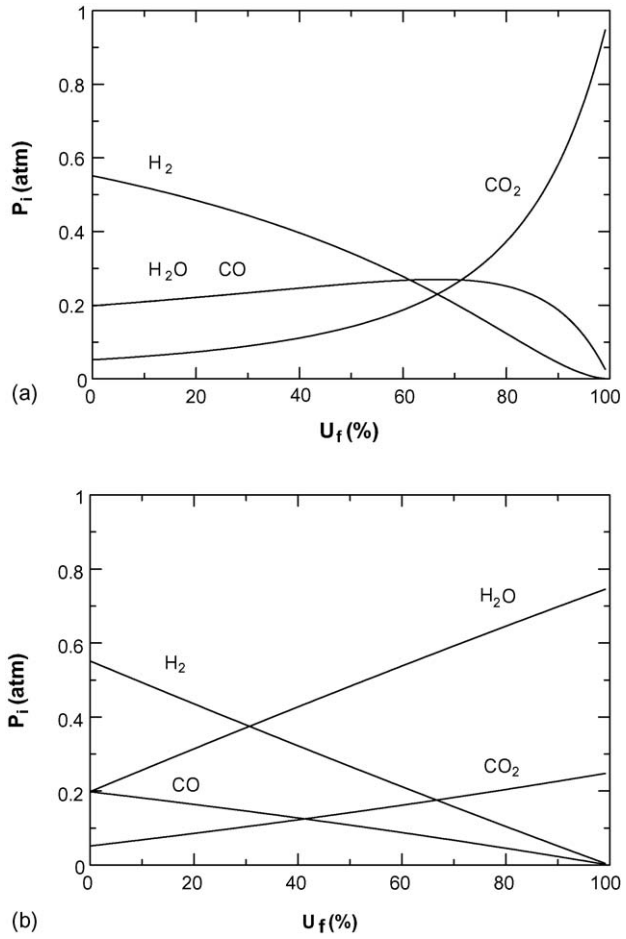

Fig. 1. Anode components' partial pressure at different fuel utilization for SOFCs with different types of electrolytes: (a) H^+ electrolyte and (b) O^{2-} electrolyte (inlet H_2O:EtOH = 3, T = 1200 K, P = 101.3 kPa, 400% excess air).

type of electrolyte on the partial pressure of each component along the cell are studied. Fig. 1 shows the anode components' partial pressure at different fuel utilizations (U_f) defined as the moles of hydrogen consumed by the electrochemical reaction divided by the maximum number of moles of hydrogen produced from ethanol (6 mol of hydrogen:1 mol of ethanol). The inlet H_2O:EtOH ratio is at the stoichiometic value of 3 and the temperature is 1200 K. For the WM mode, the partial pressure along the cell is equal to the value at the exit U_f due to the well-mixed condition. In contrast, in the PF mode, the composition change along the cell is represented by the partial pressure profiles from U_f of 0 to the exit U_f. The type of electrolyte has a significant effect on the anode partial pressure as shown in Fig. 1(a) and (b). The partial pressure of steam for the SOFC-H^+ and SOFC-O^{2-} are considerably different due to the different location of steam generation. In the SOFC-H^+ case, the partial pressure of steam increases slightly with increasing U_f because the total moles in the anode chamber decreases as hydrogen is consumed. However, at high fuel utilizations, the partial pressure of steam drops significantly because the hydrogen consumption shifts the water–gas shift reaction and results in higher carbon dioxide production as shown in Fig. 1(a). In contrast, for the SOFC-O^{2-} case, the partial pressure of steam increases dramatically over the entire anode chamber due to the major effect of electrochemical steam production at the anode side. The partial pressure of hydrogen in the SOFC-H^+ case is higher than that in the SOFC-O^{2-} case because there is no dilution effect of the electrochemical steam at the anode side in the SOFC-H^+ case. It should be noted that there is a negligible amount of ethanol and methane observed from the calculations due to the complete reforming reaction and insignificant methanation at this operating temperature.

As mentioned in the previous section, two feeding patterns (i.e. SOFC-(PF-Co) and SOFC-(PF-CC)) were considered for the PF mode. No difference in the profile of anode components' partial pressure for different feeding patterns was observed because it was assumed in our calculations that all anode components are in equilibrium which relates to the fuel utilization (U_f) along the anode chamber. Therefore, at the same operating fuel utilization the profiles of anode components in both feeding patterns are similar. In other words, the feeding patterns have no effect on the profile of anode components' partial pressure for both electrolytes.

The influence of mode of operation, feeding pattern, and type of electrolyte on the cathode components' partial pressure at various fuel utilizations are shown in Fig. 2. The partial pressure of oxygen in the SOFC-H^+ case is always lower than that in the SOFC-O^{2-} case due to the presence of the electrochemical steam at the cathode for the SOFC-H^+. However, the differences are not significant due to high value of excess air (400%) used in the calculations. It should be noted that 300–600% excess air is commonly used in SOFC operations for good heat management in SOFC cell stacks [13]. The mode of operation and feeding pattern show a slight impact on the partial pressure of oxygen in the cathode. For the SOFC (PF-Co) cases, air is fed cocurrently with the fuel. The partial pressure of oxygen decreases whereas the partial pressure of steam increases (for the SOFC-H^+ case) with increasing fuel utilization. The partial pressure profiles within the cell of the SOFC (PF-Co) cases are represented by the partial pressures between the fuel utilization at 0 and the exit U_f; however, those of the SOFC (WM) correspond to the value at the exit fuel utilization. In contrast, for the SOFC (PF-CC), air is introduced to the cathode entrance located at the exit of the anode stream and, therefore, the partial pressure profile is different among different fuel utilizations. The partial pressure of oxygen in the cathode is 0.21 atm at the entrance to the cathode side and decreases along the cathode chamber until the cathode exit located at the entrance of the anode feed.

From the obtained partial pressure profiles, the EMF at different fuel utilization for all SOFCs can be calculated using Eqs. (18) and (19). From Fig. 3, it is shown that the EMF distributions in all SOFC-H^+ cases are higher than those in all SOFC-O^{2-} cases. This can be explained by considering the partial pressure of components involved in the Nerstian term of Eqs. (19) and (20). Because the partial pressure of hydrogen in the anode for the SOFC-H^+ case is higher than that for the SOFC-O^{2-} case due to no dilution effect of the electrochemical steam at the anode side in the SOFC-H^+ case and the partial pressure of steam in the cathode side for the SOFC-H^+ case is much lower than that in the anode side for the SOFC-O^{2-} case

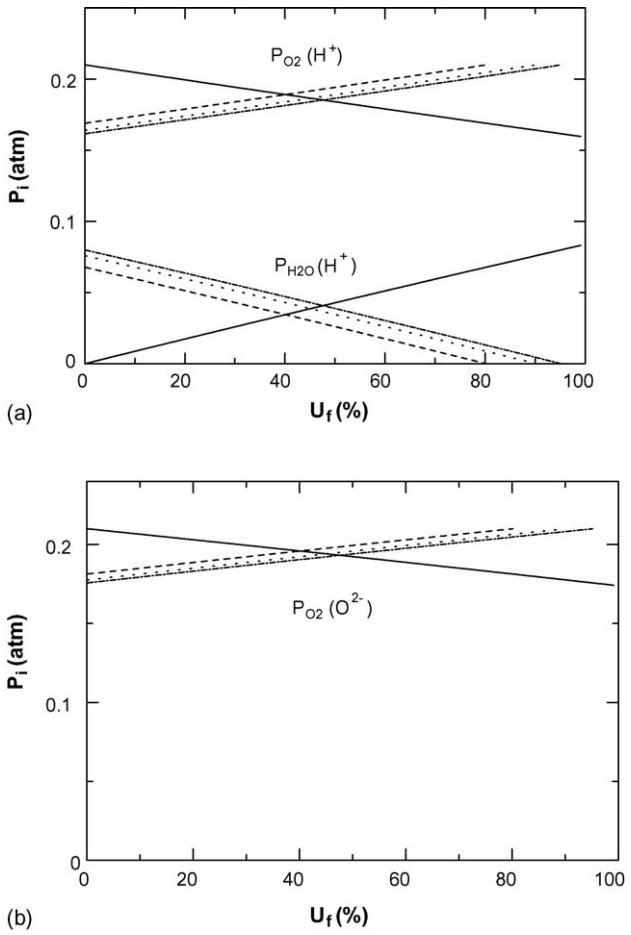

Fig. 2. Cathode components' partial pressure at different fuel utilization for SOFCs with different types of electrolytes for co-current (solid line) and counter-current at 80% U_f (dashed line), 90% U_f (dotted line), 95% U_f (dashed dotted line): (a) H^+ electrolyte and (b) O^{2-} electrolyte (inlet H_2O:EtOH = 3, T = 1200 K, P = 101.3 kPa, 400% excess air).

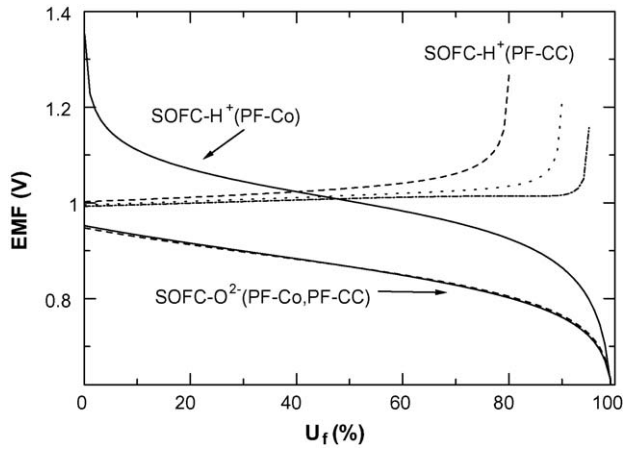

Fig. 3. EMF distribution along the SOFC-O^{2-} and SOFC-H^+ operated under PF and WM modes for co-current (solid line) and counter-current at 80% U_f (dashed line), 90% U_f (dotted line), 95% U_f (dashed dotted line): (a) H^+ electrolyte and (b) O^{2-} electrolyte (inlet H_2O:EtOH = 3, T = 1200 K, P = 101.3 kPa, 400% excess air).

(see Figs. 1 and 2), the Nerstian term of the SOFC-O^{2-} case shows a more negative value than that in the SOFC-H^+ case, and consequently, the SOFC-H^+ cell gives a higher EMF than does the SOFC-O^{2-} cell. It should be noted that the partial pressures of oxygen in the cathode for both SOFCs are not taken into account in the Nerstian term comparison due to the use of excess air in the operation. The result confirms that the SOFC-H^+ cell has a higher performance than the SOFC-O^{2-} cell when the steam:fuel feed ratio is the same as reported earlier in other system [7]. From Fig. 3, it is noticed that the feeding pattern has a significant impact on the EMF distribution in the SOFC-H^+ cell whereas only a slight effect is observed in the SOFC-O^{2-} cell. For the SOFC-H^+ case, the value of EMF is strongly dependent on both the partial pressures of oxygen and steam in the cathode. The components' partial pressures in the anode are not considered as they are similar for both feeding patterns as mentioned earlier. The feeding pattern significantly impacts the partial pressure profile of steam in the cathode as shown in Fig. 2(a) and, therefore, the EMF distribution is different with different feeding patterns. For the SOFC-O^{2-} case, the value of the EMF depends on the partial pressure of oxygen in the cathode, but it is not significantly dependent on the feeding pattern due to the high excess air. Consequently, with the same partial pressure profile in the anode, partial pressure profile of oxygen in the cathode for both feeding patterns and nearly identical, the observed values of the EMF are almost the same. The average value of the EMF for the SOFC (PF) can be obtained by the numerical calculation of the EMF distribution, while the EMF of SOFC (WM) can be achieved directly from the value at the corresponding fuel utilization. At 80% operating fuel utilization, the SOFC-H^+(WM) and the SOFC-O^{2-}(WM) yield EMF of 0.92 and 0.80 V, respectively, whereas the average values of the EMF are 1.03 and 0.89 V for the SOFC-H^+(PF) and the SOFC-O^{2-}(PF), respectively. It was found that the feeding pattern has no significant effect on the average EMF for both electrolytes although the EMF distributions are different. The average EMF of SOFCs at a inlet H_2O:EtOH ratio of 3 and 80% fuel utilization can be ordered as follows SOFC-H^+(PF-Co) ≈ SOFC-H^+(PF-CC) > SOFC-H^+(WM) > SOFC-O^{2-}(PF-Co) ≈ SOFC-O^{2-}(PF-Co) > SOFC-O^{2-}(WM).

Fig. 4(a) and (b) show the comparative results of average EMF and efficiency of SOFCs for various fuel utilizations, respectively. From Fig. 4(a), it is clear that the SOFC-H^+ provides greater EMF than the SOFC-O^{2-} for both PF and WM modes. Furthermore, it can be noticed that the WM mode results in a lower EMF than the PF mode for both electrolytes because the partial pressure of hydrogen in the WM mode is kept at its lowest value along the cell. In addition, there is no effect of feeding patterns on the average EMF in SOFCs although EMF distribution in both feeding patterns is different.

The electrochemical efficiency, η, is one indicator to identify the performance of fuel cells. The efficiency calculated from Eq. (22) is shown in Fig. 4(b). The efficiency increases in sequence SOFC-H^+(PF) > SOFC-H^+(WM) > SOFC-O^{2-}(PF) > SOFC-O^{2-}(WM); however, at high fuel utilization, the SOFC-O^{2-}(PF) case shows a higher efficiency than the SOFC-H^+(WM) case. It is obvious that under

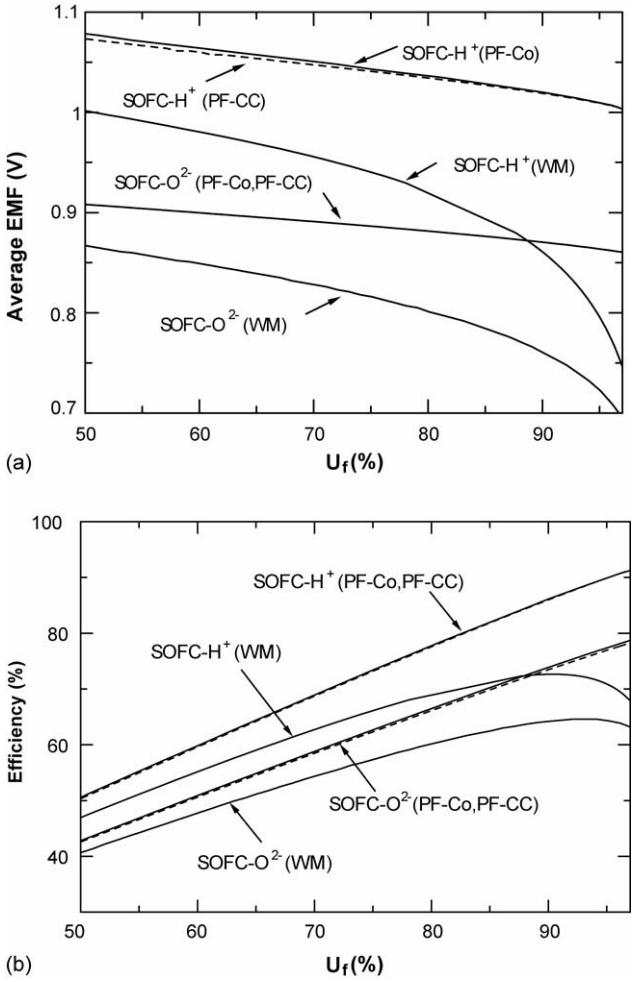

Fig. 4. Performances of SOFC-O^{2-} and SOFC-H^+ operated under PF and WM modes: (a) average EMF and (b) efficiency (inlet H_2O:EtOH = 3, T = 1200 K, P = 101.3 kPa, 400% excess air).

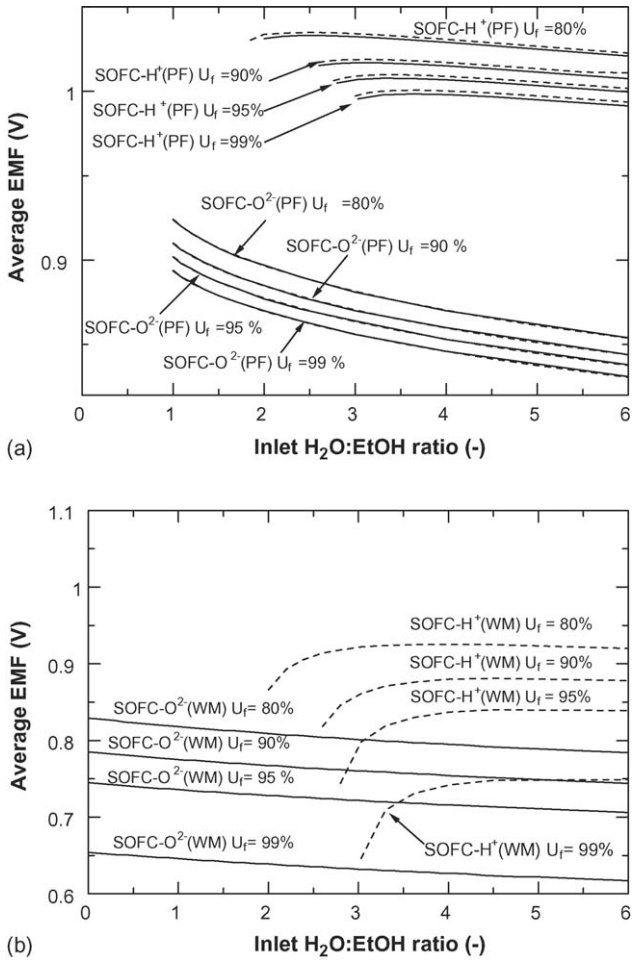

Fig. 5. Influence of inlet H_2O:EtOH ratio on SOFCs average EMF at different values of fuel utilization: (a) PF mode and (b) WM mode (T = 1200 K, P = 101.3 kPa, 400% excess air).

the same operation mode, the SOFC-H^+ cell is superior to the SOFC-O^{2-} cell. This is in good agreement with the previous work [7] which reported that the SOFC-H^+ case gives a maximum efficiency 15% higher than that of the SOFC-O^{2-} case in the range of inlet H_2O:CH_4 ratio of 2.0–3.0. Furthermore, it can be noticed that the feeding pattern has no influence on the calculated efficiency of SOFCs for both types of electrolyte.

It was reported in our previous study [9] that the SOFC-O^{2-} cell can be operated at much lower inlet H_2O:EtOH ratios than the SOFC-H^+ cell due to the difference in location of water production. Therefore, in order to compare the performance of SOFCs with different electrolyte types, it is necessary to take this SOFC-O^{2-} benefit into account in the calculations. The influence of the inlet H_2O:EtOH ratio on EMF and efficiency of SOFCs is investigated.

Figs. 5 and 6 show the influence of the inlet H_2O:EtOH ratio on the EMF and efficiency of SOFCs at different fuel utilizations. The inlet H_2O:EtOH ratio is considered only in the range where carbon formation is thermodynamically infeasible. The minimum ratio for the SOFC-O^{2-}(WM) and SOFC-O^{2-}(PF) cells is almost 0 and 1, respectively. However, the minimum ratio is higher for the SOFC-H^+ cell particularly at high fuel utilization for both modes of operation. The SOFC-O^{2-}(WM) cell can be operated without steam input because steam is produced from the electrochemical reaction of hydrogen. It should be noted that some steam is still needed in the feed during the start-up period before the cell can be self-sustaining. For both SOFC-O^{2-}(PF) and SOFC-O^{2-}(WM) cases, the EMF and efficiency decrease with increasing inlet H_2O:EtOH ratio. Therefore, their highest values are at the limit of carbon formation for each value of the fuel utilization. This indicates that the introduction of steam into the cell decreases the EMF and efficiency due to hydrogen dilution. In the SOFC-H^+(WM) and SOFC-H^+(PF) cases, the minimum inlet H_2O:EtOH ratios are 1.9 and 3.2 at 80 and 90% fuel utilization, respectively. The greater fuel utilization requires greater steam input. This is consistent with our previous work [9]. From Figs. 5 and 6, it is found that there is an optimum steam input in the SOFC-H^+ for both modes of operation at each fuel utilization. The introduction of steam initially increases the EMF and efficiency but has the negative effect at higher values. An appropriate inlet H_2O:EtOH ratio should be selected because steam is essential for the hydrogen production from the ethanol steam reforming but, on the other hand, it also acts as a diluent in the system. All optimum points found for

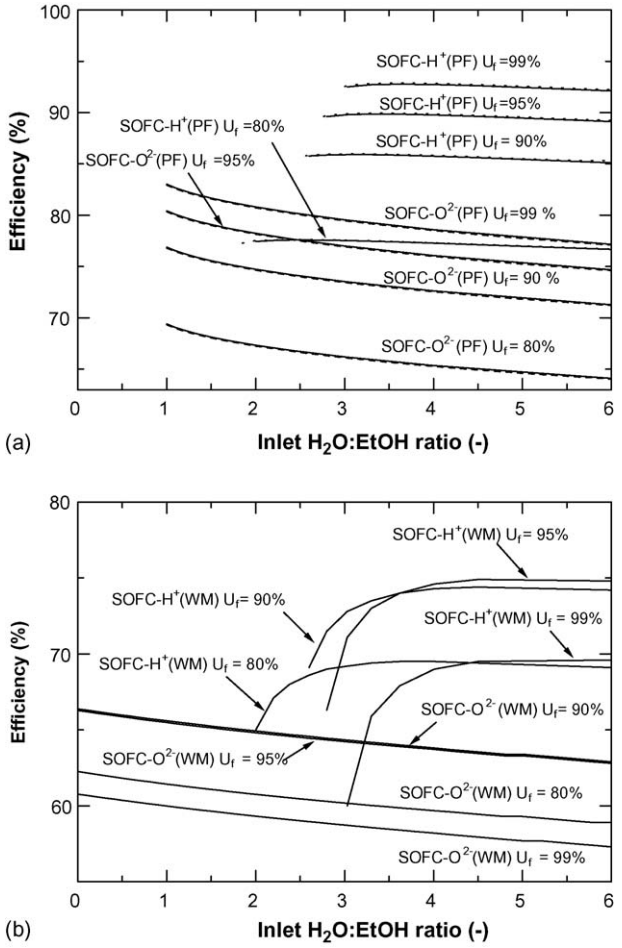

Fig. 6. Influence of inlet H_2O:EtOH ratios on SOFCs efficiency at different values of fuel utilization: (a) PF mode and (b) WM mode ($T = 1200$ K, $P = 101.3$ kPa).

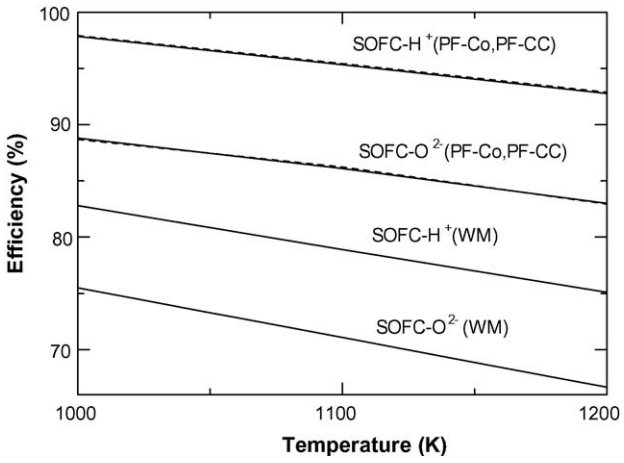

Fig. 7. Maximum efficiency of SOFC-O^{2-} and SOFC-H^+ at different operating temperatures ($P = 101.3$ kPa, 400% excess air).

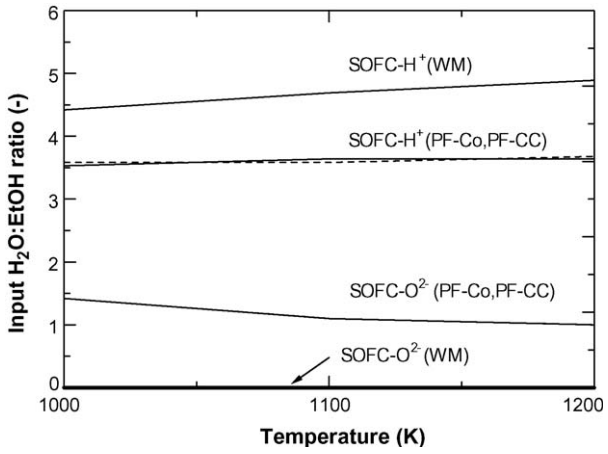

Fig. 8. Inlet H_2O:EtOH ratio at maximum efficiency ($P = 101.3$ kPa, 400% excess air).

each value of fuel utilization are beyond the limit of carbon formation. Furthermore, it is confirmed that there is no influence of feeding patterns on the EMF and efficiency for all ranges of the inlet H_2O:EtOH ratio.

By performing the calculations at various values of inlet H_2O:EtOH ratio and fuel utilization, it is possible to determine the maximum efficiency and the corresponding conditions for both SOFC-O^{2-} and SOFC-H^+ cells at each temperature level as shown in Figs. 7–9. It is obvious that the maximum SOFC efficiency follows the sequence of SOFC-H^+(PF) > SOFC-O^{2-}(PF) > SOFC-H^+(WM) > SOFC-O^{2-}(WM) for all temperatures (1000–1200 K). The maximum efficiency for all cases decreases with increasing temperature. This is consistent with the decrease in the EMF due to Gibb's free energy. The corresponding inlet H_2O:EtOH ratio is always approximately 0 for the SOFC-O^{2-}(WM). For the SOFC-O^{2-}(PF), the corresponding ratio is about 1.4 and 1 at 1000 and 1200 K, respectively. In the case of the proton conducting electrolyte, the SOFC-H^+(PF) requires a lower inlet H_2O:EtOH ratio than the SOFC-H^+(WM). For the SOFC-H^+(PF), the corresponding inlet H_2O:EtOH ratio is about 3.5 at 1000 K and increases with increasing temperature. While that for the SOFC-H^+(WM), is about 4.4 at 1000 K and also increases when operating temperature increases. This is probably because the water–gas shift reaction is exothermic and therefore more steam is required to move the reaction to the right to produce hydrogen. The corresponding fuel utilization at the maximum efficiency of the SOFC (PF) for both electrolytes is almost constant at approximately 99% but it slightly decreases

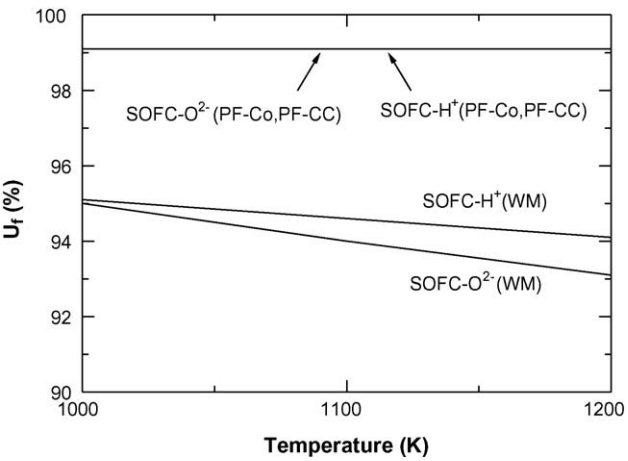

Fig. 9. Fuel utilization at maximum efficiency ($P = 101.3$ kPa, 400% excess air).

for the SOFC (WM) in both electrolytes when the temperature increases from 1000 to 1200 K.

From the above studies, it was found that although the benefit of lower steam requirement in the SOFC-O^2 is taken into account in the calculations, the SOFC-H^+ cell still shows higher efficiency than the SOFC-O^{2-} cell. This implies that the development of SOFCs should be directed to the use of a proton conducting electrolyte.

4. Conclusions

Thermodynamic analysis of ethanol-fuelled SOFCs using proton and oxygen ion conducting electrolytes in different modes of operation (plug flow and well-mixed) and feeding patterns (co-current and counter-current) has been presented in this article. At stoichiometric inlet H_2O:EtOH ratios, the SOFC-H^+(PF) provides the highest EMF and efficiency among various electrolytes and modes of operation. In order to compare the theoretical performances of SOFCs with different electrolytes, the benefit of reduced inlet steam requirement for the oxygen ion conducting electrolyte is taken into account.

It was demonstrated from the theoretical calculations assuming no polarization losses that the use of proton conducting electrolytes is more attractive than the use of oxygen ion conducting electrolytes. The SOFC-H^+(PF) gives the highest efficiency. Moreover, it was found that there is no influence of the feeding patterns on the average EMF and efficiency even though the EMF distribution along the cell is different.

Although the proton conducting electrolyte seems to be the most appropriate one for use in a solid oxide fuel cell from the theoretical calculations, it has a higher resistance than that of oxygen ion conducting electrolyte. If the ohmic loss of the electrolyte and other losses are considered, proton conducting electrolyte might perform worse than oxygen ion conducting electrolyte. If the overall resistance of proton conducting electrolyte could be reduced to be comparable with the oxygen ion conducting electrolyte, the proton conducting electrolyte is recommended as the most interesting electrolyte in the future. More details of the electrolyte selection including all resistances (i.e. ohmic loss and activation loss) must be calculated and justified.

Acknowledgements

The support from the Thailand Research Fund, Commission on Higher Education, and National Metal and Materials Technology Center are gratefully acknowledged.

References

[1] S. Freni, G. Maggio, S. Cavallaro, Ethanol steam reforming in a molten carbonate fuel cell: a thermodynamic approach, J. Power Sources 62 (1996) 67–73.
[2] G. Maggio, S. Freni, S. Cavallaro, Light alcohols/methane fuelled molten carbonate fuel cells: a comparative study, J. Power Sources 74 (1998) 17–23.
[3] T. Tsiakaras, A. Demin, Thermodynamic analysis of solid oxide fuel cell system fueled by ethanol, Chem. Eng. Sci. 102 (2001) 210–217.
[4] S.L. Douvartzides, F.A. Coutelieris, A.K. Demin, P.E. Tsiakaras, Fuel options for solid oxide fuel cell: a thermodynamic analysis, AIChE J. 49 (2003) 248–257.
[5] A. Demin, P. Tsiakaras, Thermodynamic analysis of a hydrogen fed solid oxide fuel cell based on a proton conductor, Int. J. Hydrogen Energy 26 (2001) 1103–1108.
[6] R. Salar, H. Taherparvar, I.S. Metcalfe, M. Sahibzada, SOFCs Based on $SrCe_{0.95}Yb_{0.05}O_3$ Proton Conductor, in 2001 Joint International Meeting—the 200th Meeting of The Electrochemical Society Inc. and the 52nd Annual Meeting of the International Society of Electrochemistry, San Francisco, California, 2001.
[7] A.K. Demin, P.E. Tsiakaras, V.A. Sobyanin, S.Yu. Hramova, Thermodynamic analysis of a methane fed SOFC system based on a protonic conductor, Solid State Ionics 152–153 (2002) 555–560.
[8] T. Shimada, C. Wen, N. Taniguchi, J. Otomo, H. Takahashi, The high temperature proton conductor $BaZr_{0.4}Ce_{0.4}In_{0.2}O_{3-\alpha}$, J. Power Sources 131 (2004) 289–292.
[9] S. Assabumrungrat, V. Pavarajarn, S. Charojrochkul, N. Laosiripojana, Thermodynamic analysis for solid oxide fuel cell with direct internal reforming fueled by ethanol, Chem. Eng. Sci. 59 (2004) 6015–6020.
[10] E.Y. Garcia, M.A. Laborde, Hydrogen production by the steam reforming of ethanol: thermodynamic analysis, Int. J. Hydrogen Energy 16 (1991) 307–312.
[11] K. Vasudeva, N. Mitra, P. Umasankar, S.C. Dhinggra, Steam reforming of ethanol for hydrogen production: thermodynamic analysis, Int. J. Hydrogen Energy 21 (1996) 13–18.
[12] E. Hernandez-Pacheco, D. Singh, P.N. Hutton, N. Patel, M.D. Mann, J. Power Sources 138 (2004) 174.
[13] K.W. Bedringas, I.S. Ertesvag, S. Byggstoyle, B.F. Magnussen, Energy analysis of solid-oxide fuel cell (SOFC) systems, Energy 22 (1997) 403–412.

Appendix 2

Performance Assessment of Bioethanol-Fed Solid Oxide Fuel Cell System Integrated with a Distillation Column

W. Jamsak[a], S. Assabumrungrat[a,†], P.L. Douglas[b,†], E. Croiset[b], N. Laosiripojana[c], R. Suwanwarangkul[d] and S. Charojrochkul[e]

[a] Center of Excellence in Catalysis and Catalytic Reaction Engineering, Department of Chemical Engineering, Faculty of Engineering, Chulalongkorn University, Thailand
[b] Department of Chemical Engineering, University of Waterloo, Canada
[c] The Joint Graduate School of Energy and Environment, King Mongkut's University of Technology Thonburi, Thailand
[d] Sirindhorn International Institute of Technology, Thammasat University, Thailand
[e] National Metal and Materials Technology Center (MTEC), Thailand
([†] Corresponding authors: suttichai.a@chula.ac.th or pdouglas@cape.uwaterloo.ca)

This paper investigated the performance of a bioethanol-fed Solid Oxide Fuel Cell (SOFC) system integrated with a distillation column (SOFC-D). Excess heat from the SOFC system was directly utilized in the distillation column where bioethanol (5 mol%) was purified to a desired concentration before feeding to the SOFC system consisting of an air heater, an ethanol/water heater, a reformer, an SOFC preheater, an SOFC stack and an afterburner. The SOFC-D system was simulated using Aspen Plus^{TM} for the distillation portion and Matlab^{TM} for the SOFC portion. The effects of operating parameters; i.e., ethanol concentration, ethanol recovery, fuel utilization and operating voltage on the performance and energy involved in the SOFC-D system (e.g. distillation energy: Q_D and the net exothermic heat of the SOFC system: $Q_{SOFC,Net}$) were examined. In addition, the performance of the SOFC-D system at the energy sufficient point where $Q_D = Q_{SOFC,Net}$ was considered. The integration of the distillation column with the SOFC system was found to offer superior SOFC performance. The ethanol recovery and fuel utilization significantly influenced the overall electrical efficiency and power density. Quite low performances are obtained when one operated the SOFC-D without an external heat source. The maximum overall efficiency and power density (~35% and 0.22 W cm^{-2}) occured at an ethanol recovery of 80% and U_f of 90%.

Introduction

A Solid Oxide Fuel Cell (SOFC) is considered to be an attractive power generation system nowadays. With high operating temperatures, it offers a wide range of applications, potential operation with an internal reformer and high system efficiency. Usually, an SOFC system consists of preheaters, a reformer, an SOFC stack and an afterburner. It has been known that there is always excess heat available when operating the SOFC system due to the presence of cell irreversibility and unreacted fuels. Therefore, most of SOFC systems are usually combined with other units to enhance the overall

efficiency. Two major integrated SOFC systems under current attention are SOFC-GT (gas turbine) and SOFC-CHP (combined heat and power). From an environmental point of view, bioethanol is an attractive green fuel which can be derived from renewable resources. It is also safe and easy to store and handle (1). Most studies on ethanol-fed SOFC systems are based on a feed containing a mixture of pure ethanol and water (2, 3). This operation is not efficient for an energy point of view because energy is consumed to purify bioethanol to pure ethanol which is subsequently mixed with water before feeding to the SOFC systems.

Therefore, in this study, the new ethanol-fed SOFC system is purposed. A distillation column is integrated with the SOFC system (SOFC-D) to purify bioethanol, which is typically available at about 5 mol%, to a desired concentration before feeding to the SOFC system. With this operation, the additional energy for producing pure ethanol is avoided and the excess heat from the SOFC system can be directly utilized in the distillation column. The paper is aimed at investigating the effects of distillation operating parameters (i.e. ethanol recovery and ethanol concentration) and SOFC operating parameters (i.e. fuel utilization and voltage) on the performance of the SOFC-D system.

SOFC system modelling

In this study, the SOFC system consisted of three heaters (an EtOH/H_2O vaporizer (Heater-1), an air heater (Heater-2) and an anode preheater (Heater-3)), a fuel cell stack, an external reformer and an afterburner. A distillation column was integrated with the SOFC system as presented in Figure 1. Bioethanol (5 mol%) was fed to the distillation column and the distillate with desired ethanol concentration and recovery was then fed to the SOFC system. A distillation column with equilibrium stages, a total condenser and a kettle reboiler was chosen. The feed stream was introduced at the stage above the reboiler. The *Radfrac* rigorous equilibrium stage module in *Aspen Plus*^{TM} was used for simulating the column and determining the heat duties in the condenser and reboiler, Q_C and Q_D respectively.

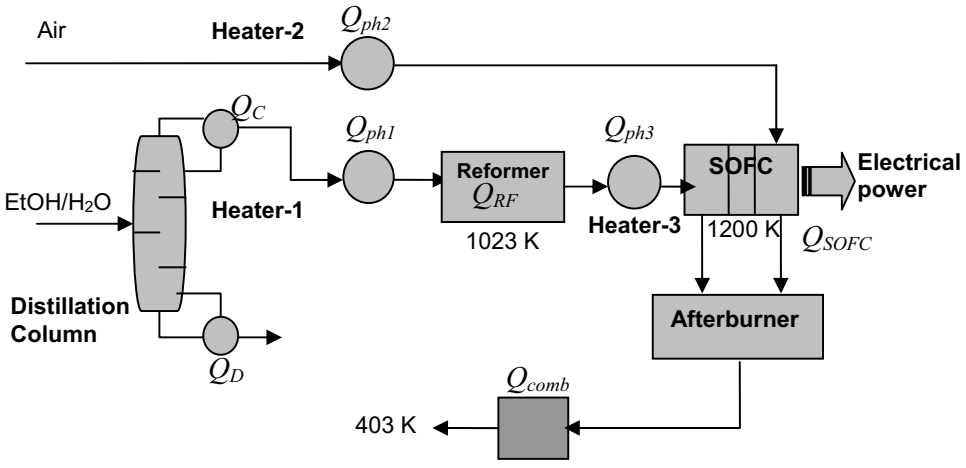

Figure 1. Schematic diagram of SOFC-D.

The minimum heat duty in the reboiler (Q_D) was obtained by varying number of stages and the reflux ratio. The distillate with a desired ethanol concentration was then heated to the reforming temperature (T_{RF}), in this case 1023 K, and reformed to generate a hydrogen-rich product, assuming that the reactions take place in an external reformer at equilibrium. The product was then heated to the SOFC temperature (T_{SOFC}) of 1200 K and introduced to the anode of the SOFC stack. In the SOFC stack, only the water gas shift reaction and electrochemical reactions were considered due to the complete ethanol reforming reaction in the reformer at high temperature. The reformer and the SOFC stack were assumed to operate under isothermal conditions and, therefore, Q_{RF} and Q_{SOFC} were involved in the reformer and the stack, respectively. Air (380% excess) was fed to the cathode chamber. In this study, the SOFC cell configuration was based on the tubular design (4). For activation losses, Achenbach's semi empirical correlation (9) was used to predict activation overpotentials for the anode and cathode. It should be noted that the chosen T_{SOFC} of 1200 K was within the accurate temperature range for Achenbach's correlation (5). The equations used in calculations are presented as follows.

$$V = E - i(r_{ohm} + r_{act}) \quad [1]$$

$$E = \frac{RT}{4F} \ln \frac{p_{O_2,c}}{p_{O_2,a}} \quad [2]$$

$$r_{act,c} = \left[\frac{4F}{RT} k (x_{O_2,c})^m \exp\left(-\frac{E_{a,c}}{RT} \right) \right]^{-1} \quad [3]$$

$$r_{act,a} = \left[\frac{2F}{RT} k (x_{H_2,a})^m \exp\left(-\frac{E_{a,a}}{RT} \right) \right]^{-1} \quad [4]$$

$$r_{ohm,i} = \rho_i \delta_i \quad [5]$$

$$P = iV \quad [6]$$

$$\eta_{elec,ov} = \frac{P}{n_{EtOH} * LHV_{EtOH}} \quad [7]$$

where E is the electromotive force of the cell, V the operating voltage, i the current density, R the gas constant, T the temperature, F the Faraday's constant, r_{act} the activation resistance, E_a the activation energy at the electrodes, $x_{O_2,c}$ and $x_{H_2,a}$ the mole fractions of oxygen in the cathode chamber and hydrogen in the anode chamber, respectively, r_{ohm} the ohmic resistance, ρ the resistivity of material, subscript i represents cell component, P the power density of the cell, n_{EtOH} the total ethanol flow rate fed to the distillation column, LHV_{EtOH} the low heating value of ethanol and $\eta_{elec,ov}$ the overall electrical efficiency. For calculating the SOFC performance, it was assumed that fuel and oxidant were well-diffused through the surface of the electrodes. Therefore, concentration loss could be omitted. Procedures for calculating composition and average EMF within SOFC stack were given in our previous works (6, 7). The values of parameters for the ohmic loss and activation polarization were adopted from the literature (4) and (5), respectively.

The effluent from the anode and the cathode were burnt in the afterburner in order to provide heat to the reformer (Q_{RF}), the EtOH/H_2O heater (Q_{ph1}), the air heater (Q_{ph2}) and

the anode preheater (Q_{ph3}). It should be noted that the heat of combustion (Q_{comb}) in the afterburner was calculated based on the exhaust gas temperature of 403 K. The values of energy involved in each unit can be determined from conventional energy balance calculations. The net exothermic heat from the SOFC part after transferring heat to the three heaters and the reformer ($Q_{SOFC,Net}$) can be calculated from Equation (8).

$$Q_{SOFC,Net} = Q_{SOFC} + Q_{Comb} - Q_{ph1} - Q_{ph2} - Q_{ph3} - Q_{RF} \quad [8]$$

Results and Discussion

Effects of ethanol concentration and recovery on SOFC performance

The effect of ethanol concentration (C_{EtOH}) on SOFC performance is shown in Figure 2. The cell is operated at T_{SOFC} = 1200 K, U_f = 80% and EtOH recovery = 90%. The range of ethanol concentration is between 5 and 41 mol%. The former value represents the concentration of bioethanol while the latter represents the boundary of carbon formation (7). Operation at higher concentrations is not recommended as deactivation of the reforming and anode catalysts by carbon formation are possible. The results indicate that the SOFC performance can be improved when the SOFC system is operated with a feed of high ethanol concentration since the presence of excessive amount of water in the feed lowers the hydrogen concentration, resulting in lower cell potential, power density and electrical efficiency.

When the distillation column is operated at different ethanol recoveries, different amounts of ethanol are introduced to the SOFC system. It is therefore not surprising, as shown in Figure 3, that the overall electrical efficiency decreases with the decreasing ethanol recovery. From the results, it is obvious that the operation of the SOFC system with a direct feed of bioethanol is not practical due to the low SOFC performance. The bioethanol should be purified to a higher concentration at high ethanol recovery prior to feeding to the SOFC system.

(a)

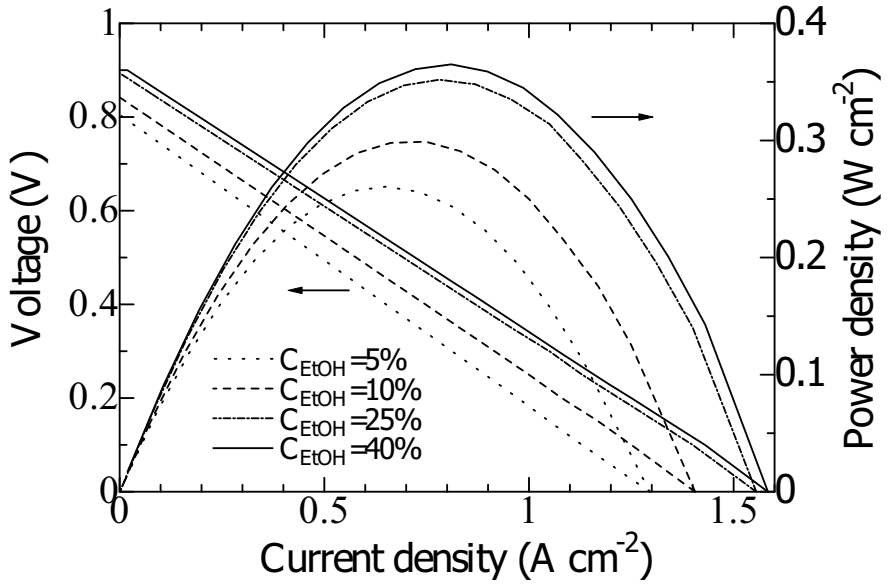

(b)

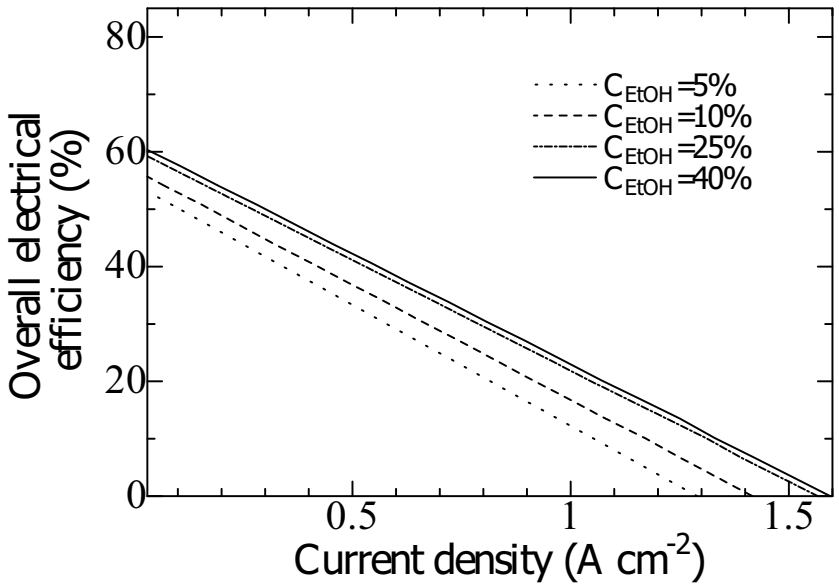

Figure 2. Effect of ethanol concentration on electrical performance: a) voltage and power density and b) overall electrical efficiency (EtOH recovery = 90%, U_f = 80%, P = 101.3 kPa).

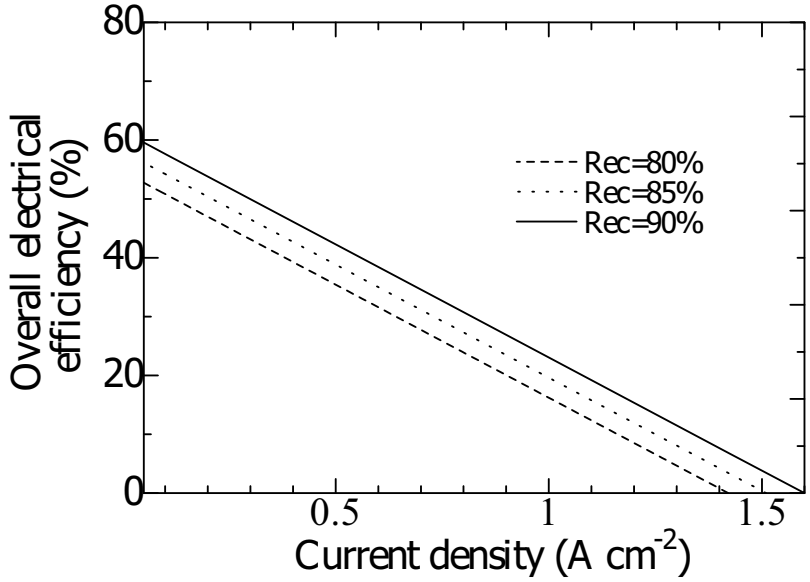

Figure 3. Effect of ethanol recovery on overall electrical efficiency (C_{EtOH} = 25% mol, U_f = 80%, P = 101.3 kPa).

Effects of ethanol concentration and recovery on energy involved in the SOFC-D system

Although the integration of the distillation column with the SOFC system is proven to offer superior SOFC performance, the energy involved in the overall SOFC-D system is another important issue of consideration for determining the potential use of the SOFC-D system. Figure 4 shows the effects of ethanol concentration and recovery on the distillation energy required for a reboiler (Q_D) and the net exothermic heat of the SOFC system ($Q_{SOFC,Net}$) operated at V = 0.7 V, U_f = 80%, T_{SOFC} =1200 K. From the results, it can be seen that both Q_D and $Q_{SOFC,Net}$ increase with increasing C_{EtOH} and EtOH recovery. For the reboiler heat duty, Q_D, it is obvious that more energy is required by the reboiler of the distillation column to produce a higher concentration product at a higher recovery. Considering the effect of ethanol concentration on $Q_{SOFC,Net}$, the increase of $Q_{SOFC,Net}$ with the increasing C_{EtOH} is mainly due to the decrease in the energy demand for heating the ethanol/water mixture (Q_{ph1}). When the system is operated at higher ethanol recoveries while keeping the fuel utilization (U_f) constant, more ethanol is present in the anode effluent stream, resulting in a higher combustion energy (Q_{comb}) and therefore $Q_{SOFC,Net}$. From the results, it should be noted that when the SOFC-D is operated at 80-90% recovery, $Q_{SOFC,Net}$ is lower than Q_D, indicating that the exothermic heat from the SOFC system is not sufficient to supply the demand from the reboiler for all ethanol concentrations (17-41%) at the base condition (V = 0.7 V, U_f = 80%) and therefore an external heat source will be needed to supply heat to the reboiler.

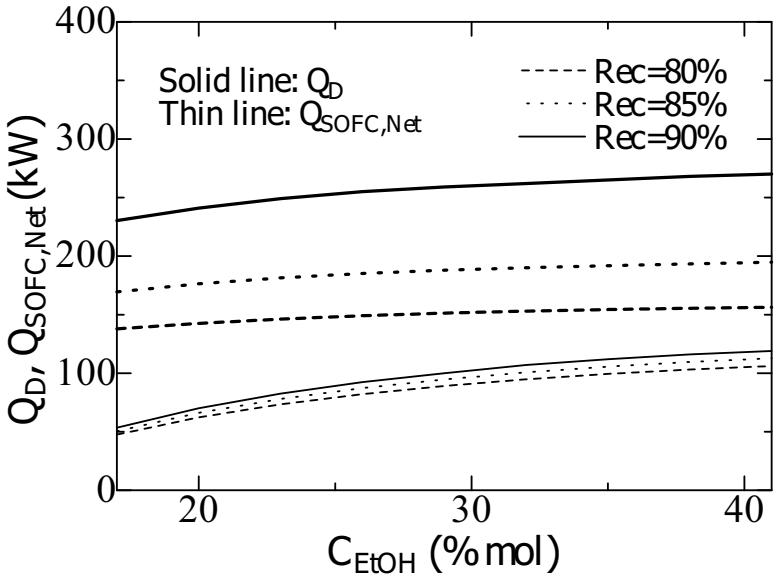

Figure 4. Effect of ethanol concentration and recovery on Q_D and $Q_{SOFC,Net}$ (V = 0.7 V, U_f = 80%, P = 101.3 kPa).

Effects of operating voltage and fuel utilization on energy involved in the SOFC-D system

When it is desired to operate the bioethanol-fed SOFC-D system without relying on other energy sources, $Q_{SOFC,Net}$ must be higher than Q_D. As mentioned earlier in Eq. (9), the exothermic heat in the SOFC system consists of two terms Q_{SOFC} and Q_{comb}. For

Q_{SOFC}, the energy arises from the irreversibility of the electrochemical reaction, in this case, entropy losses and losses due to the components of SOFC (e.g. activation losses and ohmic losses). The irreversibility due to the cell components can be observed through the difference between the maximum theoretical voltage (*EMF*) and the actual voltage. In practice, the operating voltage can be adjusted by changing an external load. For Q_{comb}, the energy is dependent on amount of unreacted fuel present in the anode effluent stream of the SOFC stack; therefore, fuel utilization (U_f) mainly influences Q_{comb}. Figure 5 shows the effects of operating voltage and fuel utilization on $Q_{SOFC,Net}$ at various values of ethanol recovery. C_{EtOH} is kept at 41 mol%. The values of Q_D are also provided in the figure. If one is to operate the bioethanol-fed SOFC-D system without relying on other energy sources, $Q_{SOFC,Net}$ must be greater than Q_D, in other words one must operate in the region above the Q_D curve. It can be seen that operating at lower fuel utilization or lower voltage can help keep $Q_{SOFC,Net}$ above Q_D. In particular, operating at low voltage (U_f = 80%, V = 0.5 V) or at low fuel utilization (U_f = 70%, V = 0.5 V), the SOFC-D can be operated at the ethanol recovery as high as 82% and 86%, respectively.

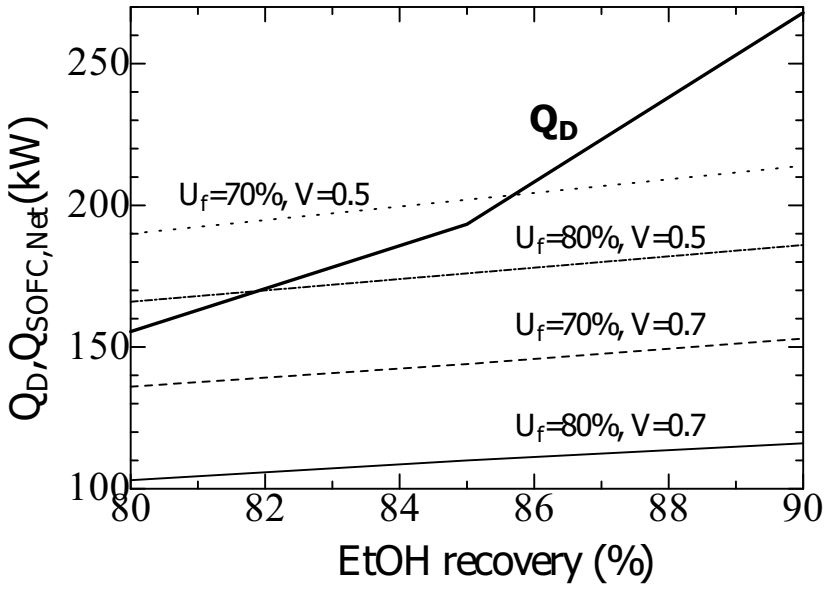

Figure 5. Effect of voltage and fuel utilization on Q_D and $Q_{SOFC,Net}$ for different values of EtOH recoveries (C_{EtOH} = 41%, P = 101.3 kPa).

Performance of the SOFC-D system at its maximum electrical power

In this section, the performance of the SOFC-D system at the energy sufficient point where $Q_D = Q_{SOFC,Net}$ is considered. The values of power density and overall electrical efficiency at different ethanol recoveries (60-90%) are shown in Figure 6. At this energy sufficient point, the maximum electrical power is obtained because no excess heat is left over from the SOFC-D system. When a value of U_f is specified, the corresponding value of the operating voltage and power density at each ethanol recovery can be determined. It is noticed that within this range of ethanol recovery, the overall electrical efficiency decreases with the increasing ethanol recovery particularly at high ethanol recovery. This is because the reboiler heat duty increases more rapidly than the energy gained from

having more ethanol in the feed to the SOFC system. The overall electrical efficiency is found to be independent on the value of fuel utilization. In contrast, the value of fuel utilization significantly influences the power density. As the fuel utilization increases, less amount of unreacted fuel is present in the anode effluent stream and therefore the value of Q_{comb} decreases. Consequently, the higher value of Q_{SOFC}, which is dependent on both the cell current and operating voltage, is required. From the results, it is obvious that the selection of the ethanol recovery and fuel utilization of the SOFC-D system is very important to achieve good SOFC-D performance. However, quite low performances are obtained when one operates the SOFC-D system without an external heat source. The maximum overall efficiency at the energy-sufficient point which does not require an external heat source as high as 35% can be obtained at an ethanol recovery of 60%. The power density of 0.22 W cm^{-2} occurs at U_f = 90%. It is likely that another ethanol purification process (such as pervaporation) which consumes less energy is essential to be integrated with the SOFC system to improve the overall electrical efficiency.

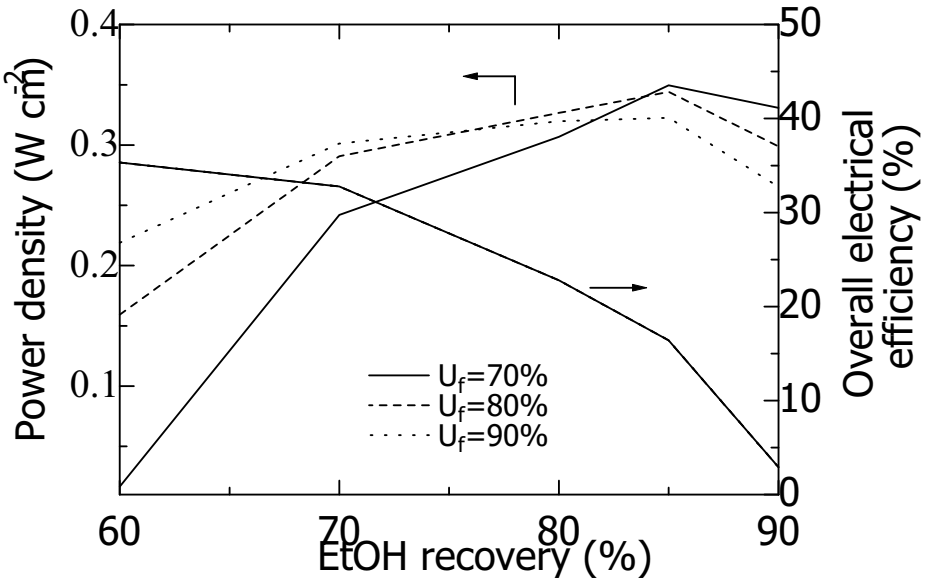

Figure 6. Performance of SOFC-D at the maximum electrical power for different values of EtOH recovery (C_{EtOH} = 41%, P = 101.3 kPa).

Conclusion

The SOFC system integrated with a distillation column (SOFC-D) has been proposed. Bioethanol with 5 mol% of EtOH in water was purified in a distillation column to a desired concentration and introduced to the SOFC system consisting of an ethanol/water vaporizer, an air heater, a reformer, an anode preheater, an SOFC stack and an afterburner. The effect of ethanol concentration and recovery on electrical performance and energy involving the SOFC system has been studied. Higher ethanol concentration and recovery yielded higher electrical performance and both increase the exothermic heat in the SOFC system; however, they require higher distillation energy. To operate the SOFC-D system without an external heat source, the effect of SOFC operating parameters (e.g. fuel

utilization and voltage) on the energy involving the SOFC-D system has been investigated. It was found that operating at lower fuel utilization or lower voltage can help in increasing the exothermic heat within the system. The conditions at the energy-sufficient point at various ethanol recoveries have been presented. The maximum overall efficiency and power density (~35% and 0.22 W cm^{-2}) occur at an ethanol recovery of 60% and U_f = 90%.

Acknowledgments

The supports from the Thailand Research Fund, Commission on High Education and National Metal and Materials Technology Center (MTEC) are gratefully acknowledged.

References

1. G. Maggio, S. Freni and S. Cavallar, *J. Power Sources*, **74**, 17 (1998).
2. S. Douvartzides, F.A. Coutelieris and P.E. Tsiakaras, *J. Power Sources*, **114**, 203 (2003).
3. S. Douvartzides, F. Coutelieris and P. Tsiakaras, *J. Power Source*, **131**, 224 (2004).
4. S.H. Chan and O.L. Ding, *Int. J. Hydrogen Energy*, **30**, 167 (2005).
5. E. Achenbach, J. Power Source, **49**, 333 (1994).
6. E. Hernandez-Pachenco, D. Singh, P. N. Hutton, N. Patel and M. D. Mann, *J. Power Source*, **138**, 174 (2004).
7. S. Assabumrungrat, V. Pavarajarn, S.Charojrochkul and N. Laosiripojana, *Chem. Eng. Sci*., **59**, 6015 (2004).
8. W. Jamsak, S. Assabumrungrat, P.L. Douglas, N. Laosiripojana and S. Charojrochkul *Chem. Eng. J.*, **119**, 11 (2006).

Appendix 3

ELSEVIER

Chemical Engineering Journal 133 (2007) 187–194

Chemical Engineering Journal

www.elsevier.com/locate/cej

Performance of ethanol-fuelled solid oxide fuel cells: Proton and oxygen ion conductors

W. Jamsak [a], S. Assabumrungrat [a,*], P.L. Douglas [b], N. Laosiripojana [c], R. Suwanwarangkul [d], S. Charojrochkul [e], E. Croiset [b]

[a] *Center of Excellence in Catalysis and Catalytic Reaction Engineering, Department of Chemical Engineering, Faculty of Engineering, Chulalongkorn University, Thailand*

[b] *Department of Chemical Engineering, University of Waterloo, Canada*

[c] *The Joint Graduate School of Energy and Environment, King Mongkut's University of Technology, Thonburi, Thailand*

[d] *Department of Chemical Engineering, Faculty of Engineering, King Mongkut's Institute of Technology, Ladkrabang, Thailand*

[e] *National Metal and Materials Technology Center (MTEC), Thailand*

Received 31 July 2006; received in revised form 8 February 2007; accepted 1 March 2007

Abstract

This paper investigates the performance of ethanol-fuelled solid oxide fuel cells (SOFCs) with two types of solid electrolytes, namely oxygen ion-conducting (SOFC-O^{2-}) and proton-conducting electrolytes (SOFC-H^+). Our previous work reported that the SOFC-H^+ shows superior theoretical performance over the SOFC-O^{2-} electrolyte. However, in this work when all resistances are taken into account, the actual performance of the SOFC-O^{2-} (Ni-YSZ|YSZ|YSZ-LSM) becomes significantly better than that of SOFC-H^+ (Pt|SCY|Pt). The maximum power density of the SOFC-O^{2-} is about 34 times higher than that of the SOFC-H^+ when operated at an inlet H_2O:EtOH ratio of 3, a fuel utilization factor of 80% and a temperature of 1200 K. Then the required values of the total resistance of the SOFC-H^+ to achieve the same power density as the SOFC-O^{2-} were determined. It was found that due to the superior theoretical performance of the SOFC-H^+, it is not necessary to reduce the SOFC-H^+ total resistance to the same values as the one for SOFC-O^{2-}. The study also indicates that reduction of only the electrolyte resistance is not sufficient to improve the SOFC-H^+ performance and, therefore, the other resistances including activation, electrodes and interconnect resistances need to be reduced simultaneously. Finally, the improvement of the electrolyte resistance by changing its resistivity and thickness is discussed.

Keywords: Solid oxide fuel cell; Oxygen conductor; Proton conductor; Performance; Losses

1. Introduction

Fuel cells are considered to be the most promising technology for chemical to electrical energy conversion. Solid oxide fuel cells (SOFC) have attracted considerable interest as they offer a wide range of potential applications, possibility for operation with an internal reformer and high system efficiency. Many fuels have been suggested for use in SOFCs; among these, ethanol is considered to be an attractive green fuel because it can be produced renewably from biomass, waste materials from agro-industries, forestry residue materials, or even organic fractions from municipal solid waste. Ethanol also offers other advantages related to natural availability and safety in storage and handling.

There are a number of published studies dealing with the use of ethanol for producing hydrogen for use in fuel cells [1–7]. However, only a few studies of ethanol utilization in SOFCs operation have been undertaken. The performance of SOFCs fuelled by products from different ethanol processes, such as ethanol steam reforming, ethanol dry reforming and ethanol partial oxidation with air were investigated. Ethanol steam reforming showed the highest maximum efficiency for high operating temperature [8]. The performance of external reforming SOFC (ER-SOFC) with different fuels, such as methane, methanol, ethanol and gasoline, were compared over a temperature range of 800–1200 K [9]. The maximum efficiency was obtained near the boundary of carbon formation for all fuels. The highest efficiency was obtained from methane (96%) followed by ethanol (94%) and then methanol (91%). By using an exergy-energy analysis, it was reported that the methane-fed SOFC provides higher efficiency than when ethanol is fed [10].

* Corresponding author. Tel.: +66 2 218 6868; fax: +66 2 218 6877.
E-mail address: Suttichai.A@chula.ac.th (S. Assabumrungrat).

1385-8947/$ – see front matter © 2007 Elsevier B.V. All rights reserved.
doi:10.1016/j.cej.2007.03.003

Nomenclature

E	electromotive force (V)
E_a	activation energy (kJ mol^{-1})
F	Faraday's constant (C mol^{-1})
i	current density (A cm^{-2})
I	current (A)
K	equilibrium constant of hydrogen oxidation reaction (kPa$^{-0.5}$)
n_i	number of moles of component i (mol)
p_i	partial pressure of component i (kPa)
P	power density (W cm^{-2})
r	resistance (Ω cm^2)
r_{act}	activation polarization area specific resistance (Ω cm^2)
r_e	electrolyte area specific resistance (Ω cm^2)
r_o	other area specific resistance (Ω cm^2)
r_{tot}	total area specific resistance (Ω cm^2)
R	gas constant (J mol^{-1} K^{-1})
T	temperature (K)
V	voltage (V)
x_i	mole fraction of component i

Greek letters

δ	thickness (cm)
ρ	resistivity (Ω cm)

Subscripts

a	anode
c	cathode

Noticeably, most SOFC studies have employed oxygen-ion conducting electrolytes although proton-conducting electrolytes are also possible for SOFC operation. There are several studies on the development of proton-conducting ceramic electrolytes for high temperature applications [11–14]; however, these studies mostly focus on the characterization of material properties, such as conductivities under various atmospheres. To date, there are very few studies using proton-conducting electrolyte in an SOFC operation [15,16]. The performance of SOFC with proton-conducting electrolytes (SOFC-H^+) in Yb-doped $SrCeO_3$ (SCY) electrolyte with platinum electrodes system (Pt|SCY|Pt) were investigated. The SOFC-H^+ was tested with various fuels (H_2 and CH_4) and atmospheres (dry and wet) at high temperatures (873–1273 K). It was shown that the SOFC-H^+ (dry-CH_4) system provided the highest performance [16].

Theoretical performance comparisons of SOFCs with different electrolytes revealed that the SOFC-H^+ provides higher efficiency than the SOFC with oxygen-ion conducting electrolytes (SOFC-O^{2-}) for a system fed with hydrogen and methane [17,18]. However, these studies were based on the same steam/methane feed ratio for the methane-fed case. It was demonstrated in our previous work [19–21] that the steam requirement for the SOFC-O^{2-} is lower than that for the SOFC-H^+ due to the presence of steam generated by the anodic electrochemical reaction. Therefore, the benefit from lower steam requirements in the SOFC-O^{2-} should be taken into account in the comparison between the two processes. When this benefit was considered, it was still observed that the SOFC-H^+ yielded higher EMF and efficiency than the SOFC-O^{2-} [22]. However, the calculations neglected the presence of actual losses encountered in a real SOFC operation. Therefore, this article aims at comparing the actual performance of SOFCs with different electrolytes. Although it is well known that current proton-conducting electrolytes have high resistivity and thus the performance of SOFC-H^+ should be inferior to SOFC-O^{2-}, it is still necessary to determine the status of the SOFC-H^+ technology compared to that of SOFC-O^{2-}. In our previous work, the theoretical performance of SOFC-H^+ and SOFC-O^{2-} was compared. Only the EMF and maximum theoretical efficiency were considered at that time and no losses were taken into consideration. In contrast, this study focuses on the actual performance of SOFC-H^+ and SOFC-O^{2-}. The losses in the SOFC cell (e.g. activation losses and ohmic losses) are now considered. The information from this theoretical study is also important in determining property targets (e.g. resistivity, electrolyte thickness and other resistance) for SOFC-H^+ in order to yield similar performance as the SOFC-O^{2-}.

2. Theory

The reaction system involving in the production of hydrogen via ethanol steam reforming reaction is represented by the following reactions [23]:

$$C_2H_5OH + H_2O \rightarrow 4H_2 + 2CO \quad (1)$$

$$CO + H_2O \rightarrow H_2 + CO_2 \quad (2)$$

$$CO + 3H_2 \rightarrow CH_4 + H_2O \quad (3)$$

Previous results [24,25] confirmed that a gas mixture in thermodynamic equilibrium contains only five components of noticeable concentration: carbon monoxide, carbon dioxide, hydrogen, steam, and methane.

The following three reactions are the most likely reactions leading to carbon formation:

$$2CO \rightarrow CO_2 + C \quad (4)$$

$$CH_4 \rightarrow 2H_2 + C \quad (5)$$

$$CO + H_2 \rightarrow H_2O + C \quad (6)$$

The Boudard reaction (Eq. (4)) has the largest Gibb's free energy; therefore, it was used to determine the possibility of carbon formation. The carbon activity (α_c) can be calculated from the following equation:

$$\alpha_c = \frac{K_c p_{CO}}{p_{CO_2}} \quad (7)$$

where K_c represents the equilibrium constant in Eq. (4) and p_i is the partial pressure of component i. The carbon formation can take place when $\alpha_c \geq 1$ [9,26]. In this study, conditions for SOFC operation under carbon formation were avoided.

Two types of solid electrolytes can be employed; namely, oxygen-conducting and proton-conducting electrolytes, which differ in the location were water is produced. For the oxygen-conducting electrolyte, water is produced in the anode chamber whereas it appears in the cathode side for the proton-conducting electrolyte.

2.1. Voltage calculations

2.1.1. Electromotive force

The electromotive force (EMF) for different electrolytes can be calculated as follows:

$$\text{SOFC-O}^{2-}: \quad E = \frac{RT}{4F} \ln \frac{p_{O_2,c}}{p_{O_2,a}} \tag{8}$$

$$\text{SOFC-H}^{+}: \quad E = \frac{RT}{2F} \ln \frac{p_{H_2,a}}{p_{H_2,c}} \tag{9}$$

where p_{O_2} and p_{H_2} are oxygen and hydrogen partial pressures, respectively, while the subscripts 'a' and 'c' represent anode and cathode, respectively. R is the universal gas constant, T the absolute temperature and F is the Faraday's constant.

In SOFC-O^{2-}, the partial pressure of oxygen in the cathode chamber is calculated directly from its mole fraction whereas the value in the anode chamber is calculated by assuming that the oxygen content is in equilibrium with hydrogen and water. Accordingly, the oxygen pressure in the anode chamber is determined from the following equation:

$$p_{O_2,a} = \left(\frac{p_{H_2O,a}}{K p_{H_2,a}} \right)^2 \tag{10}$$

where K is the equilibrium constant of the hydrogen oxidation reaction.

In contrast, for the SOFC-H^+, the partial pressure of hydrogen in the anode chamber is determined directly from its mole fraction while that at the cathode side is determined by assuming that the hydrogen content is in equilibrium with oxygen and water. Accordingly, the hydrogen pressure in the cathode chamber is calculated from the following equation:

$$p_{H_2,c} = \frac{p_{H_2O,c}}{K p_{O_2,c}^{1/2}} \tag{11}$$

Since the gas composition typically varies along the chamber, so does the local EMF. Accordingly, the average EMF ($\bar{E}$) is determined by numerical integration of the local EMF per unit cell length. It should be noted that the EMF also depends significantly on the inlet H_2O:EtOH ratio, operating temperature and fuel utilization. To simplify the calculations, it is assumed that gas compositions at the anode are at their equilibrium compositions along the cell length. For the calculation of the equilibrium composition in the SOFCs the reader can refer to our previous work [19–22]. However, it should be noted that a deviation from this equilibrium condition would result in lower EMF values as less hydrogen was generated in the anode chamber to compensate for the hydrogen consumed by the electrochemical reaction. Therefore, the results shown in this work represent the best performances for all SOFC cases.

In this paper, the electrochemical cells composed of Ni-YSZ|YSZ|YSZ-LSM and Pt|SCY|Pt are considered for the SOFC-O^{2-} and the SOFC-H^+, respectively. In this study, the state-of-the-art Ni-YSZ|YSZ|YSZ-LSM was chosen to represent SOFC-O^{2-}. Pt|SCY|Pt was chosen for SOFC-H^+ because the SCY electrolyte is known as one of the classical proton conducting materials with a high proton transport number [13]. Indeed it has high chemical stability and high proton conductivity at high temperatures.

2.1.2. Actual voltage

In practice, there is a deviation between EMF and the actual cell voltage (V) due to several losses (e.g. ohmic loss, activation loss, etc.). The actual cell voltage (V) is determined as follows:

$$V = E - i r_{tot} \tag{12}$$

$$r_{tot} = r_e + r_o \tag{13}$$

$$r_o = r_{act} + r_{ohm,electrode} + r_{ohm,interconnect} \tag{14}$$

where i is the current density (A cm^{-2}), r_{tot} the total resistance (Ω cm^2), r_e the electrolyte resistance (Ω cm^2) and r_o is the other resistance (Ω cm^2) including activation, electrodes and interconnect resistances. In this article, it is assumed that fuels and oxidants are well-diffused in/out of the electrodes. Therefore, the concentration losses can be ignored. This assumption is valid when the SOFC does not operate at too high current density.

- Activation loss:

  Activation loss is the loss caused by electrochemical reactions at the electrodes. In this study, Achenbach's correlation [26] is used for calculations of the SOFC-O^{2-}:

$$\text{cathode}: \quad r_{act,c} = \left[\frac{4F}{RT} k (x_{O_2,c})^m \exp\left(-\frac{E_{a,c}}{RT} \right) \right]^{-1} \tag{15}$$

$$\text{anode}: \quad r_{act,a} = \left[\frac{2F}{RT} k (x_{H_2,a})^m \exp\left(-\frac{E_{a,a}}{RT} \right) \right]^{-1} \tag{16}$$

  where $x_{O_2,c}$ and $x_{H_2,a}$ are mole fractions of oxygen in the cathode chamber and hydrogen in the anode chamber, respectively. The parameters used in Eqs. (15) and (16) are summarized in Table 1. It should be noted that these parameters are valid in the temperature range of 1173–1273 K [27].

- Ohmic loss:

  Ohmic losses are caused by the resistance of materials (i.e., electrodes, interconnect and current collectors) from the flow of electrons and by the resistance of electrolyte from the flow of ions passing through it. Ohmic resistances can be calculated by using the following equations:

$$r_{ohm,i} = \rho_i \delta_i \tag{17}$$

Table 1
Parameters used in Eqs. (15) and (16)

r_{act} (Ω cm^2)	k ($\times 10^{-5}$ A cm^{-2})	E_a (kJ mol^{-1})	m
$r_{act,c}$	14.9	160	0.25
$r_{act,a}$	0.213	110	0.25

Table 2
Parameters of SOFC cell components in Eqs. (17) and (18)

Materials	Parameters		Thickness (μm)
	α (Ω cm)	β (K)	
Anode (40% Ni/YSZ cermet)	2.98×10^{-5}	−1,392	150
Cathode (Sr-doped $LaMnO_3$:LSM)	8.11×10^{-5}	600	2000
Electrolyte (Y_2O_3 doped ZrO_2:YSZ)	2.94×10^{-5}	10,350	40
Interconnect (Mg doped $LaCrO_3$)	1.256×10^{-3}	4,690	100
Protonic electrolyte (Yb doped $SrCeO_3$:SCY)	7×10^{-5}	5.5×10^{-3}	1000

with

$$\rho_i = \alpha_i \, e^{(\beta_i/T)} \tag{18}$$

where subscript i represents the cell component (i.e., electrodes, electrolyte and interconnect), ρ the resistivity, δ_i the thickness of component i, and α and β are the constants specific to the materials. The parameters used in these calculations are adopted from Chan et al. [28] for the SOFC-O^{2-} and from Iwahara [13] and Salar et al. [16] for the SOFC-H^+ and are shown in Table 2.

As the SOFC-H^+ is not as developed as the SOFC-O^{2-}, the resistances of the components in the cell are not available in the open literature. Consequently, the other resistance is derived from the deviation of the total resistance and the electrolyte resistance. The values of the total resistance are obtained from the literature [13]. It should be noted that the SOFC-O^{2-} model was verified by comparing the calculated maximum power density and its corresponding current density with the results from Hernandez-Pacheco et al. [29]. Small deviations between those results were observed, i.e., the maximum power density from the calculation at the current density of 0.75 A cm^{-2} is 0.33 W cm^{-2} compared to 0.30 W cm^{-2} as reported in the literature [29].

2.2. SOFC electrical efficiency

When current is drawn from the SOFC, the power density, P, in W cm^{-2}, produced can be calculated by:

$$P = iV \tag{19}$$

The electrical efficiency is defined as the ratio of electrical work produced by SOFC to the chemical energy contained in the fuel fed to the SOFC system as shown in the following equation:

$$\eta = \frac{IV}{n_{\mathrm{EtOH}}(\mathrm{LHV}_{\mathrm{EtOH}})} \tag{20}$$

where I is the total current (A) determined by numerical integration of the local current density along the cell length, $\mathrm{LHV}_{\mathrm{EtOH}}$ the lower heating value of ethanol at the standard condition (1235 kJ/mol) and n_{EtOH} is the molar flow rate of ethanol fed to the system.

3. Results and discussion

Fig. 1 shows the main characteristics of SOFC performances at different fuel utilizations for both SOFC-O^{2-} and SOFC-H^+.

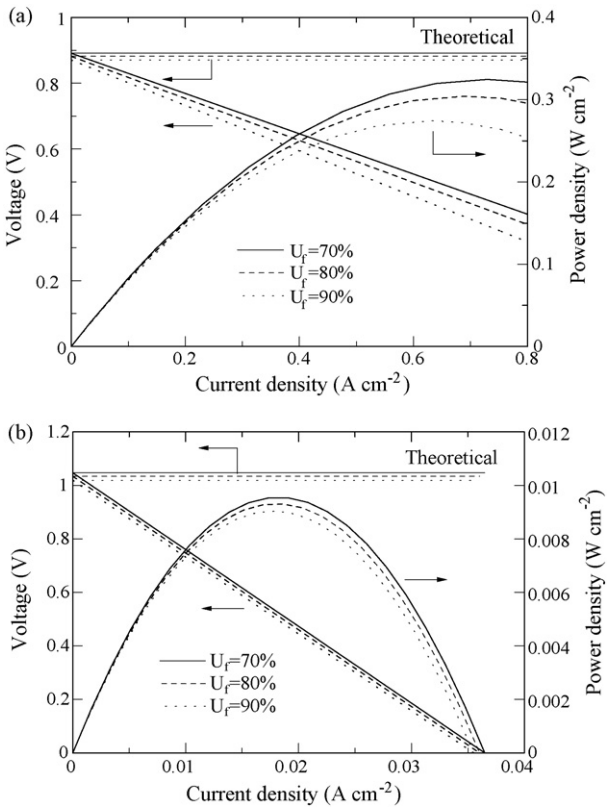

Fig. 1. Performance of SOFCs for various fuel utilizations: (a) SOFC-O^{2-} and (b) SOFC-H^+ (inlet H_2O:EtOH ratio = 3, T = 1200 K, P = 101.3 kPa, 400% excess air).

The calculations were based on a feed with an H_2O:EtOH ratio of 3 and temperature of 1200 K. The cell voltage decreases as the current density increases due to increasing losses. The power density initially increases with increasing the current density and drops at the higher values. For each value of fuel utilization, there is an optimum current density that maximizes the power density. The maximum power density decreases with increasing fuel utilization due to the effect of fuel depletion downstream. The observed values of the maximum power density of the SOFC-O^{2-} are within the range of the best value of 0.4 W cm^{-2} reported in the literature with an ethanol-fed system [30]. Fig. 1 also shows that the value of the current density for which the power density is maximum is essentially insensitive to the fuel utilization factor (at least in the range 70–90%) in the case of SOFC-H^+. The insensitivity of power density to fuel utilization in the case of SOFC-H^+ is due to the very large ohmic resis-

tance. The ohmic loss in the SOFC-H^+ electrolyte overshadows all other losses and since it is independent of the fuel utilization there is almost no difference in cell voltage for the different fuel utilizations, as seen in Fig. 1(a). As a consequence, the obtained maximum power density is insensitive to fuel utilization. For the SOFC-O^{2-}, the current density for which the power density is maximum decreases as the fuel utilization factor increases.

Performance comparisons between the two ethanol-fed SOFCs show that the SOFC-H^+ results in an EMF of around 1.01 V whereas it is approximately 0.89 V for the SOFC-O^{2-}. It is clear that the performance of SOFC-H^+ is theoretically superior to that of SOFC-O^{2-}, which is in good agreement with previous reports on SOFCs fed with H_2 and CH_4 [17,18] and ethanol [22]. The difference in the EMF between the SOFCs with different types of electrolytes is mainly due to the location of the steam generated by the electrochemical reaction, whether it is at the anode side for the SOFC-O^{2-} or at the cathode side for the SOFC-H^+. However, for an actual operation, losses strongly affect the performances of the SOFCs. It is clearly seen from Fig. 1 that the SOFC-H^+ does not perform as well as the SOFC-O^{2-}. The voltage in the SOFC-H^+ decreases significantly faster than that of the SOFC-O^{2-} as the current density increases, and the resulting maximum power density for the SOFC-H^+ is approximately 34 times lower than that of the SOFC-O^{2-}.

Another important indicator representing SOFC performance is the electrical efficiency defined in Eq. (20). The values of the electrical efficiencies at various current densities and fuel utilizations are illustrated in Fig. 2. When operating at a constant fuel utilization, the efficiency decreases with the increasing current density. The SOFC-H^+ can be operated over a much smaller range of current density than the SOFC-O^{2-} due to its higher losses. The maximum or theoretical efficiency is obtained when the current density approaches zero. At this condition, the SOFC-H^+ yields a higher efficiency than the SOFC-O^{2-} although it is not a practical operating condition as the power density is very low and, therefore, a large cell area would be required. When the fuel utilization increases, the efficiency increases although the opposite trend may be observed at high current densities, which yield low efficiency. It should be noted that the selection of suitable operating fuel utilization and current density is important as they influence the electrical efficiency and the power density, which are among the key parameters to evaluate SOFC performance.

The feed composition is another important parameter to be considered. From our previous work [22], it was reported that the SOFCs with different electrolytes required different inlet H_2O:fuel ratios to obtain their maximum EMFs. The effect of inlet H_2O:EtOH ratio on the voltage and power density is shown in Figs. 3 and 4, respectively. In the calculations, the fuel utilization was kept at 80% which is a typical operating condition used in the literature [27,29]. The inlet H_2O:EtOH ratio starts from its boundary of carbon formation which can be determined by following the procedure illustrated in our previous work [19–21]. It was found that the SOFC-O^{2-} yields the maximum voltage and power density at the boundary of carbon formation whereas those of the SOFC-H^+ are found at a ratio beyond the boundary of carbon formation. In order to compare the performance of

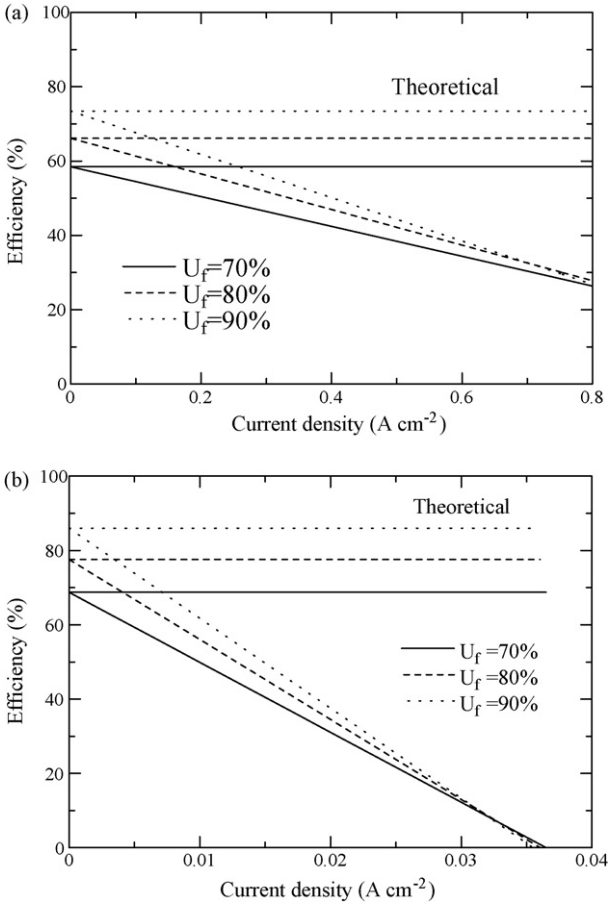

Fig. 2. Efficiency of SOFCs for various fuel utilizations: (a) SOFC-O^{2-} and (b) SOFC-H^+ (inlet H_2O:EtOH ratio = 3, T = 1200 K, P = 101.3 kPa, 400% excess air).

the SOFCs with different types of electrolytes, the best performance of each SOFC should be considered. The current density, H_2O:EtOH ratio and fuel utilization were varied to determine values which yield the highest power density for each type of SOFC.

Fig. 5 shows the maximum power density and the corresponding current density and inlet H_2O:EtOH ratio at different fuel utilizations. As expected, the maximum power density and the

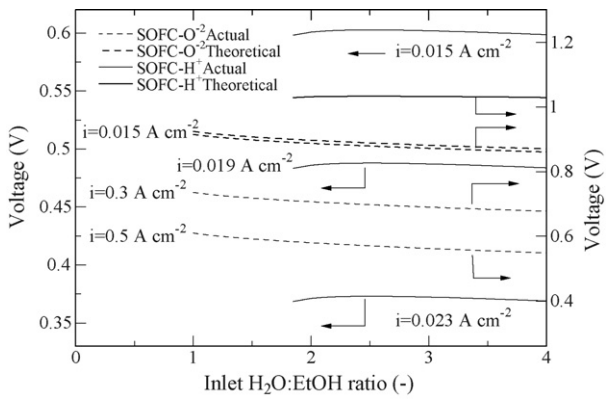

Fig. 3. Influence of inlet H_2O:EtOH ratio on voltage at various current densities (T = 1200 K, P = 101.3 kPa, U_f = 80%, 400% excess air).

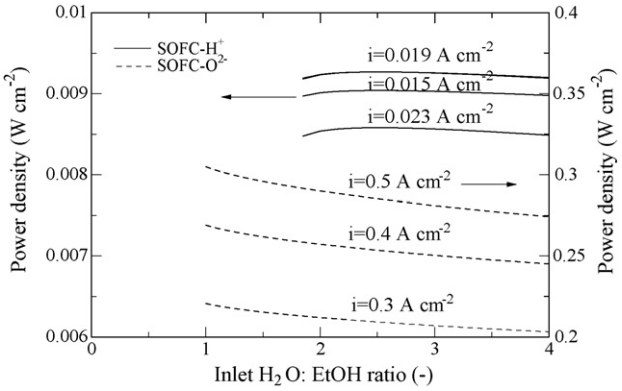

Fig. 4. Influence of inlet H_2O:EtOH ratio on power density at various current densities (T = 1200 K, P = 101.3 kPa, U_f = 80%, 400% excess air).

corresponding current density decrease with an increase in fuel utilization due to the effect of fuel depletion. Considering the corresponding values of the inlet H_2O:EtOH ratio, it can be noticed that for the SOFC-O^{2-} the values are independent of fuel utilization whereas it increases with increasing fuel utilization for the SOFC-H^+. The results can be explained by considering the influence of fuel utilization on the boundary of carbon formation. For the SOFC-O^{2-} case, the optimum H_2O:EtOH ratio is at the boundary of carbon formation. The fuel utilization does not affect the boundary of carbon formation because the critical condition for carbon formation occurs at the feed inlet in which the value of fuel utilization is zero. The possibility

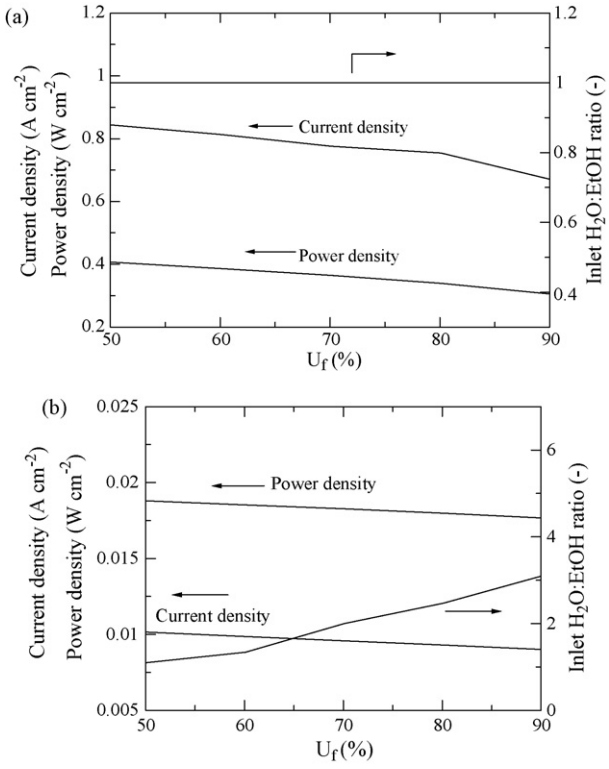

Fig. 5. Maximum power density of SOFC and their corresponding conditions (inlet H_2O:EtOH ratio and current density) at various fuel utilizations: (a) SOFC-O^{2-} and (b) SOFC-H^+ (T = 1200 K, P = 101.3 kPa, 400% excess air).

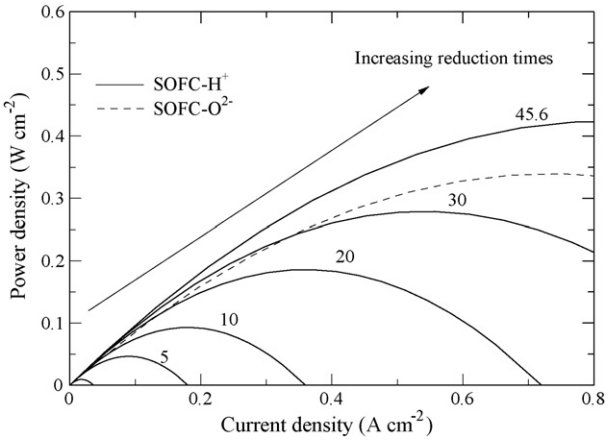

Fig. 6. Influences of total resistance on the performance of SOFC-H^+ compared with that of SOFC-O^{2-} (T = 1200 K, P = 101.3 kPa, 400% excess air).

for carbon formation becomes less severe when more hydrogen is consumed, i.e., higher fuel utilization, yielding water which helps suppress carbon formation. However, for the SOFC-H^+ case, at high fuel utilization, more hydrogen disappears without benefiting from the steam generated from the electrochemical reaction in the anode gas mixture, leading to higher possibility for carbon formation. Therefore, higher inlet H_2O:EtOH ratios are required to thermodynamically suppress carbon formation. From the results shown in Fig. 5, it is clear that the best performance of SOFC-H^+ is still lower than that of SOFC-O^{2-} for the entire range of fuel utilization, which confirms that the SOFC-H^+ does not show great promise, at least with the current extremely high resistance in SOFC-H^+.

To enhance the performance of SOFC-H^+, it is obvious that the resistance of the cell must be reduced due to the sudden drop in voltage. Fig. 6 depicts the influence of the total resistance of the SOFC-H^+ cell on the cell performances at 1200 K. It should be noted that the total resistance is termed as the summation of electrolyte resistance and the other resistances. In this section, the reduction time is defined as the ratio by which the total resistance is reduced compared to the current value. The dashed line represents the values of the SOFC-O^{2-}. Obviously, the total resistance is an important factor for improving the performance of SOFC-H^+. Higher power density can be obtained when decreasing the total resistance. It was found that when the total resistance of the SOFC-H^+ is reduced to 1/45.6 of the present value (28.7 $\Omega\,cm^2$), which would be equal to the total resistance of the current SOFC-O^{2-} (0.628 $\Omega\,cm^2$), the performance of the SOFC-H^+ is better than that of the SOFC-O^{2-}. It is clear that due to the superior theoretical performance of the SOFC-H^+, it is unnecessary to reduce the total resistance of the SOFC-H^+ to the level of that of the SOFC-O^{2-}. The total resistance in the SOFC-H^+, which yields an equivalent power density as the SOFC-O^{2-} is presented in Fig. 7 as function of temperature. It can be seen that a reduction by 1/30.7 (0.935 $\Omega\,cm^2$) is sufficient to offer the same power density as the SOFC-O^{2-} at 0.7 V and 1200 K. When increasing the operating temperature, the required resistance of SOFC-H^+ has to be further decreased due to a rapid decrease in the total resistance of SOFC-O^{2-}.

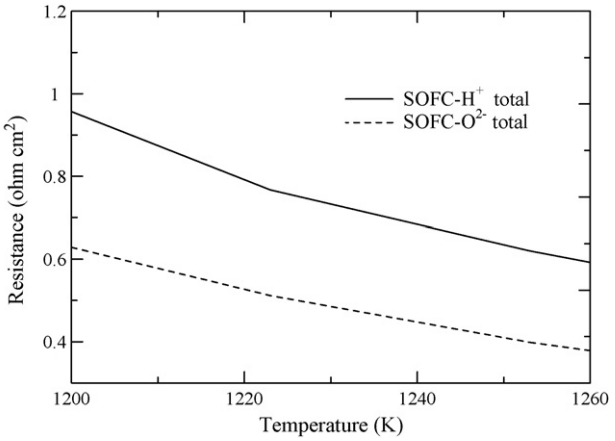

Fig. 7. Required total resistance of SOFC-H^+ with comparable SOFC-O^{2-} performance at various temperatures.

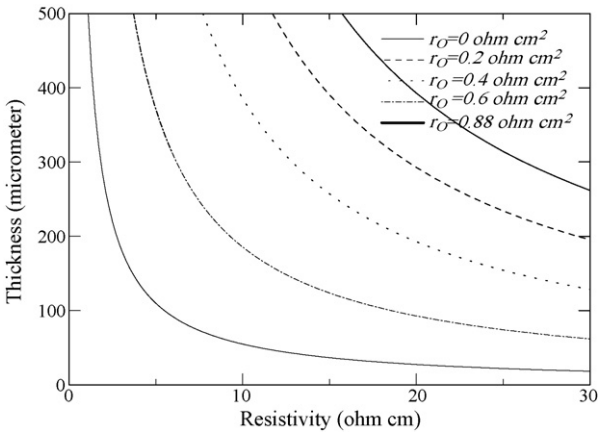

Fig. 8. Resistivity and thickness of proton-conducting electrolyte at various values of the other resistances, r_o (T = 1200 K, P = 101.3 kPa, 400% excess air).

Considering the Pt|SCY|Pt SOFC-H^+ cell in this study, the electrolyte, other and total resistances at 1200 K are 8.5, 20.2 and 28.7 $\Omega\,cm^2$, respectively. It is seen that the expected value of 0.935 $\Omega\,cm^2$ cannot be achieved by only reducing the electrolyte resistance. Both the electrolyte and the other resistances need to be improved simultaneously. At T = 1200 K, the electrolyte and the other resistances of the SOFC-H^+ are about 130 and 35 times, respectively, higher than those of the SOFC-O^{2-}. The high value of the other resistances of the SOFC-H^+ is possibly because platinum is not a good ionic conductor although it has high catalytic activity and high electronic conductivity [31]. In addition, since the cermet structure is not applied for the anode, the platinum is more likely to sinter rather than compacted to the electrolyte at high temperature [32]. These lead to low interfacial conductivity between the platinum electrodes and the electrolyte. From these comparisons, significant efforts are required to reduce both the electrolyte and the other resistances of the SOFC-H^+ cell.

Because the electrolyte resistance depends on its thickness and physical properties of material, it is possible to reduce the resistance by reducing the electrolyte thickness and/or using new materials with lower resistivity. Some materials with high proton conductivity have been reported, for example, $BaCe_{0.8}Y_{0.2}O_{3-\alpha}$ (BCY) and $BaCe_{0.9}Nd_{0.1}O_{3-\alpha}$ in which the resistivities at T = 1200 K are 12.5 and 28.6 Ω cm, respectively, compared to 85.0 Ω cm for the SCY used in this study [13]. Fig. 8 shows the required electrolyte thickness for different values of material resistivity of the electrolyte and the other resistance. It is clear that for a given value of the other resistance, the higher the material resistivity, the thinner the electrolyte is required. For the currently available high proton conducting material of SCY, when the electrolyte is reduced to a thickness as small as 150 μm which is in the range of an electrode-supported cell for 8YSZ [31], the other resistance should be reduced to 0.6 $\Omega\,cm^2$ which is approximately 1/33.7 that of the present value. To achieve the expected value of the other resistance, the electrical conductivities and activity of the cathode and anode must be significantly improved to replace the use of Pt. In addition, the interfacial resistivity between electrolyte/anode and electrolyte/cathode must be suppressed by a careful selection of material and suitable microstructure to enhance the triple-phase boundary. In addition, some other considerations such as mechanical strength, chemical compatibilities and thermal expansion compatibilities among the cell components need to be taken into account in the cell development. However, it is unfortunate that most of these data are currently not available. Therefore, considerable effort in the development of an SOFC-H^+ cell is necessary to eventually commercialize this type of fuel cell.

4. Conclusions

Although the theoretical EMF and electrical efficiency of the SOFC-H^+ are superior to those of the SOFC-O^{2-}, its actual voltage and power density are much lower than those of the SOFC-O^{2-} due to large resistance of the cell. It was calculated that in order to achieve an equivalent power density to the SOFC-O^{2-}, the total resistance of the SOFC-H^+ should be reduced to 0.935 $\Omega\,cm^2$, which is equal to 1/30.7 of the present value (28.7 $\Omega\,cm^2$), compared to the value of 0.628 $\Omega\,cm^2$ of the SOFC-O^{2-} at 1200 K. Due to the superior theoretical performance of the SOFC-H^+, it is unnecessary to reduce the total resistance of the SOFC-H^+ to the same value of the SOFC-O^{2-}. It was found that the reduction of the electrolyte resistance alone is not sufficient to reach the expected value of the total resistance. Both the electrolyte and the other resistances need to be improved simultaneously. The electrolyte resistance could be improved by reducing the electrolyte thickness and/or finding new materials with lower resistivity. When the electrolyte thickness of SCY, the currently available high proton conducting material, is reduced to 150 μm, in the range of an electrode supported cell for 8YSZ, the other resistance should be reduced to 0.6 $\Omega\,cm^2$ (1/33.7 of the present value). It is clear that the success of the SOFC-H^+ technology depends on the development of improved cell components.

Acknowledgements

The support from the Thailand Research Fund, Commission on High Education and National Metal and Materials Technology Center (MTEC) are gratefully acknowledged.

References

[1] S. Cavallaro, S. Freni, Ethanol steam reforming in a molten carbonate fuel cell. A preliminary kinetic investigation, Int. J. Hydrogen Energy 21 (1996) 465–469.

[2] G. Maggio, S. Freni, S. Cavallaro, Light alcohols/methane fuelled molten carbonate fuel cells: a comparative study, J. Power Sources 74 (1998) 17–23.

[3] T. Ioannides, S. Neophytides, Efficiency of a solid polymer fuel cell operating on ethanol, J. Power Sources 91 (2000) 150–156.

[4] T. Ioannides, Thermodynamic analysis of ethanol processors for fuel cell applications, J. Power Sources 92 (2001) 17–25.

[5] S. Cavallaro, N. Mondello, S. Freni, Hydrogen produced from ethanol for internal reforming molten carbonate fuel cell, J. Power Sources 102 (2001) 198–204.

[6] V. Klouz, V. Fierro, P. Denton, H. Katz, J.P. Lisse, S. Bouvot-Mauduit, C. Mirodatos, Ethanol reforming for hydrogen production in a hybrid electric vehicle: process optimisation, J. Power Sources 105 (2002) 26–34.

[7] N.A. Fatsikostas, D.I. Kondarides, X.E. Verykios, Production of hydrogen for fuel cells by reformation of biomass-derived ethanol, Catal. Today 75 (2002) 145–155.

[8] T. Tsiakaras, A. Demin, Thermodynamic analysis of a solid oxide fuel cell system fuelled by ethanol, J. Power Sources 102 (2001) 210–217.

[9] S.L. Douvartzides, F.A. Coutelieris, A.K. Demin, P.E. Tsiakaras, Fuel options for solid oxide fuel cell: a thermodynamic analysis, AIChE J. 49 (2003) 248–257.

[10] S. Douvartzides, F.A. Coutelieris, P.E. Tsiakaras, Exergy analysis of solid oxide fuel cell power plant fed by either ethanol or methane, J. Power Sources 131 (2004) 224–230.

[11] T. Shimada, C. Wen, N. Taniguchi, J. Otomo, H. Takahashi, The high temperature proton conductor $BaZr_{0.4}Ce_{0.4}In_{0.2}O_{3-\alpha}$, J. Power Sources 131 (2004) 289–292.

[12] T. Schober, F. Krug, W. Schilling, Criteria for the application of high temperature proton conductor in SOFCs, Solid State Ionics 97 (1997) 369–373.

[13] H. Iwahara, Proton conducting ceramics and their application, Solid State Ionics 86–88 (1996) 9–15.

[14] T. Schneller, T. Schober, Chemical solution deposition prepared dense proton conducting Y-doped $BaZrO_3$ thin films for SOFC and sensor devices, Solid State Ionics 164 (2003) 131–136.

[15] D. Browning, M. Weston, J.B. Lakeman, P. Jones, M. Cherry, J.T.S. Irvine, D.J.D. Corcoran, Proton conducting ceramics for use in intermediate temperature proton conducting fuel cells, J. New Mater. Electrochem. Syst. 5 (2002) 25–30.

[16] R. Salar, H. Taherparvar, I.S. Metcalfe, M. Sahibzada, Proceedings of the 2001 Joint International Meeting—The 200th Meeting of The Electrochemical Society Inc. and the 52nd Annual Meeting of the International Society of Electrochemistry, San Francisco, California, 2001.

[17] A. Demin, P. Tsiakaras, Thermodynamic analysis of a hydrogen fed solid oxide fuel cell based on a proton conductor, Int. J. Hydrogen Energy 26 (2001) 1103–1108.

[18] A.K. Demin, P.E. Tsiakaras, V.A. Sobyanin, S.Yu. Hramova, Thermodynamic analysis of a methane fed SOFC system based on a protonic conductor, Solid State Ionics 152–153 (2002) 555–560.

[19] S. Assabumrungrat, V. Pavarajarn, S. Charojrochkul, N. Laosiripojana, Thermodynamic analysis for solid oxide fuel cell with direct internal reforming fueled by ethanol, Chem. Eng. Sci. 59 (2004) 6015–6020.

[20] S. Assabumrungrat, N. Laosiripojana, V. Pavarajarn, W. Sangtongkitcharoen, A. Tangjitmatee, P. Praserthdam, Thermodynamic analysis of carbon formation in a solid oxide fuel cell with direct internal reformer fuelled by methanol, J. Power Sources 139 (2005) 55–60.

[21] W. Sangtongkitcharoen, S. Assabumrungrat, V. Pavarajarn, N. Laosiripojana, P. Praserthdam, Comparison of carbon formation boundary in different modes of solid oxide fuel cells fueled by methane, J. Power Sources 142 (2005) 75–80.

[22] W. Jamsak, S. Assabumrungrat, P.L. Douglas, N. Laosiripojana, S. Charojrochkul, Theoretical performance analysis of ethanol-fuelled solid oxide fuel cells with different electrolytes, Chem. Eng. J. 119 (2006) 11–18.

[23] S. Freni, G. Maggio, S. Cavallaro, Ethanol steam reforming in a molten carbonate fuel cell: a thermodynamic approach, J. Power Sources 62 (1996) 67–73.

[24] E.Y. Garcia, M.A. Laborde, Hydrogen production by the steam reforming of ethanol: thermodynamic analysis, Int. J. Hydrogen Energy 16 (1991) 307–312.

[25] K. Vasudeva, N. Mitra, P. Umasankar, S.C. Dhinggra, Steam reforming of ethanol for hydrogen production: thermodynamic analysis, Int. J. Hydrogen Energy 21 (1996) 13–18.

[26] E. Achenbach, Three-dimensional and time-dependent simulation of a planar solid oxide fuel cell stack, J. Power Sources 49 (1994) 333–348.

[27] E. Hernandez-Pacheco, D. Singh, P.N. Hutton, N. Patel, M.D. Mann, A macro-level model for determining the performance characteristics of solid oxide fuel cells, J. Power Sources 138 (2004) 174–186.

[28] S.H. Chan, C.F. Low, O.L. Ding, Energy and exergy analysis of simple solid-oxide fuel-cell power systems, J. Power Sources 103 (2002) 188–200.

[29] E. Hernandez-Pacheco, M.D. Mann, P.N. Hutton, D. Singh, K.E. Martin, A cell-level model for a solid oxide fuel cell operated with syngas from a gasification process, Int. J. Hydrogen Energy 30 (2005) 1221–1233.

[30] Fuel Cells Bulletin 8 (2005) 8.

[31] Handbook of Fuel Cells—Fundamentals, Technology and Applications, vols. 1–2, John Wiley & Sons Ltd., 2003.

[32] F.H. Garzon, R. Mukundan, R. Lujan, E.L. Brosha, Solid state ionic devices for combustion gas sensing, Solid State Ionics 175 (2004) 487–490.

Appendix 4

Available online at www.sciencedirect.com
ScienceDirect
Journal of Power Sources 174 (2007) 191–198
JOURNAL OF POWER SOURCES
www.elsevier.com/locate/jpowsour

Thermodynamic assessment of solid oxide fuel cell system integrated with bioethanol purification unit

W. Jamsak [a], S. Assabumrungrat [a,*], P.L. Douglas [b,**], E. Croiset [b], N. Laosiripojana [c], R. Suwanwarangkul [d], S. Charojrochkul [e]

[a] *Center of Excellence in Catalysis and Catalytic Reaction Engineering, Department of Chemical Engineering, Faculty of Engineering, Chulalongkorn University, Thailand*
[b] *Department of Chemical Engineering, University of Waterloo, Canada*
[c] *The Joint Graduate School of Energy and Environment, King Mongkut's University of Technology, Thonburi, Thailand*
[d] *School of Bio-Chemical Engineering and Technology, Sirindhorn International Institute of Technology, Thammasart University, Rangsit Campus, Patum Thani 12121, Thailand*
[e] *National Metal and Materials Technology Center (MTEC), Thailand*

Received 8 May 2007; received in revised form 27 August 2007; accepted 28 August 2007
Available online 7 September 2007

Abstract

A solid oxide fuel cell system integrated with a distillation column (SOFC–DIS) has been proposed in this article. The integrated SOFC system consists of a distillation column, an EtOH/H_2O heater, an air heater, an anode preheater, a reformer, an SOFC stack and an afterburner. Bioethanol with 5 mol% ethanol was purified in a distillation column to obtain a desired concentration necessary for SOFC operation. The SOFC stack was operated under isothermal conditions. The heat generated from the stack and the afterburner was supplied to the reformer and three heaters. The net remaining heat from the SOFC system ($Q_{SOFC,Net}$) was then provided to the reboiler of the distillation column. The effects of fuel utilization and operating voltage on the net energy (Q_{Net}), which equals $Q_{SOFC,Net}$ minus the distillation energy (Q_D), were examined. It was found that the system could become more energy sufficient when operating at lower fuel utilization or lower voltage but at the expense of less electricity produced. Moreover, it was found that there were some operating conditions, which yielded Q_{Net} of zero. At this point, the integrated system provides the maximum electrical power without requiring an additional heat source. The effects of ethanol concentration and ethanol recovery on the electrical performance at zero Q_{Net} for different fuel utilizations were investigated. With the appropriate operating conditions (e.g. $C_{EtOH} = 41\%$, $U_f = 80\%$ and EtOH recovery = 80%), the overall electrical efficiency and power density are 33.3% (LHV) and 0.32 W cm^{-2}, respectively.

Keywords: Solid oxide fuel cell; Combined process; Bioethanol; Distillation unit

1. Introduction

A solid oxide fuel cell is an attractive power generation system as it offers a wide range of applications, low emissions, fuel flexibility and high system efficiency. Generally, the major components of an SOFC system are preheaters, a fuel processor, a fuel cell stack and an afterburner. It is known that useful heat is always available when operating the SOFC because of the presence of irreversibility and unreacted fuel [1]. To enhance the system efficiency, an SOFC is usually integrated with other energy devices for further utilization of excess heat to generate extra electrical power and/or hot water/steam. Nowadays, the two most promising systems are SOFC–Gas Turbine system (SOFC–GT) [2–4] and SOFC–Combined Heat and Power system (SOFC–CHP) [5–8].

For the SOFC–GT system, Palsson et al. [2] investigated a 500 kW methane-fuelled SOFC–GT system. The system consisted of preheaters, a pre-reformer, an SOFC stack, a combustor, an air compressor, a booster and an expander. Part of the anode effluent was recycled in order to supply heat and steam to the external reformer. The rest of the anode effluent was combined with the cathode effluent and burnt in the combustor. The out-

* Corresponding author. Tel.: +662 218 6868; fax: +662 218 6877.
** Corresponding author.
E-mail addresses: Suttichai.A@chula.ac.th (S. Assabumrungrat), pdouglas@cape.uwaterloo.ca (P.L. Douglas).

0378-7753/$ – see front matter © 2007 Elsevier B.V. All rights reserved.
doi:10.1016/j.jpowsour.2007.08.105

Nomenclature

C_{EtoH}	ethanol concentration (% mol)
E	electromotive force of a cell (V)
E_a	activation energy (J mol^{-1})
F	Faraday constant (C mol^{-1})
i	current density (A cm^{-2})
I	current (A)
LHV_{EtOH}	lower heating value of ethanol (J mol^{-1})
n_{EtOH}	total ethanol flow rate fed to the distillation column (mol s^{-1})
p_i	partial pressure of component i (kPa)
P	pressure (kPa)
P_{den}	power density (A cm^{-2})
Q_1	the energy required for Preheater 1 (kW)
Q_2	the energy required for Preheater 2 (kW)
Q_3	the energy required for Preheater 3 (kW)
Q_4	the energy required for a reformer (kW)
Q_5	the exothermic heat released from an SOFC stack (kW)
Q_6	the energy involved the combustion of exhausted gases and cooled to the exit temperature (kW)
Q_{Con}	condenser duty (kW)
Q_D	reboiler duty (kW)
Q_{Net}	net useful heat (kW)
$Q_{SOFC,Net}$	net exothermic from SOFC (kW)
r	area specific resistance (Ω cm^2)
r_{act}	activation polarization area specific resistance (Ω cm^2)
r_{ohm}	ohmic polarization area specific resistance (Ω cm^2)
$r_{H_2,cons}$	rate of hydrogen consumed by the electrochemical reaction (mol s^{-1})
R	gas constant (J mol^{-1} K^{-1})
T_{SOFC}	SOFC temperature (K)
T_{RF}	reforming temperature (K)
U_f	fuel utilization (%)
V	operating voltage (V)
W_e	electrical power (kW)

Greek letters

$\eta_{elec,ov}$	overall electrical efficiency (%)
ρ	resistivity (Ω cm)

Subscripts

a	anode
c	cathode

let stream from the combustor was then delivered to the gas turbine for generating additional electrical power whereas the exhaust gas from the gas turbine was used for preheating the feeds. The influences of operating parameters such as pressure, air flow rate, fuel flow rate and air inlet temperature on the system performance were analyzed. Fredriksson Möller et al. [3] studied a methane-fuelled SOFC–GT system integrated with a CO_2 capture plant. The desulfurizer unit was also implemented in the SOFC system. The CO_2 capture plant consisted of a condenser, an absorber and a regenerator. Two SOFC stacks were employed in this study. The reformed gas was split between the two stacks and fed to the anode sides in parallel. The obtained electrical efficiency of the SOFC–GT system integrated with the CO_2 capture plant reached above 60%. Inui et al. [4] investigated SOFC–GTs with CO_2 recovery systems. Two new CO_2 recovery systems were proposed as a bottoming cycle, i.e. (1) CO_2 recycle system and (2) water vapor injection system. The results showed that the former system achieved an overall efficiency of 70.88% (LHV) while the latter system yielded 72.13%.

For the SOFC–CHP system, Chan et al. [5] studied a methane-fuelled SOFC system and compared its efficiency with that of a hydrogen-fuelled system. The system consisted of a vaporizer, preheaters, a pre-reformer, an SOFC stack and an afterburner. The unreacted fuel was burnt in the afterburner and the heat from the afterburner was supplied to the reformer, vaporizer, steam boiler and preheaters. Some heat from the SOFC stack was used for the steam boiler. The results indicated that the efficiency of the methane-fuelled system was higher than that of the hydrogen-fuelled system. Fontell et al. [6] examined a methane-fuelled SOFC combined with a desulfurizer unit, a power conversion unit and system controllers. The system configuration was different from Chan's work [5] as the anode effluent was re-circulated for preheating the reformed gas before being split into two streams: one was mixed with the desulfurized stream and the other was fed to the combustor. The results revealed that the system efficiency achieved was around 85%. Zhang et al. [7] also examined an SOFC fuelled with methane. The equipment setting was almost similar to that in Fontell's work [6]; however, no desulfurizer, power conversion and controllers were included. In addition, the anode effluent was also split into two streams: one for combustion and the other for anode re-circulation. No anode effluent was used for preheating the anode inlet. An electrical efficiency of 52% was obtained for the desired power of 120 kW. Omosun et al. [8] studied an SOFC fuelled by product gas from gasified biomass. The system consisted of a gasifier, separation units (i.e. cyclone and filter), a fuel cell stack and a combustor. The study focused on a performance comparison between cold and hot processes. The major differences between those processes were the gasification and clean-up processes. The hot process used a fluidized bed gasifier and a ceramic filter whereas the cold process used a fixed-bed gasifier and a wet precipitator. For a heat recovery, both anode and cathode effluents were re-circulated and mixed with the incoming streams. The results showed that the hot process yielded higher electrical and system efficiencies than the cold process. However, the cost of the hot process was higher than that of the cold process.

Among the many possible fuels for SOFC, ethanol is an attractive green fuel as it can be derived from renewable resources and it is safe and easy for storage and handling [9]. The group of Tsiakaras has been particularly active in investigating the ethanol-fuelled SOFCs [10–12]. They compared the theoretical SOFC performances for different ethanol reforming reactions (steam reforming, CO_2 reforming and par-

tial oxidation) [10]. It was reported that the products from steam reforming yielded the highest maximum efficiency when $T < 950$ and >1100 K whereas those from the CO_2 reforming was more preferable at the intermediate temperatures. For the partial oxidation, its efficiency was 20% less than the other cases. An energy–exergy analysis was also employed to examine the system comprising an external steam reformer, an SOFC stack, an afterburner, two preheaters, a water vaporizer and a mixer [11,12]. No anode and cathode recycles were considered. The heat from the combustor was provided to the preheaters, the vaporizer and the reformer. An optimization of the combustor was performed by matching appropriate reforming temperature and fuel utilization. Moreover, the minimization of SOFC loss was examined by searching for suitable reforming and air preheating temperatures. It should be noted from all studies related to SOFCs fuelled by ethanol that pure ethanol was usually mixed with water in order to obtain a desired ethanol concentration before being fed into the reformer. From an energy point of view, this might not be an efficient strategy as unnecessary energy is consumed to purify bioethanol to a needless high concentration ethanol, which is subsequently mixed with water and fed to the reformer.

In this work, it was proposed to integrate the SOFC with an ethanol purification unit. The ethanol was purified to a desired concentration using a distillation column whose required energy can be directly supplied from the excessive heat from the SOFC system. It was expected that by carefully selecting suitable operating conditions, the integrated system could be operated without any requirement of additional energy sources apart from the bioethanol feed. The influences of operating parameters including ethanol concentration, ethanol recovery, fuel utilization and voltage on electrical performance and net energy of the integrated system (Q_{Net}) were investigated.

2. SOFC system modelling

Fig. 1 shows the proposed SOFC system integrated with a distillation column (SOFC–DIS). The SOFC system consisted of three heat exchangers (for preheating feeds), a reformer and an afterburner. The distillation column was integrated with the SOFC system to purify bioethanol to desired levels of ethanol concentration and recovery. Generally, the ethanol concentration from a fermentation process is in the range of 1–7 mol% [13–16]. In this work, the value of 5 mol% was selected as a representative of bioethanol. Aspen Plus™ and the Radfrac rigorous

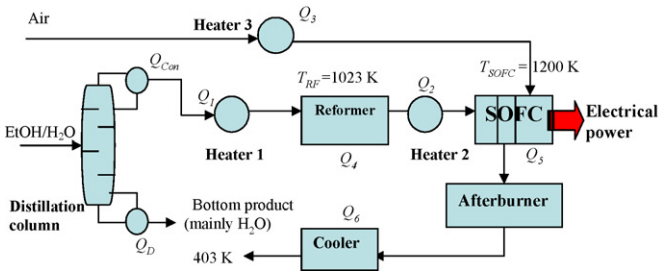

Fig. 1. Schematic diagram of SOFC system integrated with a distillation column (SOFC–DIS).

equilibrium stage distillation module were used for simulating the distillation column. A total condenser and a kettle boiler were employed. The bioethanol feed was introduced to the stage above the reboiler. The minimum reboiler heat duty, which could be obtained by adjusting the number of stages and reflux ratio, was used in the present study of the SOFC–DIS system.

The distillate leaving the distillation column was heated up to the reforming temperature (T_{RF}) by Heater 1 (here $T_{RF} = 1023$ K), and fed to the external reformer, which was assumed to operate isothermally. It should be noted that considering such high reforming temperature, negligible extent of ethanol was present in the reformed gas. The reformed gas was then heated up to the SOFC temperature (T_{SOFC}) by Heater 2 and introduced to the anode chamber of the SOFC stack. The SOFC stack was also assumed to operate isothermally ($T_{SOFC} = 1200$ K). Excess air (380%) preheated by Heater 3 was fed to the cathode chamber. The equations describing the electrochemical model are as follows:

$$V = E - i(r_{ohm} + r_{act}) \tag{1}$$

$$E = \frac{RT}{4F} \ln \frac{p_{O_2,c}}{p_{O_2,a}} \tag{2}$$

$$r_{act,c} = \left[\frac{4F}{RT} k (p_{O_2,c})^m \exp\left(-\frac{E_{a,c}}{RT}\right)\right]^{-1} \tag{3}$$

$$r_{act,a} = \left[\frac{2F}{RT} k (p_{H_2,a})^m \exp\left(-\frac{E_{a,a}}{RT}\right)\right]^{-1} \tag{4}$$

$$r_{ohm,j} = \rho_j \delta_j \tag{5}$$

$$\rho_j = \alpha_j exp\left(\frac{\beta_j}{T}\right) \tag{6}$$

$$P_{den} = iV \tag{7}$$

$$I = r_{H_2,cons} \times 2F \tag{8}$$

$$r_{H_2,cons} = r_{H_2 in,equiv.} \times U_f \tag{9}$$

$$r_{H_2 in,equivalent} = 6 \times r_{EtOH,d} \tag{10}$$

$$A = \frac{I}{i} \tag{11}$$

$$W_e = IV \tag{12}$$

where E is the electromotive force (EMF), V the operating voltage, i the current density, I the overall current, R the gas constant, T the SOFC temperature, F the Faraday's constant, r_{act} the activation resistance, $E_{a,a}$ and $E_{a,c}$ the activation energies at anode and cathode, respectively, $p_{O_2,c}$ and $p_{H_2,a}$ the mole fractions of oxygen in the cathode chamber and hydrogen in the anode chamber, respectively, r_{ohm} the ohmic resistance, ρ_j the resistivity of material j, α_j and β_j the constants specific to material j, $r_{H_2,cons}$ the molar flow rate of hydrogen consumed in the electrochemical reaction, $r_{H_2 in,equiv.}$ the maximum hydrogen molar flow rate coming into the anode chamber (6× that of ethanol flow rate), $r_{EtOH,d}$ the ethanol flow rate in the distillate fed into the SOFC system, A the total active area of SOFC stack, W_e the electrical power, P_{den} the power density, LHV_{EtOH} the low heating value

Table 1
Parameters for activation loss [17]

r_{act} (Ω cm^2)	k ($\times 10^{-13}$ A cm^2)	E_a (kJ mol^{-1} K^{-1})	m (−)
$r_{act,c}$	14.9	160	0.25
$r_{act,a}$	0.213	110	0.25

of ethanol. The parameters used for calculating the ohmic and activation overpotentials are listed in Tables 1 and 2.

It should be noted that the SOFC cell was based on the tubular configuration [5]. Concerning the activation losses, the Achenbach's semi-empirical correlation [17] was used to predict the activation overpotentials for the anode and cathode. Hernandez-Pacheco et al. [18] compared the values from the Achenbach's correlation and the Butler–Volmer equation and found that the Achenbach's correlation gave reliable results for temperatures between 1173 and 1273 K. The operating temperature of 1200 K in this study was within the reliable range of the Achenbach's correlations. For calculating SOFC performance, a concentration polarization loss could be omitted when an SOFC does not operate at high current density. The concentration losses can be estimated by using an equation given in Ref. [19]. A concentration loss of 0.03 V was thus estimated at the current densities around 0.6 A cm^{-2}. This is why the concentration polarization was neglected. Details on the calculations of composition and EMF distributions within the SOFC stack were given in our previous works [20,21]. Note that the flow rate of ethanol is kept constant for all conditions; therefore, the active area of the SOFC stack were changed when the voltage and fuel utilization changed. The appropriate size of SOFC stack was not investigated in this work.

The effluent from the anode and the cathode was burnt in the afterburner. Assuming that the combusted gas was discharged to the environment at 403 K, the useful heat remaining in the exhaust stream could be calculated. The useful heat is used to supply the energy to the energy-demanding units in the system (such as reboiler, heaters and reformer). It should be noted that the temperature of the exhaust gas to the environment should be higher than the dew point of water to avoid water condensation, which may cause corrosion due to acidic condensate in pipelines. For efficient heat utilization in the system, the exothermic heat from the SOFC stack (Q_5) and the afterburner (Q_6) were supplied to the energy-consuming units of the SOFC system (the heaters (Q_1, Q_2 and Q_3) and the reformer (Q_4)). The net useful heat from the SOFC system ($Q_{SOFC,Net}$) was defined as the difference between the exothermic heat (SOFC stack and afterburner) and the endothermic heat (preheaters and reformer) of the SOFC system. Generally, $Q_{SOFC,Net}$ was positive and could be further utilized for the distillation column. The net useful heat (Q_{Net}) of the SOFC–DIS system was calculated as the difference between the net useful heat of the SOFC system ($Q_{SOFC,Net}$) and the distillation energy (Q_D), in this case the reboiler heat duty. For energy calculation, the heat involved in each unit can be calculated using a conventional energy balance. The overall electrical efficiency was calculated as follows:

$$\eta_{elec,ov} = \frac{IV}{n_{EtOH} \times LHV_{EtOH}} \quad \text{when } Q_{Net} \geq 0 \tag{13}$$

$$\eta_{elec,ov} = \frac{IV}{(n_{EtOH} \times LHV_{EtOH}) - Q_{Net}} \quad \text{when } Q_{Net} \leq 0 \tag{14}$$

where n_{EtOH} represents the total ethanol flow rate fed to the distillation column. For $Q_{Net} \leq 0$, the SOFC–DIS system required more energy from an external heat source. To calculate the actual overall electrical efficiency, the energy required from the external heat source should be taken into account.

Table 2
Parameters of ohmic loss in SOFC cell components [5]

Materials	Parameters		Thickness (μm)
	α (Ω cm)	β (K)	
Anode (40% Ni/YSZ cermet)	2.98×10^{-5}	−1392	150
Cathode (Sr-doped $LaMnO_3$: LSM)	8.11×10^{-5}	600	2000
Electrolyte (Y_2O_3-doped ZrO_2: YSZ)	2.94×10^{-5}	10350	40
Interconnect (Mg-doped $LaCrO_3$)	1.256×10^{-3}	4690	100

3. Results and discussion

3.1. Effect of ethanol concentration on SOFC performance and energy requirement in the distillation column

It is impractical to directly reform bioethanol to generate a fuel gas for an SOFC stack due to the high water content [22]. Fig. 2 shows the performance curves of SOFCs fed by various reformed gases from the reforming of ethanol at different concentrations. The SOFC operated at a T_{SOFC} of 1200 K with a fuel utilization (U_f) of 80%. From Fig. 2 it is clear that the power density, cell voltage and electrical efficiency increase with increasing ethanol concentration. This implies that the SOFC stacks perform better when a distillation column is integrated with the SOFC system to purify the bioethanol. However, in practice, the maximum ethanol concentration should be kept below the range of carbon formation to avoid deactivation of the reforming catalyst and anode of the SOFC cell. For example, at T_{RF} = 1023 K, the boundary of carbon formation was at 41 mol% [20].

Although it is advantageous to use ethanol at high concentrations for the SOFC system, an additional energy is required to concentrate the bioethanol. Fig. 3 shows the minimum reboiler and condenser heat duties as a function of ethanol purity and recovery. It is clear that more energy is required when the distillation column is operated to achieve higher ethanol concentration and recovery. The reboiler and condenser heat duties increase dramatically at low ethanol purity and rises steadily at the higher ethanol purity. This is due to a narrow vapor–liquid equilibrium gap for ethanol–water mixture at low ethanol purity and a wider vapor–liquid gap at higher purity.

3.2. Performance of the SOFC system integrated with a distillation column (SOFC–DIS) at base case conditions

Fig. 4 indicates the temperature and energy requirement for all important units in the SOFC–DIS system operating at base

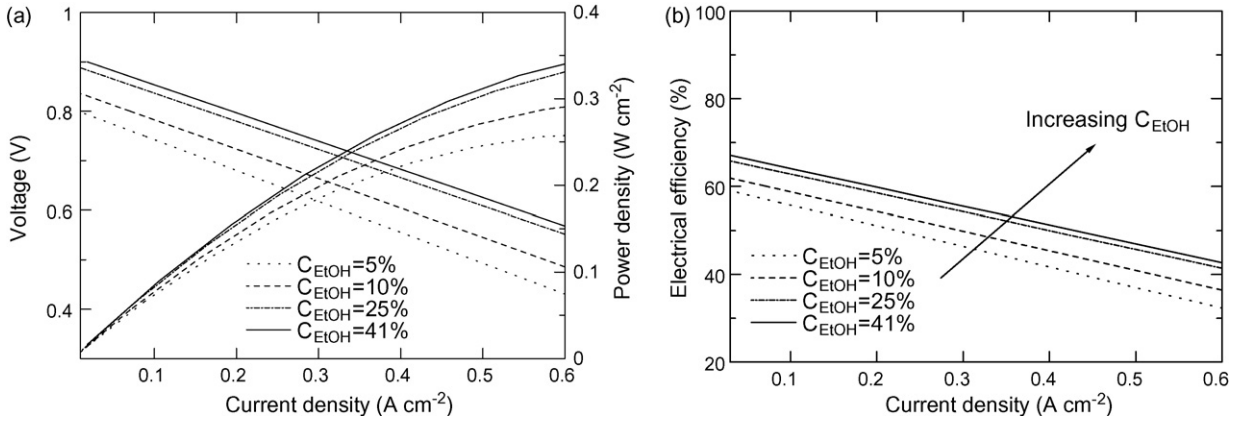

Fig. 2. Effect of ethanol concentration on SOFC performance: (a) voltage and power density and (b) electrical efficiency ($U_f = 80\%$ and $P = 101.3$ kPa).

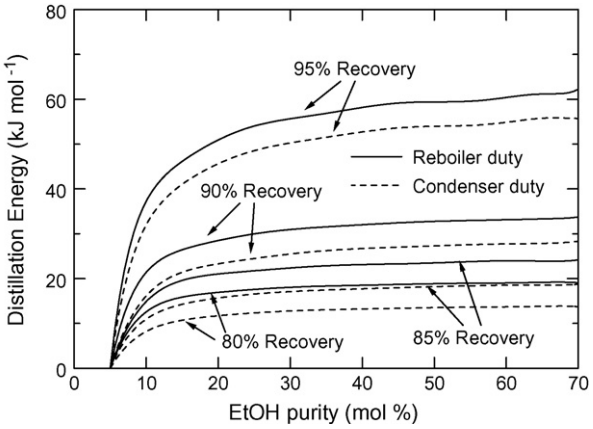

Fig. 3. Effect of ethanol concentration and ethanol recovery on distillation energy.

Table 3
Summary of operating conditions and the performance of SOFC for the base case

Parameter	Value/quality
Bioethanol flow rate (mol s^{-1})	8.42
Ethanol recovery (%)	80
Fuel option	Bioethanol with 5 mol% EtOH in water
Reforming temperature (K)	1023
SOFC temperature (K)	1200
Fuel utilization (%)	80
Voltage (V)	0.7
Power (kW)	218.77
Q_{Net} (kW)	−60.75
Overall electrical efficiency (%)	37.72

case conditions, i.e. $C_{EtOH} = 25$ mol%, EtOH recovery = 80%, cell operating voltage = 0.7 V and $U_f = 80\%$. An electrical power (W_e) of 218.77 kW with an overall electrical efficiency (based on LHV) of 37.72% was achieved. The net useful heat of the SOFC system ($Q_{SOFC,Net}$) and the heat required for the distillation column (Q_D) are 88.36 and 149.11 kW, respectively. In this case, although $Q_{SOFC,Net}$ can be used for supplying heat to the reboiler directly, it is obvious that the amount of $Q_{SOFC,Net}$ is not enough for the required Q_D under these base conditions. The conditions and the performance of SOFC–DIS system (power, power density, Q_{Net}) at the base case are presented in Table 3. However, by carefully adjusting the operating conditions such as operating voltage, fuel utilization, ethanol concentration and recovery, excess heat from the SOFC system can be increased to satisfy the energy requirements of the reboiler in the distillation column. A proper adjustment of these operating conditions for the system to be self-sufficient ($Q_{Net} = Q_{SOFC,Net} - Q_D = 0$) is the subject of the subsequent sections.

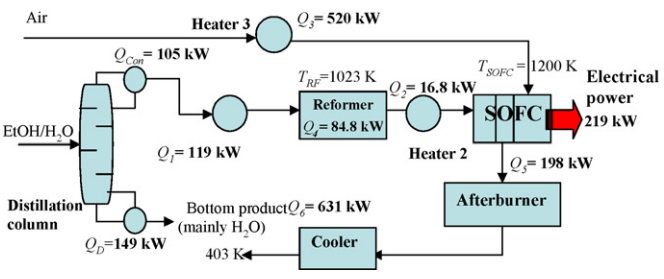

Fig. 4. Energy and temperature for various units in the SOFC–DIS system (EtOH recovery = 80%, $C_{EtOH} = 25$ mol%, $U_f = 80\%$, and $P = 101.3$ kPa).

3.3. Effects of operating parameters

3.3.1. Effects of SOFC operating voltage and fuel utilization

Fig. 5 represents the effect of operating voltage and fuel utilization on the overall efficiency and electrical power, W_e, (Fig. 5a), net useful heat, Q_{Net}, (Fig. 5b) and power density (Fig. 5c). As mentioned earlier, Q_{Net} is $Q_{SOFC,Net}$ subtracted by Q_D. Therefore, the value of Q_{Net} can be positive, zero or negative. A positive value of Q_{Net} indicates that some extra heat is left from the overall SOFC–DIS system. For the case where Q_{Net} is negative, $Q_{SOFC,Net}$ is not enough to supply all the required heat to the distillation column; therefore, an external heat source is required. At the point where Q_{Net} is equal to zero, $Q_{SOFC,Net}$ satisfies exactly the reboiler demand. Consequently, this condition offers the maximum electrical power for the SOFC–DIS system without requiring an external heat source. From Fig. 5b it can be seen that higher Q_{Net} (i.e. the system becomes more energy sufficient) can be obtained when the SOFC–DIS system operates

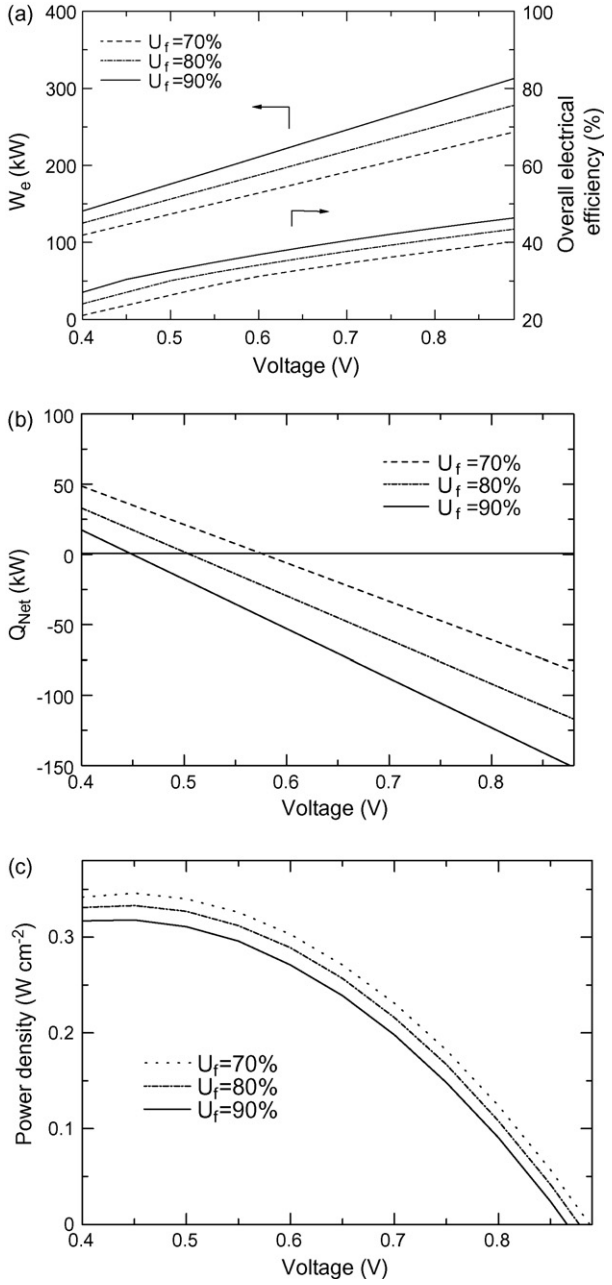

Fig. 5. Effect of operating voltage and U_f on SOFC–DIS performance: (a) W_e and overall efficiency, (b) Q_{Net} and (c) power density (EtOH recovery = 80%, C_{EtOH} = 25 mol%, and P = 101.3 kPa).

at lower voltage and/or lower fuel utilization. For lower voltage operation, the difference between the theoretical voltage and the actual one is large and results in higher heat losses emitted from the SOFC stack and therefore, Q_{Net} increases. For operation at a lower fuel utilization, more unreacted fuel exiting the SOFC stack is burnt in the afterburner. This leads to higher combustion energy and, as a result, higher Q_{Net}. However, lower electrical power and overall efficiency are obtained at higher Q_{Net}. There is an appropriate voltage for which $Q_{Net} = 0$ for U_f ranging from 70 to 90% (at C_{EtOH} = 25% and EtOH recovery = 80%). The corresponding voltages are 0.58, 0.51 and 0.45 V, for U_f = 70, 80 and 90%, respectively. Operation at higher fuel utilization requires lower operating voltage for generating more heat from the stack to compensate for the heat required in the overall system.

Another important SOFC performance indicator, which should be of concern, is the power density. The effects of voltage and fuel utilization on power density are shown in Fig. 5(c). An operation at low voltage is of no practical value (hence, not shown in Fig. 5). However, at high voltage Fig. 5c shows a rapid decrease in power density, resulting in larger (increased area) and more expensive SOFC stacks. Fig. 5b and c also indicate that for voltages corresponding to Q_{Net} equal to zero, the power densities are equal to 0.31, 0.33 and 0.32 W cm^{-2} for U_f = 70, 80 and 90%, respectively, which also corresponds to an overall electrical efficiency of 30.3% for all fuel utilizations. The fuel utilization factor (at least in the range of 70–90%) has thus no notable influence on the overall electrical efficiency and power density when Q_{Net} is kept at zero (at constant ethanol concentration).

In summary, the SOFC–DIS system can be made self-sufficient by adjusting the fuel utilization and operating voltage. However, it should be noted that a number of operating parameters must be carefully examined. An operation of SOFC at too low voltage may result in a significant reduction in power density. Moreover, the excessive heat generated in the stack will directly damage the thermophysical property of the SOFC cell components and raises the issue of how to remove this high amount of heat from the stack. It is recommended that adjusting fuel utilization is a better option to control $Q_{SOFC,Net}$. Also, for practical operation, the electrical power, overall efficiency and power density should be acceptably high.

3.3.2. *Effect of ethanol concentration*

From the previous section, it was found that an adjustment of voltage and fuel utilization can render the system self-sufficient. However, Q_{Net} also depends on the amount of required distillation energy (Q_D), which is strongly influenced by ethanol concentration (C_{EtOH}) and ethanol recovery (Fig. 3). In this section, the effect of ethanol concentration on electrical performance (W_e, overall efficiency, and corresponding voltage and power density) at conditions for which $Q_{Net} = 0$ is investigated. The ethanol recovery was kept at 80%. The results shown in Fig. 6(a) indicate that, for ethanol concentrations between 15 and 41%, W_e, and overall efficiency increase with increasing ethanol concentration, independent of the fuel utilization (U_f = 70–80%). We know that increasing ethanol concentration is beneficial in terms of power produced, but is detrimental in terms of energy demand in the column reboiler (see Fig. 3). Fig. 6a illustrates the fact that, for ethanol concentrations between 15 and 41%, the benefit of increasing ethanol concentration is more important than the negative effect of increased reboiler duty. This could be explained by the relatively gentle increase in reboiler duty for ethanol concentrations greater than 15%, as seen in Fig. 3. The effect of fuel utilization on SOFC performance when Q_{Net} equals zero is also presented in Fig. 6(b). It can be seen that the SOFC would run at lower voltage for an operation at higher fuel utilization. This result is in good agreement with the results described earlier. It can be seen that the operating voltage is around 0.6 and 0.5 V at U_f = 70 and 80%,

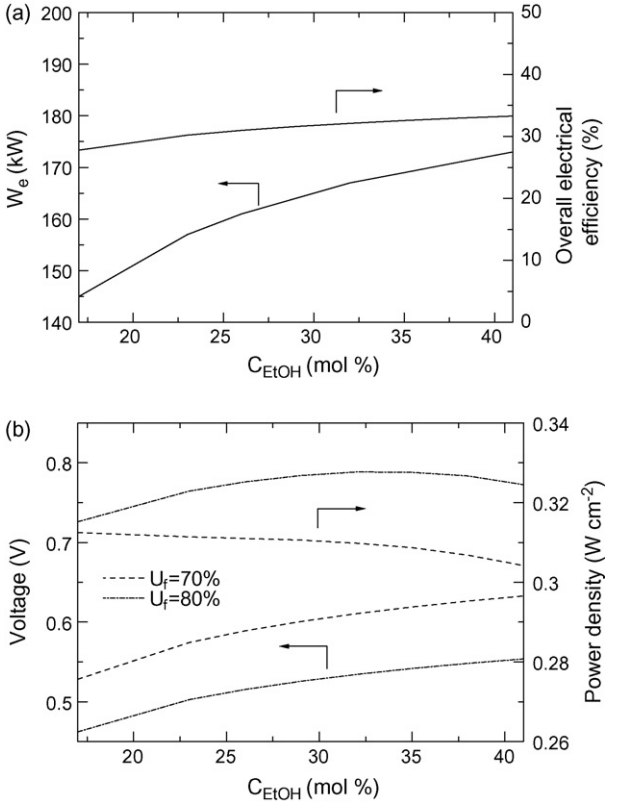

Fig. 6. Effect of ethanol concentration on SOFC–DIS performance for various U_f when $Q_{Net} = 0$: (a) W_e and overall efficiency and (b) corresponding voltage and power density (EtOH recovery = 80%, and $P = 101.3$ kPa).

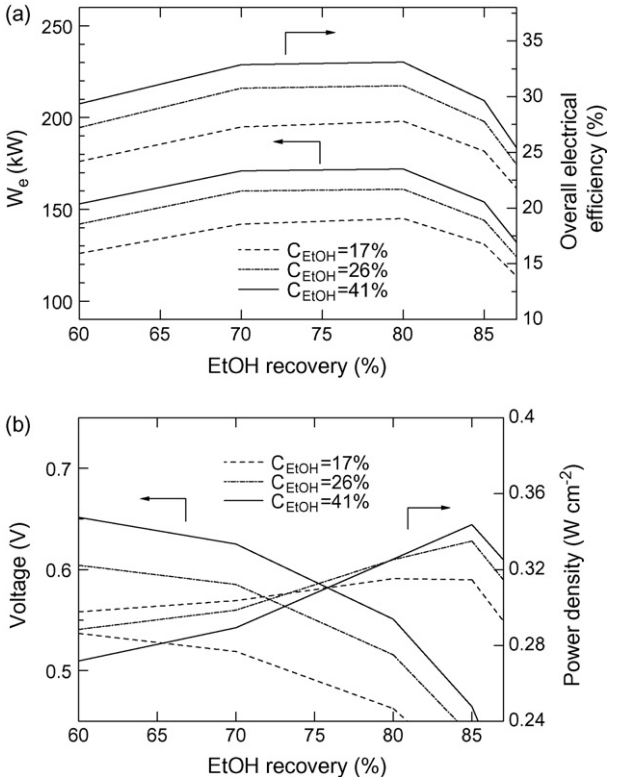

Fig. 7. Effect of ethanol recovery on SOFC–DIS performance when $Q_{Net} = 0$ at different C_{EtOH}: (a) W_e and overall efficiency, and (b) corresponding voltage and power density ($U_f = 80\%$ and $P = 101.3$ kPa).

respectively. Fig. 6(b) also presents the effect of ethanol concentration on power density. For $U_f = 80\%$, the power density slightly increases when operated at higher C_{EtOH} whereas the opposite is true for $U_f = 70\%$. As expected, the power density is consistently higher at $U_f = 80\%$ than at 70%.

In summary, Fig. 6 indicates that, when keeping Q_{Net} equals to zero, better overall performance (higher overall electrical efficiency, higher power density) is achieved when operating at higher fuel utilization factor (e.g. 80%) and at the highest possible ethanol concentration (i.e. 41%). At these conditions, the overall efficiency reaches 33.3% and the power density 0.32 W cm^{-2} (corresponding to a voltage of 0.55 V and current density of 0.58 A cm^{-2}). It should be noted that in this study the SOFC cell is based on the tubular configuration. In a practical operation, a planar SOFC with higher current densities may be an attractive choice.

3.3.3. *Effect of ethanol recovery*

As mentioned earlier, an ethanol recovery is an important parameter affecting Q_D and the overall energy within the system. Fig. 7(a) presents the effect of ethanol recovery on W_e and overall efficiency at different ethanol concentrations for $Q_{Net} = 0$. Higher W_e and overall efficiency are obtained when increasing the ethanol recovery up to 80%; however, the performance significantly decreases at ethanol recoveries greater than 80%. This is because of the competition between an increase of current and a decrease of operating voltage at that point. By increasing the ethanol recovery, this effect also increases the current at the same fuel utilization while the operating voltage is also dependent on the required Q_D. It can be seen that at lower ethanol recovery, the required operating voltage is slightly changed due to a small change in Q_D. Therefore, the electrical power becomes higher because of the increase in current. However, at high ethanol recovery, Q_D is dramatically increased and causes a sudden drop in voltage as shown in Fig. 7(b). This results in a decrease in electrical power. The corresponding voltage and power density at different EtOH recovery is also shown in Fig. 7(b). It can be seen that an increase of ethanol recovery still requires lower voltage. The SOFC–DIS system still needs some energy from the SOFC stack to compensate for the higher demand in Q_D. This is different from the results in Fig. 6(b), which shows that lower voltage is not required because the SOFC–DIS system gain some benefits from the less preheating energy for EtOH/H_2O mixture. For the effect of ethanol recovery, more ethanol and water are fed to the SOFC–DIS system when operated at higher ethanol recovery. More energy is therefore required for the reformer and EtOH/H_2O preheater. The SOFC stack has to be operated at lower voltages to compensate for the heat, which results in a decrease in voltage as shown in Fig. 7(b). Moreover, it was found that at higher EtOH recovery, a higher power density is obtained.

From the above studies, it is possible to operate the SOFC–DIS system in an energy sufficient mode. The obtained efficiency and power density of SOFC–DIS system are 33.3% and 0.32 W cm^{-2} at $C_{ETOH} = 41\%$, $U_f = 80\%$ and ethanol recov-

ery = 80%. The reboiler heat duty is the limit in achieving a higher performance because the SOFC–DIS has to be operated under inferior conditions in order to provide the required heat to the distillation column. Moreover, a large amount of heat (105 kW) was emitted from the SOFC–DIS at the condenser. The management of this condenser duty could be used to enhance the SOFC–DIS performance and allow the SOFC to operate at more optimal conditions. It is expected that the performance of SOFC–DIS could be further improved.

4. Conclusions

An SOFC system integrated with a distillation column (SOFC–DIS) was studied. Bioethanol was used as a feed stream for the SOFC–DIS system. The influence of operating parameters (EtOH concentration, EtOH recovery, cell operating voltage and fuel utilization) on electrical performance (e.g. electrical power, overall efficiency and power density) and thermal energy involved in the SOFC system (e.g. reboiler heat duty and the net useful heat) was presented. The study showed that it is possible to operate the SOFC–DIS system in an energy self-sufficient mode by adjusting the operating voltage and/or fuel utilization. The effect of ethanol concentration (17–41 mol%) and ethanol recovery at the energy-sufficient point ($Q_{Net} = 0$) was presented. It was found that higher ethanol concentration yielded higher electrical power (for C_{EtOH} in the range of 15–17%), higher overall electrical efficiency and acceptably high power density. For the effect of ethanol recovery, there is an optimum ethanol recovery at 80%, which yielded the optimum electrical power and overall electrical efficiency. Higher power densities can be obtained when operating at higher ethanol recoveries. In brief, this thermodynamic study of the SOFC–DIS system showed the potential of the system when operated without external heat sources. However, the obtained performance of the SOFC–DIS system was quite low (0.32 W cm^{-2}, 173.07 kW, 33.3% overall efficiency based on total ethanol flow rate fed to SOFC–DIS system at $U_f = 80\%$, EtOH recovery = 80% and $C_{EtOH} = 41\%$). It was found that the reboiler heat duty was the limit of the SOFC–DIS system. Moreover, a huge amount of heat was lost at the condenser. To improve the performance of the SOFC–DIS system, it is recommended that (1) the heat emitted at a condenser should be utilized for other purposes and (2) another purifying process (e.g. membranes) which consumes less energy should be investigated.

Acknowledgements

The support from the Thailand Research Fund, Commission of Higher Education and National Metal and Materials Technology Center (MTEC) are gratefully acknowledged.

References

[1] EG&G Service Parsons Inc., Fuel Cell Handbook, 5th ed., Science Applications International Corporation, Morgantown, WV, 2000, pp. 234.
[2] J. Palsson, A. Selimovic, L. Sjunnesson, J. Power Sources 86 (2000) 442–448.
[3] B. Fredriksson Möller, J. Arriagada, M. Assadi, I. Potts, J. Power Sources 131 (2004) 320–326.
[4] Y. Inui, T. Matsumae, H. Koga, K. Nishiura, Energy Convers. Manage. 46 (2005) 1837–1847.
[5] S.H. Chan, C.F. Low, O.L. Ding, J. Power Sources 103 (2002) 188–200.
[6] E. Fontell, T. Kivisaari, N. Christiansen, J.B. Hansen, J. Pålsson, J. Power Sources 131 (2004) 49–56.
[7] W. Zhang, E. Croiset, P.L. Douglas, M.W. Fowler, E. Entchev, Energy Convers. Manage. 46 (2005) 181–196.
[8] A.O. Omosun, A. Bauen, N.P. Brandon, C.S. Adjiman, D. Hart, J. Power Sources 131 (2004) 96–106.
[9] G. Maggio, S. Freni, S. Cavallar, J. Power Sources 74 (1998) 17–23.
[10] P. Tsiakaras, A. Demin, J. Power Sources 102 (2001) 210–217.
[11] S. Douvartzides, F.A. Coutelieris, P.E. Tsiakaras, J. Power Sources 114 (2003) 203–212.
[12] S. Douvartzides, F. Coutelieris, P. Tsiakaras, J. Power Sources 131 (2004) 224–230.
[13] D.J. Shell, C.J. Riley, N. Dowe, J. Farmer, K.N. Ibson, M.F. Ruth, S.T. Toon, R.E. Lumpkin, Bioresour. Technol. 91 (2004) 179–188.
[14] C.A. Cardona Alzate, O.J. Sanchez Toro, Energy 31 (2006) 2447–2459.
[15] P.L. Roger, K.J. Lee, D.E. Tribe, Process Biochem. (1980) 7–11.
[16] S.E. Buchholz, M.M. Dooley, D.E. Eveleigh, Trends Biotechnol. 5 (1987) 199–204.
[17] E. Achenbach, J. Power Sources 49 (1994) 333–348.
[18] E. Hernandez-Pachenco, D. Singh, P.N. Hutton, N. Patel, M.D. Mann, J. Power Sources 138 (2004) 174–186.
[19] M.C. Williams, J.P. Starkey, S.C. Singhal, J. Power Sources 131 (2004) 79–85.
[20] S. Assabumrungrat, V. Pavarajarn, S. Charojrochkul, N. Laosiripojana, Chem. Eng. Sci. 59 (2004) 6015–6020.
[21] W. Jamsak, S. Assabumrungrat, P.L. Douglas, N. Laosiripojana, S. Charojrochkul, Chem. Eng. J. 119 (2006) 11–18.
[22] S.L. Douvartzides, F.A. Coutelieris, A.K. Demin, P.E. Tsiakaras, AIChE J. 49 (2003) 248–257.

Appendix 5

Available online at www.sciencedirect.com
ScienceDirect
Journal of Power Sources 159 (2006) 1274–1282
JOURNAL OF POWER SOURCES
www.elsevier.com/locate/jpowsour

Determination of the boundary of carbon formation for dry reforming of methane in a solid oxide fuel cell

S. Assabumrungrat [a,*], N. Laosiripojana [b], P. Piroonlerkgul [a]

[a] *Center of Excellence in Catalysis and Catalytic Reaction Engineering, Department of Chemical Engineering, Faculty of Engineering, Chulalongkorn University, Bangkok 10330, Thailand*
[b] *The Joint Graduate School of Energy and Environment, King Mongkut's University of Technology Thonburi, Bangkok 10140, Thailand*

Received 8 November 2005; received in revised form 14 December 2005; accepted 15 December 2005
Available online 20 January 2006

Abstract

The boundary of carbon formation for the dry reforming of methane in direct internal reforming solid oxide fuel cells (DIR-SOFCs) with different types of electrolyte (i.e., an oxygen ion-conducting electrolyte (SOFC-O^{2-}) and a proton-conducting electrolyte (SOFC-H^+)) was determined by employing detailed thermodynamic analysis. It was found that the required CO_2/CH_4 ratio decreased with increasing temperature. The type of electrolyte influenced the boundary of carbon formation because it determined the location of water formed by the electrochemical reaction. The extent of the electrochemical reaction also played an important role in the boundary of carbon formation. For SOFC-O^{2-}, the required CO_2/CH_4 ratio decreased with the increasing extent of the electrochemical reaction due to the presence of electrochemical water in the anode chamber. Although for SOFC-H^+ the required CO_2/CH_4 ratio increased with the increasing extent of the electrochemical reaction at high operating temperature ($T > 1000$ K) following the trend previously reported for the case of steam reforming of methane with addition of water as a carbon suppresser, an unusual opposite trend was observed at lower operating temperature. The study also considered the use of water or air as an alternative carbon suppresser for the system. The required H_2O/CH_4 ratio and air/CH_4 ratio were determined for various inlet CO_2/CH_4 ratios. Even air is a less attractive choice compared to water due to the higher required air/CH_4 ratio than the H_2O/CH_4 ratio; however, the integration of exothermic oxidation and the endothermic reforming reactions may make the use of air attractive. Water was found to be more effective than carbon dioxide in suppressing the carbon formation at low temperatures but their effect was comparable at high temperatures. Although the results from the study were based on calculations of the SOFCs with different electrolytes, they are also useful for selecting suitable feed compositions for other reactors; including conventional reformers and membrane reactors with hydrogen removal.

Keywords: Solid oxide fuel cell; Carbon formation; Thermodynamic analysis; Dry reforming of methane

1. Introduction

A solid oxide fuel cell (SOFC) is a more efficient electrical power generator than many conventional processes. Due to its high operating temperature, it offers wide potential applications, flexibility of fuel choices, possibility for operation with an internal reformer and a high system efficiency. Recent developments on SOFCs seem to move towards to two main issues: intermediate temperature operation and the use of other fuels instead of hydrogen. The uses of various alternative fuels; e.g., natural gas, bio-ethanol, coal, biomass, biogas, methanol, gasoline and other oil derivatives, in SOFCs have been investigated [1–3]. As SOFCs are operated at high temperatures, these fuels can be internally reformed at the anode side of SOFCs producing a H_2-CO rich gas, which is eventually used to generate the electrical energy and heat. This operation is called a direct internal reforming (hence, DIR-SOFCs). Regarding the global environmental problems and current fossil fuel concerns, the development of SOFCs fed by renewable fuels attract more attention as an alternative method for power generation in the near future. Among renewable sources, biogas is a promising candidate, since it is produced readily from the fermentation of biomasses and agricultural wastes. Typically, biogas consists mainly of methane and carbon dioxide. Due to the rich CO_2 in biogas, carbon dioxide (or dry) reforming reaction would be one of the most suitable processes to convert biogas to hydrogen or

* Corresponding author. Tel.: +66 2 218 6868; fax: +66 2 218 6877.
E-mail address: Suttichai.A@chula.ac.th (S. Assabumrungrat).

0378-7753/$ – see front matter © 2006 Elsevier B.V. All rights reserved.
doi:10.1016/j.jpowsour.2005.12.010

Nomenclature

a	inlet moles of methane (mol)
b	inlet moles of carbon dioxide (mol)
c	inlet moles of steam (mol)
d	inlet moles of inert (mol)
e	extent of the electrochemical reaction of hydrogen (mol)
K_1	equilibrium constant of reaction (16) (kPa)
K_2	equilibrium constant of reaction (17) (kPa)
K_3	equilibrium constant of reaction (18) (kPa)
n_i	number of moles of component i (mol)
p_i	partial pressure of component i (kPa)
x	converted moles associated with reaction (1) (mol)
y	converted moles associated with reaction (2) (mol)
z	converted moles associated with reaction (3) (mol)

Greek letter

α_c	carbon activity

synthesis gas (CO and H_2) for later utilization in SOFCs or other processes.

However, in order to operate SOFCs on the direct feed of alternative fuels (i.e., biogas) rather than hydrogen, several major problems remain to be solved. One of them is the problem of carbon deposition on the anode, causing loss of active sites and cell performance as well as poor durability. The growth of carbon filaments attached to the anode crystallites can generate massive forces within the electrode structure leading to rapid breakdown [4]. A number of efforts have been carried out to alleviate this problem. One approach is to search for appropriate anode formulations and operating conditions. A number of additives were added to the anode to lower the rate of carbon formation. For example, the addition of molybdenum and cerium metal oxides to the Ni-based anode was reported to reduce carbon deposition, and in some cases, to increase fuel conversion [5,6]. The addition of alkalis such as potassium can accelerate the reaction of carbon with steam and also neutralize the acidity of the catalyst support, hence reducing carbon deposition [7].

Another conventional approach to avoid carbon deposition is the addition of extra oxidant to the feed. According to the dry reforming of methane, it was suggested that the use of excess carbon dioxide in the dry reforming reaction could avoid carbon formation [8]. Experimental studies on dry reforming using an excess of carbon dioxide with carbon dioxide to methane (CO_2/CH_4) ratios of 3/1 and 5/1 over a nickel catalyst supported on alumina were carried out. It was reported that the rate of disintegration is smaller for the case with higher ratio. Selection of a suitable CO_2/CH_4 ratio is therefore an important issue [9,10]. Carbon formation can occur when the SOFCs are operated at low CO_2/CH_4 ratios. However, use of high CO_2/CH_4 ratios is unattractive as it lowers the electrical efficiency of the SOFCs by the dilution of fuel, the yield of hydrogen production and the system efficiency. Consequently, it is necessary to find the CO_2/CH_4 ratio at the boundary of carbon formation at which represents the minimum ratio required to operate the SOFCs in a carbon-free condition.

In this paper, a detailed thermodynamic analysis is carried out to predict the boundary of carbon formation for DIR-SOFCs fueled by mixtures of methane and carbon dioxide. The effects of electrolyte type (i.e., oxygen ion-conducting and proton-conducting electrolytes), operating temperature, and extent of electrochemical reaction on the required CO_2/CH_4 ratio have been investigated. Our previous work employed thermodynamic calculations to predict the required H_2O/fuel ratio for SOFCs fed by methane [11] and methanol [12]. It was found that the SOFCs with an oxygen-conducting electrolyte (SOFC-O^{2-}) require less H_2O/fuel ratio than those with a hydrogen-conducting electrolyte (SOFC-H^+) because extra water generated from the electrochemical reaction is available for use in the anode chamber. In this present work, alternative methods to alleviate the carbon formation by adding water or air to the system were considered as it is practical to add these components along with methane and carbon dioxide in the feed to reduce the degree of carbon deposition.

2. Theory

The main reaction involved in the production of hydrogen from methane and carbon dioxide is the dry reforming of methane (Eq. (1)). When the SOFC is operated using an oxygen ion-conducting electrolyte, water is also generated by the electrochemical reaction of hydrogen and oxygen ion, and therefore, the steam reforming of methane (Eq. (2)) and the water gas shift reaction (WGS) (Eq. (3)) also take place.

$$CH_4 + CO_2 = 2H_2 + 2CO \quad (1)$$

$$CH_4 + H_2O = 3H_2 + CO \quad (2)$$

$$CO + H_2O = H_2 + CO_2 \quad (3)$$

The dry and steam reforming reactions are strongly endothermic while the WGS is mildly exothermic. Both steam and dry reforming reactions have similar thermodynamic characteristics except that the carbon formation in the dry reforming is more severe than in the steam reforming due to the lower H/C ratio of this reaction [13]. The activities toward steam and dry reforming over several catalysts were investigated [14]. It was observed that replacing water with carbon dioxide gave similar activation energies, which indicated a similar rate-determining step in these two reactions. Nickel and cobalt are usually applied as the catalysts for this reaction. The dry reforming reaction with a stoichiometric feed ratio over several catalysts was studied [15]. It was found that Ni/SiO_2 exhibited this reaction near equilibrium and had high selectivity to carbon monoxide. The activity of the catalyst over other supports was found to be deactivated rapidly due to carbon deposition.

When a SOFC is operated with an internal reformer, hydrogen produced from the reforming process is consumed simultaneously by the electrochemical reaction generating electricity. Theoretically, two types of solid electrolytes can be employed in the SOFC: oxygen ion- and proton-conducting electrolytes. The reactions taking place in the anode and the cathode can be summarized as follows:

Oxygen ion-conducting electrolyte:

Anode:

$$H_2 + O^{2-} = H_2O + 2e^- \quad (4)$$

$$CO + O^{2-} = CO_2 + 2e^- \quad (5)$$

Cathode:

$$O_2 + 4e^- = 2O^{2-} \quad (6)$$

Proton-conducting electrolyte:

Anode:

$$H_2 = 2H^+ + 2e^- \quad (7)$$

Cathode:

$$2H^+ + \tfrac{1}{2}O_2 + 2e^- = H_2O \quad (8)$$

The difference between the SOFCs with the two electrolyte types is the location of the water produced. For the SOFC with the oxygen ion-conducting electrolyte (SOFC-O^{2-}), water is produced in the anode chamber whereas it appears in the cathode chamber for the SOFC with the proton-conducting electrolyte (SOFC-H^+). It should be noted that for the SOFC-H^+, carbon monoxide cannot be electrochemically consumed. It is, therefore, not so practical to use only the dry reforming of methane in the SOFC-H^+ unless water is included in the feed to enhance the hydrogen production by steam reforming (Eq. (2)) and WGS (Eq. (3)). For the SOFC-O^{2-}, both hydrogen and carbon monoxide can electrochemically react with oxygen. However, the electrochemical reaction of hydrogen is much faster than that of CO [16]. Therefore, in this study it was assumed that only hydrogen reacts electrochemically with oxygen supplied from the cathode side. For comparative purpose between the SOFCs with different electrolytes, only the range of possible electrochemical reaction from hydrogen in the SOFC-H^+ was considered in the study.

The number of moles of each component in the anode gas mixture is given by the following expressions:

$$n_{CH_4} = a - x - y \quad (9)$$

$$n_{CO_2} = b - x + z \quad (10)$$

$$n_{CO} = 2x + y - z \quad (11)$$

$$n_{H_2} = 2x + 3y + z - e \quad (12)$$

$$n_{H_2O} = c - y - z + e \text{ (for oxygen ion-conducting electrolyte)}$$
$$n_{H_2O} = c - y - z \text{ (for proton-conducting electrolyte)} \quad (13)$$

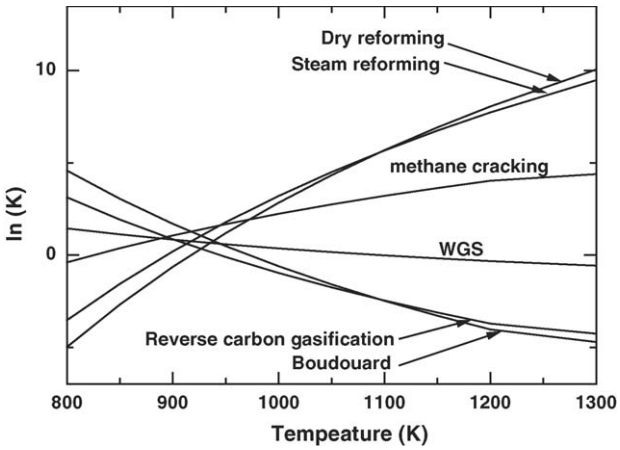

Fig. 1. Values of the equilibrium constants.

$$n_{inert} = d \quad (14)$$

$$n_{total} = \sum_{i-1}^{6} n_i \quad (15)$$

where a, b, c and d represent the inlet moles of methane, carbon dioxide, steam and inert respectively, e the extent of the electrochemical reaction of hydrogen, and x, y and z represent the converted moles associated to the reactions (1)–(3), respectively. The thermodynamic equilibrium composition can be determined by solving a system of nonlinear equations relating the moles of each component to the equilibrium constants of the reactions whose values are given in Fig. 1.

The following reactions are the most probable carbon formation reactions in the system [17]:

$$2CO = CO_2 + C \quad (16)$$

$$CH_4 = 2H_2 + C \quad (17)$$

$$CO + H_2 = H_2O + C \quad (18)$$

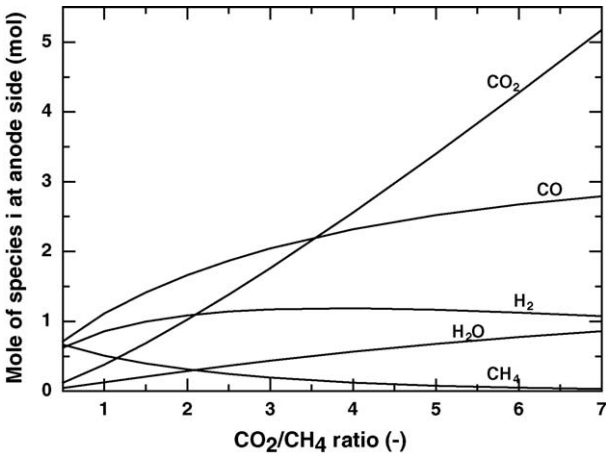

Fig. 2. Effect of inlet CO_2/CH_4 ratio on the moles of each component in a conventional reformer (a = 1 mol, P = 101.3 kPa and T = 900 K).

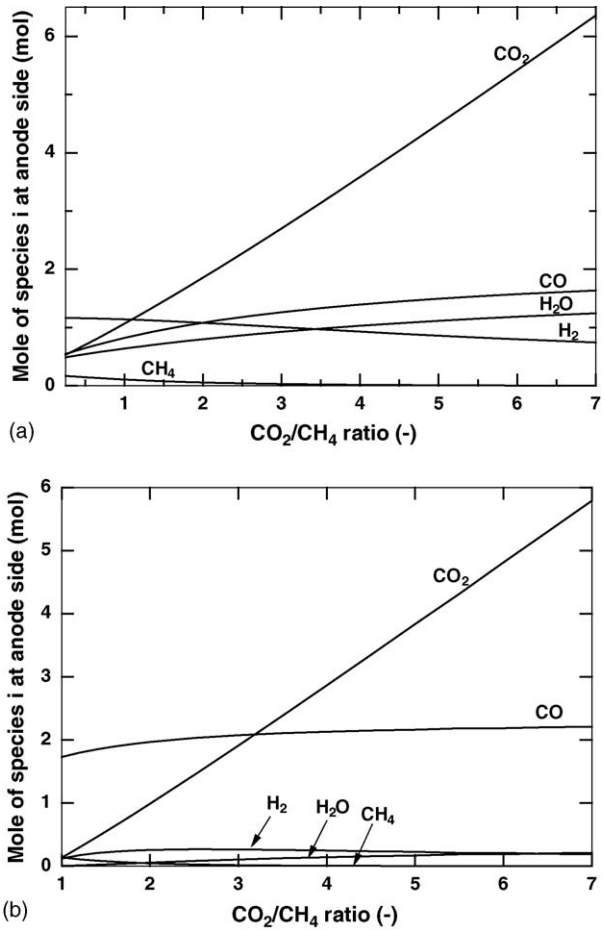

Fig. 3. Effect of inlet CO_2/CH_4 ratio on the moles of each component: (a) SOFC-O^{2-} and (b) SOFC-H^+ ($a = 1$ mol, $e = 1.6$ mol, $P = 101.3$ kPa and $T = 900$ K).

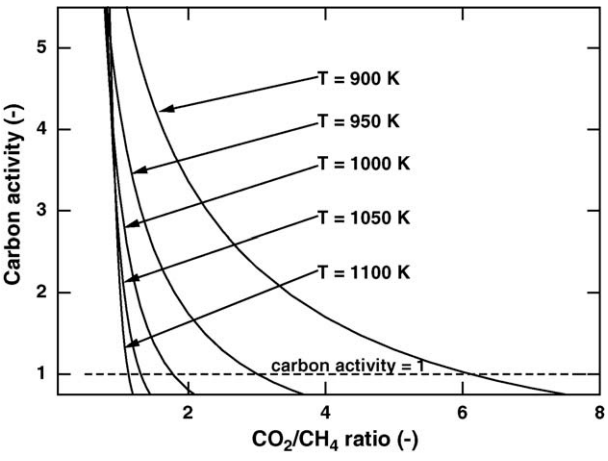

Fig. 4. Effect of inlet CO_2/CH_4 ratio on carbon activity ($a = 1$ mol, $e = 1.6$ mol, $P = 101.3$ kPa and $T = 900$ K).

It should be noted that due to the endothermic nature of the dry reforming of methane (Eq. (1)) and the mildly exothermic nature of the WGS reaction (Eq. (3)), the amount of CO becomes significant at high operating temperatures [18]. All reactions are employed to examine the thermodynamic possibility of carbon formation by calculating the values of their carbon activities (α_c)

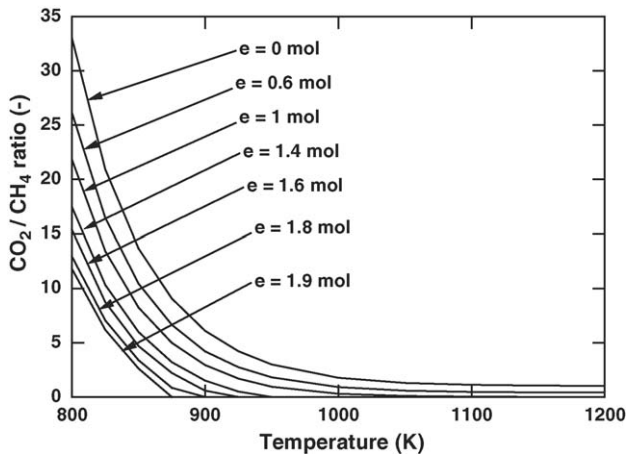

Fig. 5. Influence of the extent of the electrochemical reaction of H_2 on the requirement of the inlet CO_2/CH_4 ratio at different operating temperature (SOFC-O^{2-}, $a = 1$ mol and $P = 101.3$ kPa).

as defined in Eqs. (19)–(21).

$$\alpha_{c,\mathrm{CO}} = \frac{K_1 p_{\mathrm{CO}}^2}{p_{\mathrm{CO_2}}} \tag{19}$$

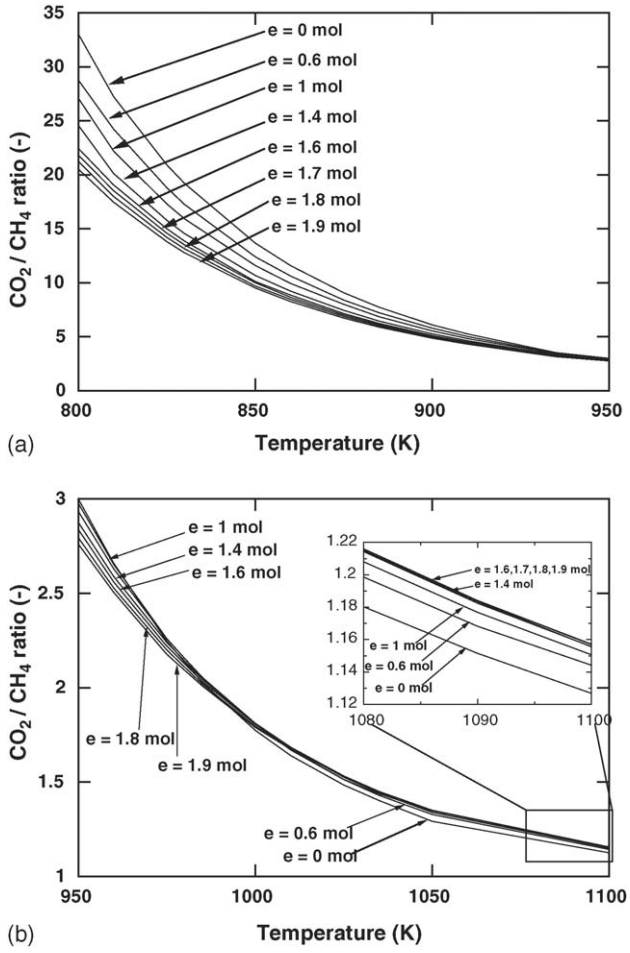

Fig. 6. Influence of the extent of electrochemical reaction of H_2 on the requirement of inlet CO_2/CH_4 ratio at different operating temperature: (a) $T = 800$–950 K and (b) 950–1100 K (SOFC-H^+, $a = 1$ mol and $P = 101.3$ kPa).

$$\alpha_{c,CH_4} = \frac{K_2 p_{CH_4}}{p_{H_2}^2} \quad (20)$$

$$\alpha_{c,CO\text{-}H_2} = \frac{K_3 p_{CO} p_{H_2}}{p_{H_2O}} \quad (21)$$

where K_1, K_2 and K_3 represent the equilibrium constants of the reactions (16)–(18), respectively, and p_i represents the partial pressure of component i. When $\alpha_c > 1$, the system is not in equilibrium and carbon formation is observed. The system is at equilibrium when $\alpha_c = 1$. It is noted that the carbon activity is only the indicator for the presence of carbon in the system. It does not give the information regarding the amount of carbon formed. Finally, when $\alpha_c < 1$, carbon formation is thermodynamically impossible.

To find the range of SOFC operation which does not suffer from the carbon formation, the operating temperature and the extent of the electrochemical reaction of hydrogen are specified. Then, the initial value of the CO_2/CH_4 ratio is varied and the corresponding values of α_c are calculated. The carbon formation boundary is defined as the value of CO_2/CH_4 ratio whose value of $(1 - \alpha_c)$ is approaching zero. This value represents the minimum inlet CO_2/CH_4 ratio at which carbon formation in the equilibrium mixture is thermodynamically impossible. When the inlet CO_2/CH_4 ratio is fixed at a certain value and water is added to the feed for the purpose of suppressing the carbon formation, the same calculation procedure can be applied to find the value of H_2O/CH_4 ratio whose value of $(1 - \alpha_c)$ is approaching zero. When air is employed instead of water, the calculation is carried out by assuming the complete combustion of oxygen in air with methane to yield water and carbon dioxide. Then the obtained feed composition is used to calculate the carbon activity. The value of air/CH_4 ratio is varied until the value of $(1 - \alpha_c)$ approaching zero is obtained.

It should be noted that although recent investigators have estimated the carbon concentration in the reforming reactions by the method of Gibbs energy minimization [19], the principle of equilibrated gas to predict the carbon formation in this study is still meaningful since the calculations are carried to find the carbon formation boundary where the carbon just begins to form. In addition, other factors such as mass and heat transfer or rate of reactions may also affect the prediction of the carbon formation boundary. Local compositions which allow the local carbon formation may exist, although the carbon formation is unfavorable according to the calculations based on equilibrium bulk compositions. Moreover, other forms of carbonaceous compounds such as C_nH_m may be formed and result in comparable damages.

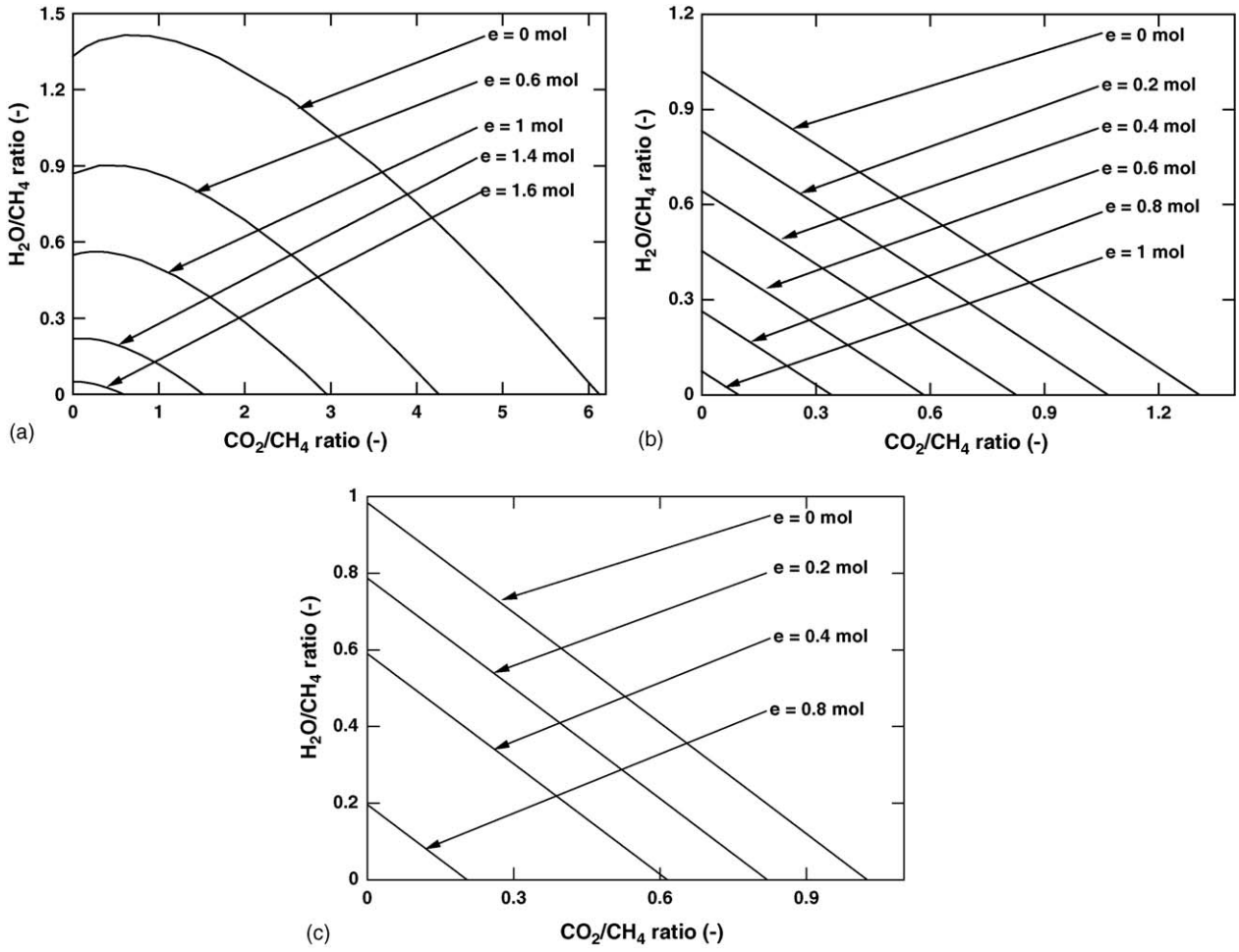

Fig. 7. Required inlet H_2O/CH_4 ratio at different inlet CO_2/CH_4 ratios: (a) $T = 900$ K, (b) $T = 1050$ K and (c) $T = 1200$ K (SOFC-O^{2-}, $a = 1$ mol and $P = 101.3$ kPa).

3. Results and discussion

The influences of the inlet CO_2/CH_4 ratio on equilibrium composition of the dry reforming reaction in a conventional reactor at the isothermal condition ($T = 900$ K) are shown in Fig. 2. It was found that the amounts of carbon monoxide and hydrogen increased with increasing moles of carbon dioxide in the feed, and that some hydrogen was converted to water particularly at high CO_2/CH_4 ratios due to the reverse water gas shift reaction (RWGS) and methanation reaction (reverse steam reforming of methane). However, at higher operating temperatures, the contribution of the methanation reaction was much less pronounced due to the high value of the equilibrium constant of the steam reforming of methane as shown in Fig. 1. It should be noted that some methane still existed even with high CO_2/CH_4 ratios at a moderate temperature of 900 K. For SOFC-O^{2-} operation, hydrogen was electrochemically consumed and water was generated in the anode chamber. It is shown in Fig. 3(a) that negligible amount of methane was observed because the consumption of hydrogen moved the dry reforming of methane forward and, in addition, the steam reforming of methane promoted the methane consumption. When the extent of carbon dioxide in the feed was increased, a lower amount of hydrogen and a higher amount of water were observed according to the RWGS reaction. For SOFC-H^+ operation, hydrogen was also electrochemically consumed; however, the electrochemical water appeared in the cathode chamber and played no role in the anode reactions unlike in the SOFC-O^{2-}. It should be noted that the SOFC-H^+ behaved quite similarly to a membrane reactor in which the forward reaction is enhanced by removing some products (e.g., hydrogen) from the reaction zone. From Fig. 3(b), it was observed that the amounts of hydrogen and water involved in the SOFC-H^+ were much less than those in the SOFC-O^{2-}. Moreover, when higher amount of carbon dioxide was added in the feed, more hydrogen was converted to water and a slight increase of carbon monoxide was observed.

The effect of the inlet CO_2/CH_4 ratio on the carbon activity for the conventional reformer is shown in Fig. 4. The carbon activity decreased dramatically with increasing CO_2/CH_4 ratio and operating temperature, implying that the chance of carbon formation can be rapidly decreased by adding CO_2 to the system or operating the system at a high temperature. Increasing the amount of CO_2 in the feed promoted the consumption of methane and generation of water, which reduced the possibility of carbon formation. Because the Boudard (Eq. (16)) and reverse carbon gasification (Eq. (18)) reactions are exothermic,

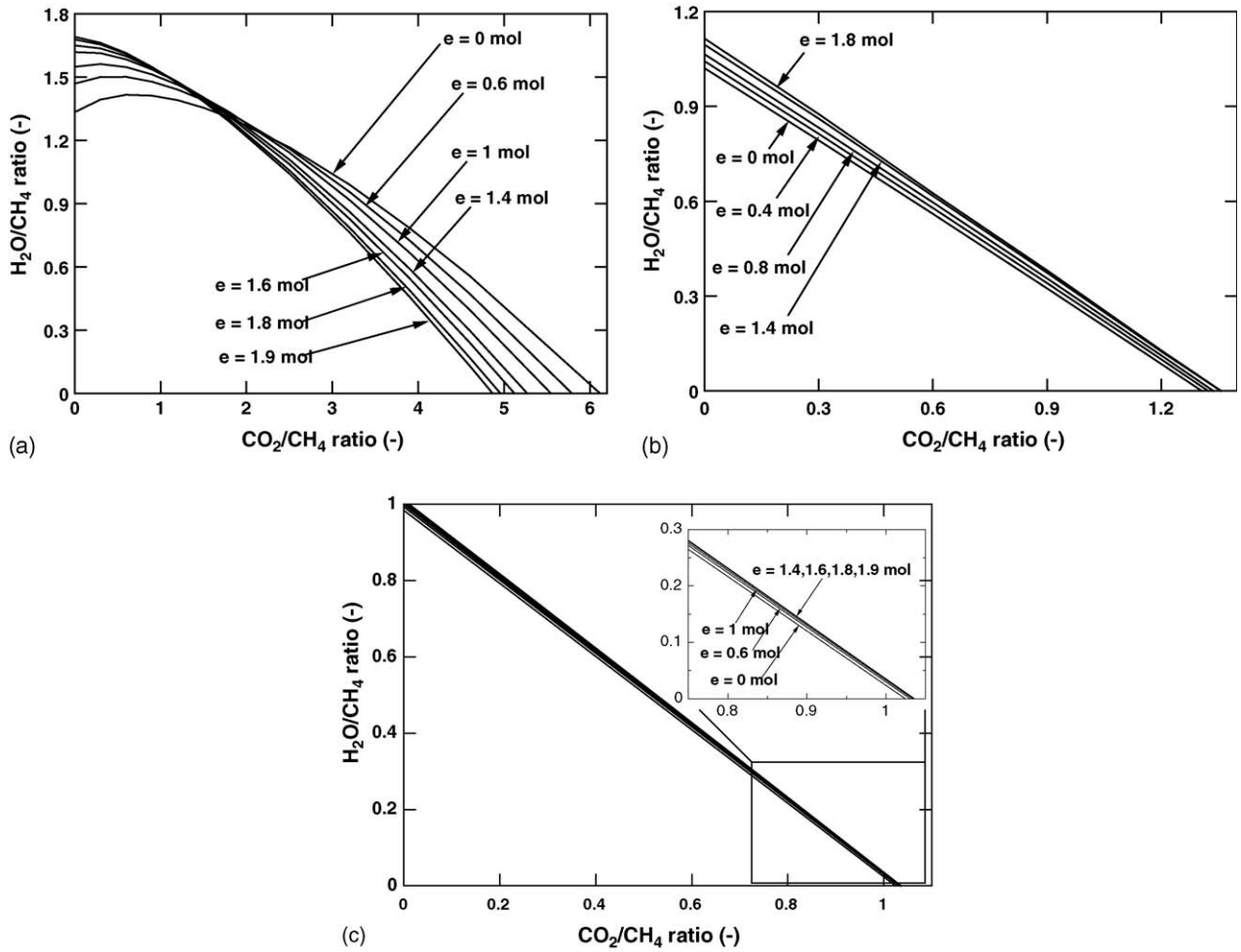

Fig. 8. Required inlet H_2O/CH_4 ratio at different inlet CO_2/CH_4 ratios: (a) $T = 900$ K, (b) $T = 1050$ K and (c) $T = 1200$ K (SOFC-H^+, $a = 1$ mol and $P = 101.3$ kPa).

the carbon activity was significantly reduced at high operating temperatures. Although the carbon formation from methane cracking (Eq. (17)) should be more significant at high temperature, the much higher values of the equilibrium constants of the dry and steam reforming reactions compared to that of the methane cracking make it become less likely at high operating temperatures (see Fig. 1). It should be noted that the carbon activity calculated from Eqs. (19)–(21) yield the same value, which is in good agreement with previous literature [11,20]. Fig. 5 shows the required CO_2/CH_4 ratio at the boundary of carbon formation for the SOFC-O^{2-} at different temperatures and extent of electrochemical reaction of hydrogen (e). Lower CO_2/CH_4 is required for the SOFC-O^{2-} compared to that of the conventional reformer due to the presence of electrochemical water in the anode chamber. The difference was particularly pronounced at for a higher extent of the electrochemical reaction. For the SOFC-H^+, at moderate operating temperatures (T = 800–1000 K) when the extent of the electrochemical reaction (e) was increased, the lower CO_2/CH_4 ratio was sufficient to alleviate carbon formation as shown in Fig. 6(a). However, the opposite trend was observed at higher operating temperatures (T > 1000 K) as shown in Fig. 6(b). The trend at lower operating temperatures was quite unusual as it has been reported earlier for the systems of the steam reforming of methane [11] and methanol [12] that a higher H_2O/fuel ratio was required at the higher extent of electrochemical reaction because hydrogen was consumed and no benefit of electrochemical water was realized in the anode gas mixture in the SOFC-H^+. In addition, there was a general concern in using a membrane reactor for dehydrogenation reactions where the carbon formation problem could be more severe due to the removal of hydrogen from the reaction system. Therefore, it is likely that for the SOFC-H^+, more carbon dioxide would be needed when the extent of the electrochemical reaction is higher in the dry reforming system.

To explain the reasons for the unusual behavior of the dry reforming of methane in the SOFC-H^+ at moderate temperatures (800–1000 K), the moles of each species at different CO_2/CH_4 ratios at T = 900 K for the conventional reactor (Fig. 2) and the SOFC-H^+ (Fig. 3(b)) were compared. Note that because the carbon activity of all the possible carbon formation reactions provided the same value when the gas mixtures are at their equilibrium conditions, for simplicity the carbon activity based on the Boudard reaction (Eq. (19)) is considered as an example for understanding the behavior of the system when carbon dioxide is added to the system. From the figures, when hydrogen was electrochemically removed from the anode gas mixture, the dry

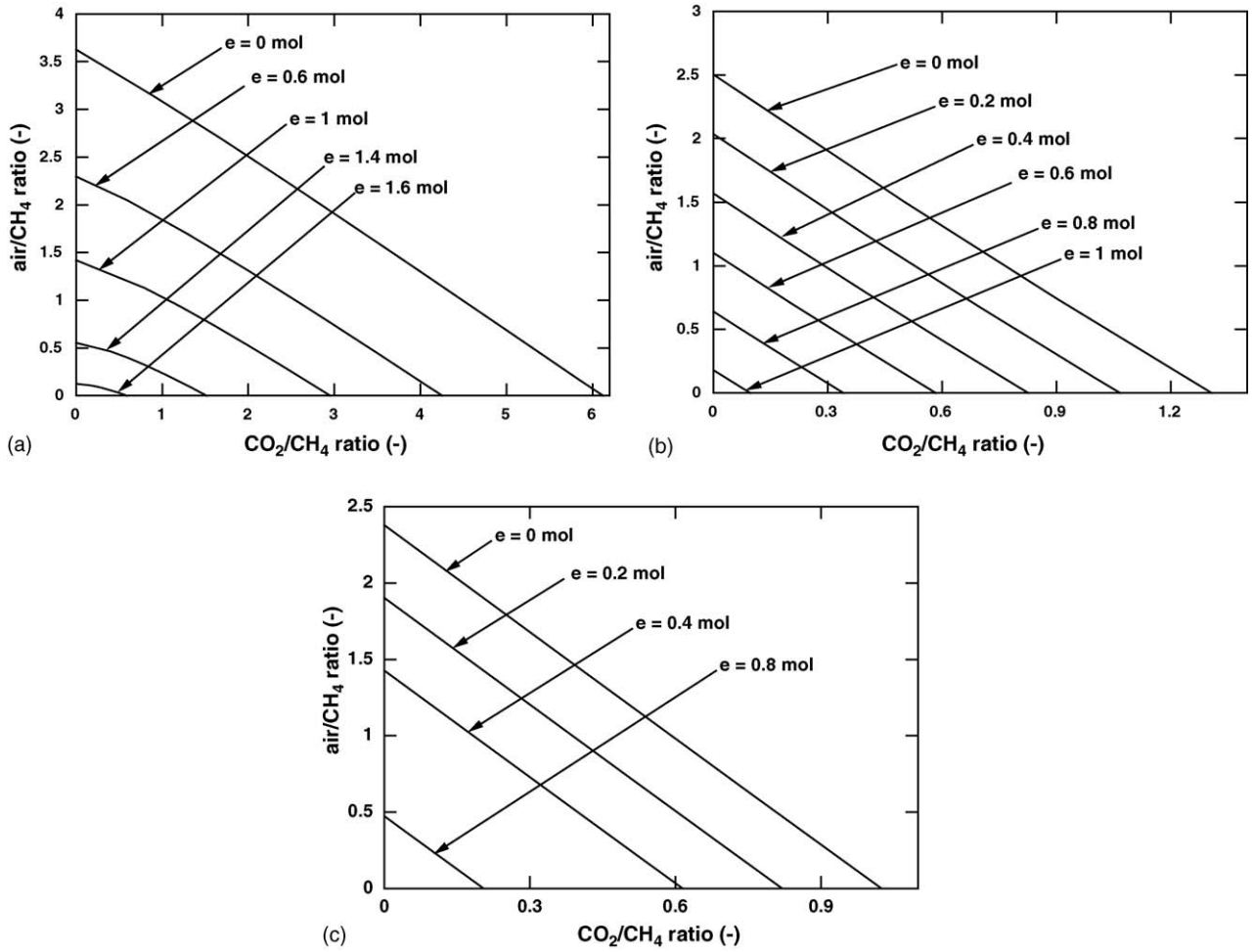

Fig. 9. Required inlet air/CH_4 ratio at different inlet CO_2/CH_4 ratios: (a) T = 900 K, (b) T = 1050 K and (c) T = 1200 K (SOFC-O^{2-}, a = 1 mol and P = 101.3 kPa).

reforming of methane moved forward, resulting in a low content of CH_4 in the gas mixture. It is observed that the moles of CO in the gas mixture for the SOFC-H^+ were less dependent on the CO_2/CH_4 ratio than for the conventional reactor because the RWGS played a less significant role when smaller amounts of hydrogen was present in the system. Consequently, the value of the carbon activity ($K_1 p_{CO}^2/p_{CO_2}$) for the SOFC-H^+ decreased with increase of the CO_2/CH_4 ratio more rapidly than that for the conventional reactor and, therefore, reached the boundary of carbon formation ($\alpha_c = 1$) at a lower value of CO_2/CH_4 ratios.

In practical operation, carbon dioxide is unlikely to be added to the system to suppress carbon formation. Other components such as water and air are more practical additive choices. The calculations were carried out to find the required H_2O/CH_4 or air/CH_4 ratio for different inlet CO_2/CH_4 ratios, the extent of the electrochemical reaction and the operating temperature. This information is important for selecting a suitable feed composition which avoids the carbon formation problem. Figs. 7 and 8 show the H_2O/CH_4 ratio at the boundary of carbon formation for different CO_2/CH_4 ratios in the feed for SOFC-O^{2-} and SOFC-H^+, respectively. It was found that for the SOFC-O^{2-}, the required H_2O/CH_4 ratio decreased with the increases of inlet CO_2/CH_4 ratio, extent of electrochemical reaction and operating temperature. The operation at a high extent of the electrochemical reaction and high temperature significantly reduced the risk of carbon formation. For the SOFC-H^+, the required H_2O/CH_4 ratio also decreased with increase of the inlet CO_2/CH_4 ratio and operating temperature. Higher H_2O/CH_4 ratios were required at higher extents of the electrochemical reaction. However, the reverse trend was observed when the system was operated at a moderate operating temperature ($T = 900$ K) with high inlet CO_2/CH_4 ratio (approximately higher than 1.5) which is in good agreement with the previous case in which only carbon dioxide was used as the carbon suppresser. When comparing between the required H_2O/CH_4 ratio for the case with no carbon dioxide present in the inlet feed (CO_2/CH_4 ratio = 0) and the required CO_2/CH_4 of the case without the addition of water for both SOFC-O^{2-} and SOFC-H^+, it is clear that water showed a more pronounced influence on inhibiting the carbon formation than carbon dioxide particularly at low operating temperatures. The results also revealed that for the SOFC-H^+ the extent of the electrochemical reaction had no significant effect on the required H_2O/CH_4 ratio at high temperatures. It should be noted that when comparing between the dry reforming and the steam reforming of methane with addition of carbon dioxide and water, respectively, as the components for inhibiting the carbon formation, the addition of water always provided a beneficial effect to the system as water reacted with methane to reduce the extent

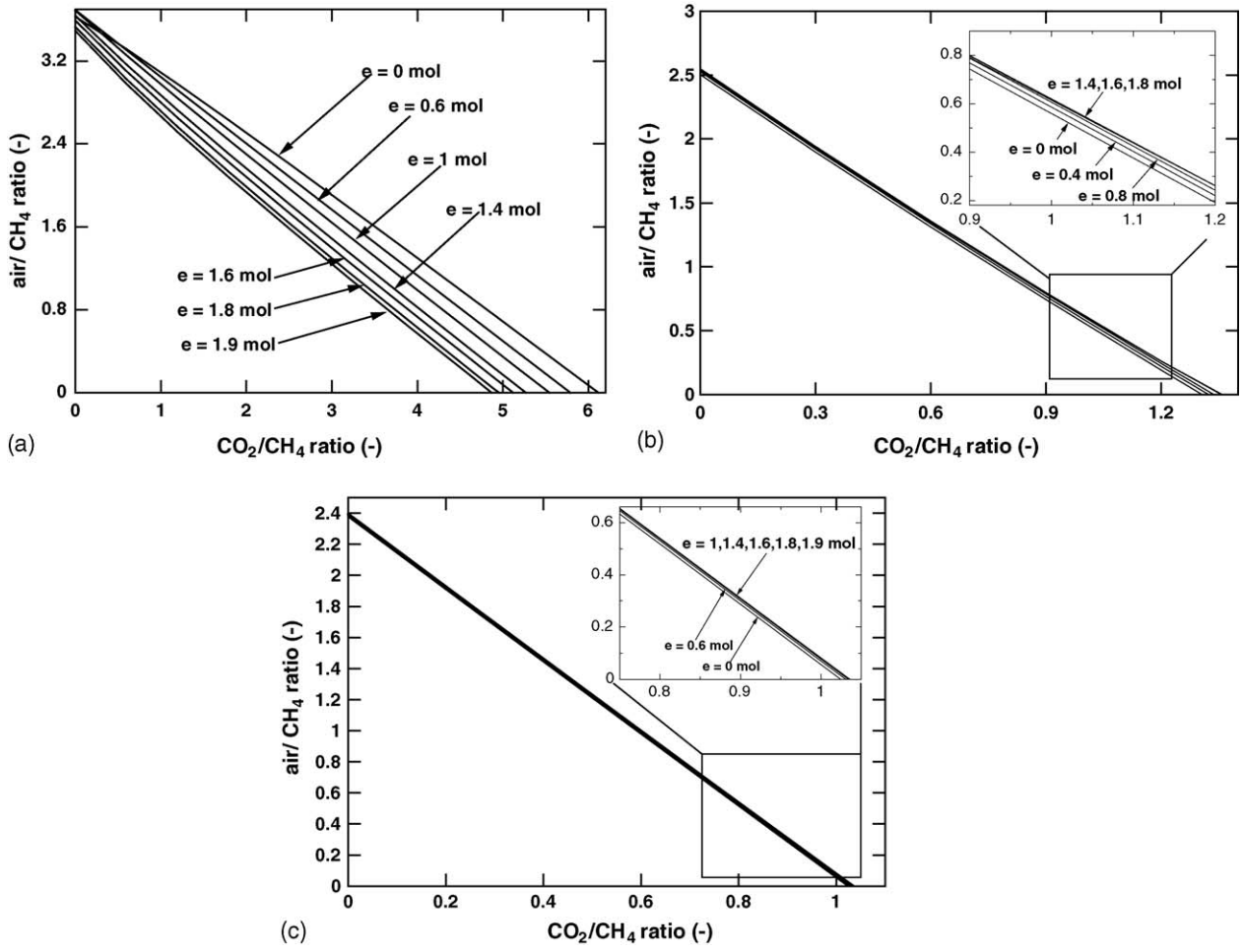

Fig. 10. Required inlet air/CH_4 ratio at different inlet CO_2/CH_4 ratios: (a) $T = 900$ K, (b) $T = 1050$ K and (c) $T = 1200$ K (SOFC-H^+, $a = 1$ mol and $P = 101.3$ kPa).

of methane and with carbon monoxide to reduce the extent of carbon monoxide, forming hydrogen and carbon dioxide. The presence of high amounts of carbon dioxide, hydrogen and water was important in preventing the carbon formation in the system. For the case of addition of carbon dioxide, although extra carbon dioxide promoted the consumption of methane from the dry reforming reaction, unlike water, carbon dioxide did not help reduce the extent of carbon monoxide in the system. In addition, more carbon monoxide could be generated by the RWGS reaction.

When air is used as an alternative oxidant for preventing carbon formation, oxygen in air can react with methane, carbon monoxide or hydrogen whose products are beneficial for preventing the carbon formation. Figs. 9 and 10 show the required air/CH_4 ratios for the SOFC-O^{2-} and SOFC-H^+, respectively. It was found that the similar trend as that of the addition of water was observed for both cases. It should be noted that, the advantage of air addition, that although the presence of nitrogen diluted the partial pressure of hydrogen in the anode gas mixture, which resulted in lower fuel cell performance, the exothermic heat from the oxidation reactions was useful for the endothermic dry reforming reaction in the system.

4. Conclusion

Thermodynamic analysis was employed to predict the boundary of carbon formation for DIR-SOFCs. The required CO_2/CH_4 ratio to prevent carbon formation has been determined by varying the operating temperature, electrolyte type and the extent of the electrochemical reaction. Operation at high temperatures dramatically reduced the required inlet CO_2/CH_4 ratio. The benefit of the presence of electrochemical H_2O in the anode chamber on suppression of carbon formation was realized in the SOFC-O^{2-} which resulted in a lower requirement for the CO_2/CH_4 ratio. For the SOFC-H^+, due to the disappearance of H_2 without gaining the benefit of the electrochemical H_2O in the anode chamber, a higher CO_2/CH_4 ratio was necessary. However, at moderate temperatures ($T = 800$–1000 K) an unexpected and opposite trend was observed. The additions of water and air to a feed with a certain inlet CO_2/CH_4 ratio were considered as alternative strategies for suppressing the carbon formation. Water was a more effective choice than CO_2 particularly at low temperatures. Although air is less attractive to water, the benefit of the exothermic heat from the reactions with oxygen may make the system more practical.

It should be noted that although the thermodynamic calculations can be used to predict the boundary of carbon formation, the deactivation of the anode is not solely the result of the deposition of carbon. Deposition of other forms of carbonaceous compounds such as polymeric coke (C_nH_m) may result in comparable damage. Therefore, the results obtained in this study should be considered only as a crude guideline for selecting suitable operating conditions for SOFCs and other related reactors.

Acknowledgements

This research is financially supported by the Thailand Research Fund and Ministry of University Affairs. The support from Professor Piyasan Praserthdam is also gratefully acknowledged.

References

[1] S.L. Douvartzides, F.A. Coutelieris, K. Demin, P.E. Tsiakaras, AIChE J. 49 (2003) 248–257.
[2] L.F. Brown, Int. J. Hydrogen Energy 26 (2001) 381–397.
[3] G. Maggio, S. Freni, S. Cavallaro, J. Power Sources 74 (1998) 17–23.
[4] S.H. Clarke, A.L. Dicks, K. Pointon, T.A. Smith, A. Swann, Catal. Today 38 (1997) 411–423.
[5] C.M. Finnerty, R.M. Ormerod, J. Power Sources 86 (2000) 390–394.
[6] S. Park, R.J. Gorte, J.M. Vohs, Appl. Catal. A 200 (2000) 55–61.
[7] C.M. Finnerty, N.J. Coe, R.H. Cunningham, R.M. Ormerod, Catal. Today 46 (1998) 137–145.
[8] L. Topor, L. Bejan, E. Ivana, N. Georgescu, Rev. Chim. Bucharest 30 (1979) 539.
[9] T.A. Chubb, Sol. Energy 24 (1980) 341.
[10] T.A. Chubb, J.H. McCrary, G.E. McCrary, J.J. Nemecek, D.E. Simmons, Proc. Meet. Am. Sect. Int. Sol. Eng. Soc. 4 (1981) 166.
[11] W. Sangtongkitcharoen, S. Assabumrungrat, V. Pavarajarn, N. Laosiripojana, P. Praserthdam, J. Power Sources 142 (2005) 75–80.
[12] S. Assabumrungrat, N. Laosiripojana, V. Pavarajarn, W. Sangtongkitcharoen, A. Tangjitmatee, P. Praserthdam, J. Power Sources 139 (2005) 55–60.
[13] J.H. Edwards, A.M. Maitra, Fuel Proc. Tech. 42 (1995) 269.
[14] J.R. Rostrup-Nielsen, J.H.B. Hansen, J. Catal. 144 (1993) 38.
[15] T. Sodesawa, A. Dobashi, F. Nozaki, React. Kinet. Catal. Lett. 12 (1979) 107.
[16] J.H. Hirschenhofer, D.B. Stauffer, R.R. Engleman, M.G. Klett, Fuel Cell Handbook, fourth ed., Parsons Corporation, Reading, 1998, p. 2.
[17] P. Pietrogrande, M. Bezzeccheri, in: L.J.M.J. Blomen, M.N. Mugerwa (Eds.), Fuel Cell Systems, Plenum Press, New York, 1993, p. 142.
[18] L.F. Brown, Int. J. Hydrogen Energy 26 (2001) 381–397.
[19] J.R. Grace, X. Li, C.J. Lim, Catal. Today 64 (2001) 141–149.
[20] S. Nagata, A. Momma, T. Kato, Y. Kasuga, J. Power Sources 101 (2001) 60–71.

Appendix 6

Available online at www.sciencedirect.com
ScienceDirect
Journal of Power Sources 167 (2007) 139–144
JOURNAL OF POWER SOURCES
www.elsevier.com/locate/jpowsour

Short communication

Improvement of solid oxide fuel cell performance by using non-uniform potential operation

S. Vivanpatarakij [a], S. Assabumrungrat [a,*], N. Laosiripojana [b]

[a] *Center of Excellence in Catalysis and Catalytic Reaction Engineering, Department of Chemical Engineering, Faculty of Engineering, Chulalongkorn University, Bangkok 10330, Thailand*

[b] *The Joint Graduate School of Energy and Environment, King Mongkut's University of Technology Thonburi, Bangkok 10140, Thailand*

Received 7 November 2006; received in revised form 6 February 2007; accepted 6 February 2007
Available online 21 February 2007

Abstract

Theoretical study was carried out to investigate the possible improvement of SOFC performance by using a non-uniform potential operation (SOFC-NUP) in which the operating voltage was allowed to vary along the cell length. Preliminary results of a simple SOFC-NUP with a cell divided into two sections of equal size in term of range of fuel utilization (U_f) indicated that the SOFC-NUP can offer higher power density than an SOFC with uniform potential operation (SOFC-UP) without a reduction of the electrical efficiency. In this work, voltages and section splits were optimized to obtain the maximum power density of the SOFC-NUP. At the optimum splits ($S_{p,1} = 0.55$ and $S_{p,2} = 0.45$), the power density improvement as high as 9.2% could be achieved depending on the level of electrical efficiency. It was further demonstrated that the increase in the number of separated section (n) of the cell could increase the achieved maximum power density but the improvement became less pronounced after $n > 3$.

Keywords: SOFC; Non-uniform potential; Power generation

1. Introduction

Fuel cells are promising electrochemical devices that convert the chemical energy of a fuel directly into electrical energy. Compared to conventional power generation processes, fuel cells are attractive due to their better environmental friendliness, practical noise-free operation, and higher efficiency. A number of researches have been carried out in many directions with a major aim to improve performances of the fuel cells and their systems. For instance, several gas turbine cycles such as steam injected gas turbine cycle, gas turbine/steam turbine combined cycle, and humid air turbine cycle have been combined with solid oxide fuel cell (SOFC) for efficiency improvement [1]. An operation with anodic offgas recirculation was proposed for a polymer electrolyte membrane fuel cell (PEMFC) system equipped with a fuel processor. Under this operation, a significant efficiency increase for the fuel processor and the gross efficiency of the combined system of 30% were reported [2]. A novel gas distributor with current-collecting elements distributed in gas-delivery fields for effective current collection and heat/mass transfer enhancement was designed to improve power density [3,4]. In addition, many researches have been devoted on development of cell components with superior characteristics [5–7]. The performance improvement of PEMFC from operation at a higher pressure was reported although the power loss due to air compression was taken into account in the comparisons [8].

Among several procedures for improving fuel cell performance, the use of non-uniform potential operation concept for fuel cells in which the cell voltage is allowed to vary along the cell length is another interesting approach. However, until now only some works have focused on the potential benefits of this approach. It was demonstrated that an improvement in electrical efficiency of about 1% could be achieved by splitting the cell of a molten carbonate fuel cell (MCFC) into two sections [9]. Selimovic and Plasson [10] examined performances of networked solid oxide fuel cell (SOFC) stacks combined with a gas turbine cycle. Two multistage configurations, i.e. (i) both anode and cathode flows were serially connected and (ii) only the anode

* Corresponding author. Tel.: +66 2 216 6868; fax: +66 2 218 6877.
E-mail address: Suttichai.A@chula.ac.th (S. Assabumrungrat).

0378-7753/$ – see front matter © 2007 Elsevier B.V. All rights reserved.
doi:10.1016/j.jpowsour.2007.02.026

Nomenclature

a	constant in Eq. (11) (Ω m)
A	area (m^2)
b	constant in Eq. (11) (K)
E	activation polarization energy in Eqs. (12) and (13) (kJ mol^{-1})
E_0	open circuit voltage (V)
F	Faraday constant (96485.34) (C mol^{-1})
i	current density (A m^{-2})
LHV	lower heating value of methane feed (W)
m	constant polarization parameters in Eqs. (12) and (13)
n	number of separated section
p	partial pressure (atm)
P	power density (W cm^{-2})
r	activation polarization parameters in Eqs. (12) and (13) (A m^{-2})
R	universal gas constant (8.31447×10^{-3}) (kJ mol^{-1} K^{-1})
S_p	section split
T	absolute temperature (K)
U_f	fuel utilization (%)
V	operating voltage (V)
W	electrical work (W)

Greeks letters

δ	thickness (m)
ε	electrical effiency (%)
η	overpotential (Ω m^2)
φ	potential (V)
ρ	specific ohmic resistance (Ω m)

Subscript

A	anode
Act	activation
C	cathode
Conc	concentration
k	section number
Ohm	ohmic

flow was serially connected while the cathode flow was parallel connected, were considered. An increase of system efficiency of about 5% was reported for the former configuration mainly due to an improved thermal management. The similar multi-stage configurations were also considered for a combined heat and power MCFC plant [11]. Detailed flowsheet calculations showed that the improvement in efficiency was about 0.6% for the former configuration, and 0.8% for the latter configuration. The concept was also extended to PEMFCs divided into many stages (or stacks) of equal size [12]. It was demonstrated that the non-uniform cell potential operation allowed for enhanced maximum power densities compared to the traditional concept involving a uniform cell potential distribution. The improvement within 6.5% was reported.

In this study, the concept of non-uniform potential operation implemented to SOFCs fed by methane was investigated in an effort to optimize cell operating voltages and sizes so that a maximum power density could be achieved without a reduction of electrical efficiency. Values of power density of a simple SOFC with a cell divided into two sections whose operating voltages and sizes were allowed to vary were compared to those of a typical SOFC with uniform cell potential at various electrical efficiencies. Additionally, the effect of number of cell section on the obtained performance was determined.

2. Theory

The schematic diagram of an SOFC with non-uniform potential operation (SOFC-NUP) is illustrated in Fig. 1. Compositions of fuel and air streams change along the cell channel according to changes in value of fuel utilization defined as the mole of hydrogen electrochemically consumed divided by the theoretical mole of hydrogen generated from complete reforming of the methane feed. In section k, the fuel utilization changes from $U_{f,k-1}$ to $U_{f,k}$, and the cell is operated at a constant potential of V_k within the section. In practice, the non-uniform cell potential can be realized by using segmented current collectors for a single-cell SOFC or it can be carried out in a series of SOFC stacks operated at different stack potentials. The section split of section k ($S_{p,k}$) is defined by

$$S_{p,k} = \frac{U_{f,k} - U_{f,k-1}}{U_{f,final}} \quad (1)$$

When the SOFC is fed by a non-hydrogen fuel (e.g. methane), a reformer is generally required to reform the fuel with an oxidant (e.g. steam) to a hydrogen-rich stream before feeding to the SOFC stack. The main reactions involved in the production of hydrogen from methane and steam are the methane steam reforming and water gas shift reactions as shown in Eqs. (2) and (3), respectively.

$$CH_4 + H_2O = 3H_2 + CO \quad (2)$$

$$CO + H_2O = H_2 + CO_2 \quad (3)$$

In the SOFC stack, both hydrogen and CO can react electrochemically with oxygen. However, it is assumed that the CO electro-oxidation is neglected. It was estimated earlier that about 98% of current is produced by H_2 oxidation in common situations [13]. This is due to the fast rate of water gas shift reaction at an SOFC operating temperature. The electrochemical reactions of hydrogen and oxygen take place according to Eqs. (4) and (5).

$$\text{Anode}: \quad H_2 + O^{2-} = H_2O + 2e^- \quad (4)$$

$$\text{Cathode}: \quad O_2 + 4e^- = 2O^{2-} \quad (5)$$

Electromotive force (E_0) of the cell is a difference of potentials between both electrodes of the cell. It can be represented as follows:

$$E_0 = |\varphi_C - \varphi_A| \quad (6)$$

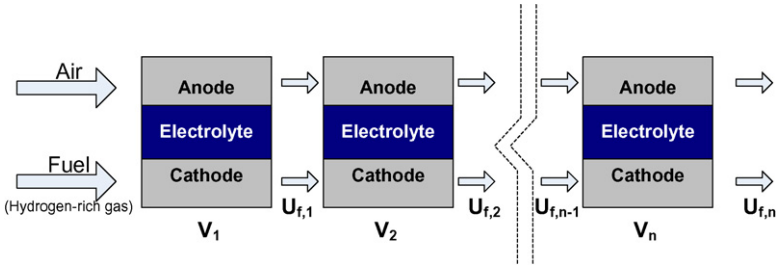

Fig. 1. Schematic diagrams of SOFC-NUP.

where φ_C and φ_A are the potentials of the cathode and the anode, respectively. The electrode potential can be calculated from Nernst equation which can be expressed as follows:

$$\varphi = \left(\frac{RT}{4F}\right) \ln p_{O_2} \tag{7}$$

where R is the universal gas constant, T the absolute temperature and F is the Faraday's constant. The partial pressure of oxygen in the cathode chamber is calculated from its mole fraction while the partial pressure of oxygen in the anode chamber is given by:

$$p_{O_2} = \left(\frac{p_{H_2O}}{K p_{H_2}}\right)^2 \tag{8}$$

where p_i is the partial pressure, and K is the equilibrium constant of the hydrogen oxidation reaction.

When the SOFC is operated at a potential of V_k, the local current density can be determined according to Eq. (9). It should be noted that as the value of E_0 changes along the cell length within the section due to the change in gas compositions, the current density varies within the cell section.

$$i = \frac{E_0 - V_k}{\eta_{Ohm} + \eta_{Act,A} + \eta_{Act,C} + \eta_{Conc,A} + \eta_{Conc,C}} \tag{9}$$

where

$$\eta_{Ohm} = \sum \rho_j \delta_j \tag{10}$$

$$\rho_j = a_j \exp(b_j T) \tag{11}$$

$$\eta_{Act,C} = \left(\frac{4F}{RT} r_C \left(\frac{p_{O_2}}{p}\right)^m \exp\left(\frac{-E_C}{RT}\right)\right)^{-1} \tag{12}$$

$$\eta_{Act,A} = \left(\frac{2F}{RT} r_A \left(\frac{p_{H_2}}{p}\right)^m \exp\left(\frac{-E_A}{RT}\right)\right)^{-1} \tag{13}$$

The parameters used in the calculations are provided in Table 1 [14] and Table 2 [15]. It was reported that the correlations of the activation polarization can predict the cell performance close to the Butler–Volmer equation within the temperature range of 1173–1273 K [16]. In this study, the operating temperature is kept at 1173 K which is in the reliable limit.

To simplify the calculations of the SOFC performance, it is assumed that both fuel and oxidant are well-diffused through the surface of the electrodes. Therefore, concentration polarization losses ($\eta_{Conc,A}$ and $\eta_{Conc,C}$) can be omitted. This assumption is valid when the cell is not operated at too high current density or too low concentration. In addition, it is further assumed that the cell is operated at isothermal condition and the fuel stream is always at its equilibrium composition along the length of the SOFC cell. It should be noted that an external reformer is usually connected to the SOFC system in order to generate hydrogen-rich feed for the stack and to suppress the cell deactivation due to the carbon formation. In addition, state-of-the-art SOFC nickel cermet anodes are usually active for the steam reforming and shift reactions particularly at high operating temperature of SOFC [16,17]. Calculations of the thermodynamic equilibrium composition are accomplished by following details given in our previous work [18].

Table 1
Resistivity and thickness of cell component [12]

Material used	Ni–YSZ/YSZ/LSM–YSZ
Anode thickness (μm)	150
Anode ohmic resistance constant	$a = 0.0000298$, $b = -1392$
Cathode thickness (μm)	2000
Cathode ohmic resistance constant	$a = 0.0000811$, $b = 600$
Electrolyte thickness (μm)	40
Electrolyte ohmic resistance constant	$a = 0.0000294$, $b = 10350$
Interconnect thickness (μm)	10
Interconnect ohmic resistance constant	$a = 0.001256$, $b = 4690$

When the current density is known, the cell area (A_k) and electrical power (W_k) involved in each cell section can be determined. The values of overall electrical efficiency (ε) and average power density (P) can be determined according to Eqs. (14) and (15), respectively.

$$\varepsilon = \sum_{k=1}^{n} \frac{W_k}{LHV} \times 100\% \tag{14}$$

$$P = \frac{\sum_{k=1}^{n} W_k}{\sum_{k=1}^{n} A_k} \tag{15}$$

where LHV is the lower heating value of methane feed.

Table 2
Summary of activation polarization parameters [13]

	r (A m^{-2})	$E_{A,pol}$ (kJ mol^{-1})	m
Cathode	1.489×10^{10}	160	0.25
Anode	2.128×10^{8}	110	0.25